5HT Modulates the Mode of Fusion through the Interaction of Gβγ, Calcium-synaptotagmin and SNARE Proteins

BY

SHELAGH RODRIGUEZ
B.S., University of Illinois at Chicago, Chicago, 2010

THESIS

Submitted as partial fulfillment of the requirements
for the degree of Doctor of Philosophy in Biological Sciences
in the Graduate College of the
University of Illinois at Chicago, 2019

Chicago, Illinois

Defense Committee:

        Janet E. Richmond, Chair
        Simon T. Alford, Advisor
        Thomas J. Park
        Liang-Wei Gong
        Mitchell F. Roitman, Psychology

This work is dedicated to my family, here and gone; those related by blood and those related by circumstance.

ACKNOWLEDGEMENTS

I would like to thank Simon Alford for his extensive help, kindness and understanding over the years, without which this thesis would not have been possible. I would like to thank all of my committee members, Janet Richmond, Thom Park, Liang-Wei Gong, and Mitch Roitman for their patience and adaptability. I'd like to acknowledge the difficult work done by Shankar Ramachandran that laid the foundation for my own experiments. I'd like to thank Mariana Potcoava for her work with the lattice light sheet microscope and for always having snacks. I'd also like to thank all former and current members of the Alford lab who welcomed me and assisted me in all my scientific endeavors, particularly Emily Church and Michael Alpert.

CONTRIBUTION OF AUTHORS

Chapters 3 and 4 of this work are adapted from published papers that were a collaborative effort between the Alford (University of Illinois at Chicago) and Hamm (Vanderbilt University) laboratories. The figures that the author of this work contributed to are delineated in the full figure legends. Experiments performed by the author of this work have been noted in the body of the text. All other experiments were carried out by the talented group of individuals in both laboratories.

TABLE OF CONTENTS

TABLE OF CONTENTS (continued)

LIST OF TABLES

LIST OF FIGURES

LIST OF ABBREVIATIONS

$[Ca^{2+}]$	Calcium concentration
5-HT	5-hydroxytryptamine
AHP	afterspike hyperpolarization
ATP	Adenosine triphosphate
BAPTA	1,2-bis(2-aminophenoxy)ethane-N,N,N',N'-tetraacetic acid
BSA	Bovine Serum Albumin
BoNT	Botulinum Neurotoxin
BRP	Bruchpilot
Ca^{2+}	Calcium
CaM	Calmodulin
CaMKII	Ca^{2+}/calmodulin-dependent protein kinase II
CaV	Voltage gated calcium channels
CDK5	cyclin-dependent kinase 5
CNS	central nervous system
CNAα	calcineurin Aα (CNAα)
EGTA	ethylene glycol-bis(β-aminoethyl ether)-N,N,N',N'-tetraacetic acid
EM	Electron Micrograph
EPSC	Excitatory Post-Synaptic Current
F-actin	F-actin
G Protein	guanine-nucleotide binding proteins
GDP	Guanosine 5´-diphosphate
GIRK	G-protein activated inward rectifying potassium channels

GPCR	G Protein Coupled Receptors
GRK	G protein coupled receptor kinase
GST	glutathione S-transferase
GTP	Guanosine 5´-triphosphate
HRP	Horseradish Peroxidase
HVA	High Voltage Activated
K_D	Equilibrium dissociation constant
K_{ON}	Rate constant for association
KO	Knock Out
LLSM	Lattice Light Sheet Microscope
LVA	Low Voltage Activated
MIANS	2-(4′-maleimidylanilino) naphthalene-6-sulfonate
Munc-13	mammalian uncoordinated-13
Munc-18	mammalian uncoordinated-18
NSF	N-ethylmaleimide Sensitive Fusion protein
Ni-NTA	Ni-nitrilotriacetic acid
P_r	Release probability
RIM	Rab-3 Interacting Molecule
RMS	Root Mean Square
RRP	Readily Releasable Pool
SM-like Proteins	Sec1/Munc18-like proteins
SNAP-25	synaptosome-associated protein of 25 kDa
SNARE Proteins	Soluble N-ethylmaleimide Sensitive Fusion Attachment Proteins
STD	Short Term Depression
STF	Short Term Facilitation

STP	Short Term Plasticity
SV	Synaptic Vesicles
Syt	Synaptotagmin
t-SNAREs	Target-membrane associated SNAREs
TRP	Total Releasable Pool
UFE	Ultrafast Endocytosis
v-SNAREs	Vesicle associated SNARES
VAMP	Vesicle Associated Membrane Protein
VGCC	Voltage-Gated Calcium Channel
WT	Wild-Type

SUMMARY

Fast synchronous neurotransmission occurs when an action potential triggers Ca^{2+} influx through voltage-gated calcium channels. In turn, Ca^{2+} binds to synaptotagmin forcing it to interact with the SNARE complex and the plasma membrane. This interaction results in the fusion of the two membranes and the release of neurotransmitter from the newly formed fusion pore. The creation of a full fusion pore is inhibited in a Ca^{2+}-dependent manner by the $G\beta\gamma$ subunit of a $G_{i/o}$-coupled serotonin receptor. This inhibition causes neurotransmission to favor transient, kiss-and run, exocytosis. Thereby, the action of $G\beta\gamma$ and Ca^{2+} have direct impacts on short term synaptic plasticity.

Of particular interest is the C-terminal region of SNAP-25. When the C-terminal of SNAP-25 is cleaved by 26 residues, the formation of SNARE complexes is completely abolished. However, when only the 9 C-terminal residues of SNAP-25 are cleaved, synaptic transmission remains but is no longer tightly coupled to the influx of Ca^{2+}. In addition, the cleavage of these same 9 residues prevents inhibition by $G\beta\gamma$. Therefore, the inhibition of $G\beta\gamma$ appears to be caused by competition with Synaptotagmin binding of SNAP-25 at the C-terminal.

Our collaborators at Vanderbilt determined the residues at which $G\beta\gamma$ bound SNAP-25. Through a novel approach of direct injection of mutant SNAP-25 into lamprey reticulospinal axons I further determined which of these binding domains was responsible for 5-HT mediated inhibition without impairing synaptic transmission. This work directly led to the creation of a mouse model which shows a decrease in 5-HT mediated inhibition. This model has now been used to study the action of $G\beta\gamma$ on synaptic transmission without confounding factors from previous studies.

Under high frequency stimulation, inhibition of $G\beta\gamma$ is relieved. This has been linked to the ability of Synaptotagmin-1 to outcompete $G\beta\gamma$ for binding under high Ca^{2+} concentrations. The interaction of Ca^{2+} and synaptotagmin happens on a very short time scale and is assisted

by the tight coupling of VGCCs to SNARE complexes. The microarchitecture of the active zone, as well as the probability of VGCC opening directly effects Ca^{2+} transients at release sites. It is of interest then, how VGCCs behave under a single stimulus as well as during high frequency stimulation. I looked at Ca^{2+} influx at high spatio-temporal resolution over several active zones simultaneously by utilizing Lattice Light Sheet Microscopy. I have shown that Ca^{2+} entry at a given active zone is variable and stochastic, and that this variability is independent between active zones. Additionally, in short high frequency bursts of stimulation, VGCCS display a high degree of heterogeneity in evoked transients. I propose that this variability is due to VGCCs opening in cassettes, with subsequent stimulation causing Ca^{2+}-dependent inactivation or facilitation of a subset of VGCCs.

1. INTRODUCTION

1.1   Synaptic Transmission

1.1.1   Overview

Exocytosis and endocytosis are essential components of all eukaryotic life. They offer a fundamental process for cells to fuse lipid compartments, to move proteins between membranes, to process proteins in the Golgi apparatus, and to exchange information both intracellularly and extracellularly (Bennett and Scheller, 1994; Ferro-Novick and Jahn, 1994; Südhof, 2004). These processes are so essential that they are conserved throughout all eukaryotic organisms, from a simple strain of yeast or the noble lamprey all the way to the less noble human (Ferro-Novick and Jahn, 1994). The machinery that exists for cell to cell and intracellular communication, finds a highly specialized role in neuronal chemical synaptic transmission (Südhof, 2004).

Chemical synaptic transmission requires exocytosis and endocytosis (Südhof, 2004). It occurs when an action potential causes voltage-gated calcium channels (VGCCs) to open at specialized active zones in a presynaptic neuron. In turn, this influx of calcium (Ca^{2+}) causes a rise in intracellular Ca^{2+} concentration ($[Ca^{2+}]$) which triggers fusion between the vesicle and plasma membrane leading to neurotransmitter release. The neurotransmitter in the synaptic cleft then interacts with a receptor, or receptors, on the postsynaptic cell causing depolarization and thus propagating the signal. (Dodge and Rahamimoff, 1967; Katz and Miledi, 1970; Südhof, 2004) This is the process at its most simplistic however there are nuances, complexities and complications at every step with many of the key interactions still under debate.

In this work I examine the interactions between Ca^{2+}, synaptotagmin, as well as the $G\beta\gamma$ subunit of the 5-Hydroxytryptamine (5-HT) -1B receptor, and how these interactions participate in the modulation of fusion events. Due to the interconnectedness of so many protein-protein interactions it is crucial to understand many of the underlying mechanisms of synaptic transmission.

1.1.2   Docking, Priming, Exocytosis and Endocytosis

Release of neurotransmitter from synaptic vesicles (SVs) occurs over three steps: docking, priming and exocytosis. These steps are fluid and dynamic, placing hard borders between them is difficult, but it is useful to define them in order to establish a vocabulary for SVs exhibiting different properties. Vesicles are said to be docked when they are in close association with the plasma membrane in a readily reversible manner (Weimer and Richmond, 2005; Fernandez-Busnadiego et al., 2010). Although they are in close proximity to the membrane, they are not yet fusion competent, meaning they cannot immediately fuse in response to increasing $[Ca^{2+}]$ (Südhof, 2014; Weimer and Richmond, 2005). Docking requires a synaptic vesicle to approach the plasma membrane, prompting assembly of clusters of syntaxin-Munc-18 as well as the slow (1-2min) trafficking of Munc-13 and SNAP-25 to the site (Gandasi and Barg, 2014).

Munc-13 has recently been shown to be co-localized with all functioning release sites, making it absolutely essential for proper organization of the active zone (Böhme et al., 2016; Reddy-Alla et al., 2017; Sakamoto et al., 2018). The active zone scaffold protein Rab-3 Interacting Molecule (RIM) is essential for Munc-13 activity by undoing Munc-13 homodimerization (Betz et al., 2001). As its name suggests, RIM also interacts with vesicle associated GTPases Rab3 as well as Rab27, aiding in the recruitment of synaptic vesicles to the active zone. (Wang et al., 1997; Gracheva et al., 2008). Munc-13 and RIM form a protein scaffold with ∝-liprins, this protein scaffold is necessary for the proper functioning of active zones. (Aravamudan et al., 1999; Augustin et al., 1999; Richmond et al.,1999; Zhen and Jin, 1999; Schoch et al., 2002) The putative Ca^{2+} sensor for exocytosis, a Synaptotagmin, has also been shown to enhance the docking of synaptic vesicles in a Ca^{2+} dependent manner (Chieregatti et al., 2002). Once vesicles have docked, additional protein-protein interactions transition the vesicle into a primed state.

Primed vesicles are fusion competent. The physiological underpinnings of what makes a vesicle primed are still under debate. It appears that, by the action of regulatory proteins Munc-13 and RIM, partially zippered SNARE (Soluble N-ethylmaleimide Sensitive Fusion Attachment) complexes form and sit on the membrane waiting for a Ca^{2+} signal before undergoing exocytosis (Aravamudan et al., 1999; Augustin et al., 1999; Richmond et al., 1999; Betz et al., 2001; Koushika et al., 2001; Hatsuzawa et al., 2003, Fernandez-Busnadiego et al., 2010). The full priming of vesicles may happen through a series of protein-protein interactions such as these that progressively make the SV more likely to undergo exocytosis (Taschenberger et al., 2016).

Exocytosis occurs when the fusing of membranes results in the creation of a fusion pore through which neurotransmitter is released. The pore expands to the point it becomes indistinguishable from the plasma membrane itself or the pore closes (Breckenridge and Almers, 1987; Sharma and Lindau, 2018). Exocytosis occurs through several mechanisms: synchronous release which occurs rapidly after an action potential and is short lived, asynchronous release which is also evoked by an action potential but persists well after the action potential, and spontaneous release which is not evoked by an action potential. Rising $[Ca^{2+}]$ triggers synchronous release and utilizes vesicles in the primed state, known as the readily releasable pool (RRP). The RRP exists separately from a larger pool of reserve vesicles (2000-5000 in the lamprey) that do not exocytose in response to an action potential (Gerachshenko, 2005). Probability of any given SV undergoing exocytosis is low with only 10%-20% of SVs releasing neurotransmitter after a single action potential (Alabi and Tsien, 2012).

Endocytosis serves multiple functions. For one, endocytosis must occur in order to prevent infinite expansion of the plasma membrane by vesicle fusion. In addition, endocytosis provides a mechanism for replenishing the vesicle pool as well as clearing the active zone of previously used fusion machinery and relocalizing these proteins to vesicles or the plasma lemma as needed. (Heuser and Reese, 1973; Kononenko and Haucke et al., 2015). After

neurotransmitter release via full fusion, it takes tens of seconds before the synaptic vesicle can complete a classical cycle of clathrin-mediated endocytosis and be reprimed for release (Heuser and Reese, 1973; Ryan et al., 2003). In synapses within the central nervous system (CNS), the RRP is small, consisting of only 30-45 vesicles (Harata et al., 2001). The traditional, slow repriming of vesicles can limit the rate of synaptic transmission as the RRP is depleted. There are more rapid forms of recycling methods, dubbed kiss and run and ultrafast endocytosis (UFE), occurring over just 20-50 ms, which can be utilized to prevent vesicle depletion (Ceccarelli et al., 1972; Fesce et al., 1994; Watanabe et al., 2013). However, there is much disagreement and many unanswered questions about how, where and when these different forms of endocytosis occur. Synaptic activity and $[Ca^{2+}]$ may directly influence which form of endocytosis is used by Ca^{2+}/calcineurin-dependent dephosphorylation of dynamin among other factors (Armbruster et al., 2013; Wu et al., 2014; Kononenko and Haucke, 2015).

1.1.3   The SNARE Complex in Detail

Fusion of vesicles to the presynaptic plasma membrane requires the participation of an array of proteins and ions, including proteins known as the SNARE proteins (Südhof, 2013). The SNARE protein synaptobrevin (also vesicle associated membrane protein or VAMP) located on the vesicle twists with the plasma membrane-associated SNARES (t-SNAREs) forming the superficial structure known as the ternary SNARE complex. (Söllner et al., 1993; Hanson et al., 1997) By constructing isolated liposomes that lack their endogenous proteins it is possible to reincorporate proteins, such as SNAREs, into these isolated liposomes to determine if they are sufficient for membrane fusion; in isolation the formation of even one SNARE complex links two membranes and is sufficient for spontaneous liposome fusion. (Weber et al., 1998; Schuette et al., 2004; van den Bogaart et al., 2010)

SNARE complex formation occurs when synaptobrevin begins twisting, in the N to C terminal direction with the t-SNARE heterodimer of syntaxin-1 and SNAP-25 (Sutton et al., 1998; Fiebig et al.,1999; Sørensen et al., 2006). This zippering occurs at four homologous 60 residue coiled-coil domains known as SNARE motifs; one on each of the N and C terminal of SNAP-25 and one on each of the C terminals of syntaxin and synaptobrevin (Weimbs et al., 1997) These SNARE motifs form a twisted parallel four $\propto$-helical bundle known as the ternary SNARE complex. (Söllner et al., 1993; Hanson et al., 1997; Sutton et al., 1998).

Syntaxin-1 and synaptobrevin contain transmembrane domains that anchor them to the plasma membrane and vesicle membrane respectively (Teng et al., 2001, Betke et al., 2012) SNAP-25, however, does not have a transmembrane domain and is instead palmitoylated to the plasma membrane by four cysteine residues at the center of the molecule (Hess et al., 1992) While the majority of the cytoplasmic portions of Synaptobrevin and SNAP-25 are intrinsic parts of the fully formed ternary SNARE complex, for syntaxin-1, only the C-terminal directly participates. (Dulubova et al., 1999).

Although in liposomal fusion assays VAMP and t-SNAREs will form SNARE complexes without the action of additional proteins, in physiological conditions, the SNARE complex requires additional machinery to form and function (Weber et al., 2008). Multiple proteins, such as Munc-18, Munc-13 and $G\beta\gamma$, interact with SNAREs either individually or in complexes to modulate their formation and function (Hatsuzawa et al., 2003; Gerachshenko et al., 2005; Hammarlund et al., 2007). In addition, in order for continued synaptic transmission, ternary SNARE complexes within the plasma membrane are disassembled by NSF in an adenosine triphosphate (ATP) dependent manner following exocytosis. (Otto et al.,1997; Xu et al.,1998)

Sec1/Munc18-like (SM) proteins are essential for both the formation of SNARE complexes and for membrane fusion (Hata et al., 1993; Grote et al., 2000, Misura et al.,2000). The H_{abc} domain at the non-SNARE N-terminal of syntaxin-1 autonomously folds in on itself, covering the SNARE motif, and must unfold in order to form the ternary SNARE complex

(Fernandez et al., 1998; Teng et al., 2001). SM like proteins bind to the closed form of syntaxin, preventing formation of SNARE complexes prematurely (Misura et al., 2000; Gerber et al., 2008; Smyth et al., 2010). The opening of syntaxin requires the binding of Munc-13, which allows SNARE complexes to form (Hammarlund et al., 2007). After SNARE complex formation, Munc-18 switches its interaction from syntaxin to the SNARE complex itself and must remain associated with the complex, possibly acting to keep the complex from disassociating or being disassembled before fusion can occur (Dulubova et al., 1999; Richmond et al., 2001; Dulubova et al., 2007; Südhof and Rothman, 2009). The molecular mechanisms of SM protein association with syntaxin and the SNARE complex varies from system to system.

The partial formation of the SNARE complex in addition to the actions by its accessory proteins results in the priming of synaptic vesicles (Sørensen et al., 2006). Once vesicles are primed they are available to rapidly release neurotransmitter through a fusion pore in response to an action potential (Südhof, 2014; Weimer and Richmond, 2005). Some primed vesicles rest on the plasma membrane in a hemifused state, a stable intermediary step in which the outer lipid leaflet of the two interacting membranes fuse, but the inner leaflets remain separate (Chernomordik et al., 1998; Zampighi et al., 2006; Zhao et al., 2016). Hemifusion can lead to either full fusion or the membranes can revert back to two distinct entities: the vesicular membrane and plasma membrane (Chernomordik and Kozlov, 2008).

Although primed vesicles exist in an energetically favorable position to undergo fusion, spontaneous fusion is rare, occurring at an estimated rate of 0.01Hz at individual presynaptic boutons (Geppert et al., 1994; Kavalali, 2015). Primed vesicles may persist without undergoing spontaneous fusion due to the clamping function of complexin which tightly binds SNARE complexes; this keeps the vesicles fusion competent but prevents exocytosis until a sufficient Ca^{2+} (~1 mM) signal enables synaptotagmin to knock off the complexin clamp (McMahon et al., 1995; Ishizuka et al., 1995; Schaub et al., 2006; Tang et al., 2006). An additional, but not contradictory role, of complexin may be to hold the SNARE complex firmly together in a primed

state, overcoming the repulsive forces of bent unfused membranes in close proximity to one another (Chen et al., 2002). This, and many aspects of priming, hemifusion, and the action of complexin are not agreed upon.

SNAREs are critical to the fusion of synaptic vesicles. The full, tight zippering of SNAREs alters the shape of the fusing membranes. Part of the SNARE complexes role as a fusogenic complex seems to be to increase membrane curvature; lipid membranes with low curvature require more energy to fuse than those with a higher degree of curvature, by increasing membrane curvature SNAREs reduce the energy barrier for fusion. (Martens et al., 2007; Hernandez et al., 2012) The nature of the fusion pore is not fully elucidated. However, there is growing evidence that the fusion pore is not purely lipidic or proteinaceous but contains both lipids and protein domains, possibly including the transmembrane domains of synaptobrevin and syntaxin (Han et al., 2004; Bao et al., 2016, Sharma and Lindau, 2018). Upon full SNARE complex zippering, the C terminal of synaptobrevin is tilted towards the vesicular membrane forcing its transmembrane domain to become further embedded, aiding in pore formation (Risselada, 2011; Gao, 2012; Lindau, 2012)

Although it has been shown that one SNARE complex is sufficient for membrane fusion, it may be that in the complex physiological environment, the SNARE complex is competing with other processes that reduce its efficacy (van den Bogaart et al., 2010). For example, a quarter of the surface area of the lipid membrane of a synaptic vesicle is made up of the transmembrane domains of vesicle associated proteins, this alone may have a huge impact on the energy required for membrane fusion (Takamori et al., 2006). In physiological assays as few as 3 SNARE complexes are involved in the creation of a competent fusion pore, however, the number of SNAREs involved in each instance of fusion is highly variable. (Takamori et al., 2006; Sieber et al., 2007; Mohrmann et al., 2010, Gao et al., 2012) This is initially confounding when considering there are 70 copies of synaptobrevin on a typical synaptic vesicle and 15 copies of syt-1. (Takamori et al., 2006) This is a large number if only 1-3 SNARE complexes are

necessary for fusion, but this level of redundancy may assure that the SVs can readily dock and participate in repetitive docking events without being limited by synaptobrevin. There is also evidence to show that although only a few SNARE complexes are required for fusion, the kinetics of pore formation are faster when more SNAREs are present (Zhao, 2013). The abundance of SNAREs may serve to assist in rapid docking and priming.

1.1.4 Synaptotagmin is the Putative Calcium Sensor for Fast Synchronous Neurotransmitter Release

Liposomal fusion can be seen in liposomes containing either only v-SNAREs or only t-SNAREs, however, this fusion occurs much more slowly than the millisecond response seen physiologically (Sabatini and Regehr, 1996; Weber et al., 1998). The speed of synchronous release seen *in vivo* requires Ca^{2+} influx and detection. Once the SNARE complex has formed, Ca^{2+} influx in response to an action potential signals fast, synchronous release by interacting with the vesicular membrane associated protein synaptotagmin at cytoplasmic Ca^{2+} binding domains (Perin et al., 1990; Brose et al., 1992; Geppert et al., 1994; Fernández-Chacón et al., 2001; Mahal et al., 2002). Synaptotagmin has relatively low affinity for Ca^{2+} which ensures that it will only trigger release in response to the massive and brief increase in $[Ca^{2+}]$ that occurs during stimulation. Intracellular $[Ca^{2+}]$ is supralinearly related to neurotransmitter release, suggesting cooperativity between multiple Ca^{2+} interactions (Dodge and Rahamimoff, 1967). This cooperativity can be attributed to the binding of three to five Ca^{2+} ions (Dodge and Rahamimoff, 1967; Schneggenburger and Neher, 2000; Bollmann et al., 2000).

There are several isoforms of synaptotagmin. Synaptotagmin-1 (Syt-1) and to some extent syt-2, has been shown to be specifically important for fast evoked Ca^{2+}-dependent release (Geppert et al.,1994; Schiavo et al., 1998). Additional isoforms have been shown to impact neurotransmission, but either not in the same manner as Syt-1 or not as ubiquitously.

Syt-2 and Syt-9 evoke synchronous neurotransmitter release in some cell-types and Syt-7 may be involved in asynchronous release, short term plasticity, and Ca^{2+}-dependent replenishment of SVs (Xu et al., 2007; Wen et al., 2010; Bacaj et al., 2013; Liu et al., 2014; Jackman et al., 2016). Syt-1 is attached to synaptic vesicles by an N-terminal transmembrane domain (Perin et al., 1990). As $[Ca^{2+}]$ increases in response to an action potential, Ca^{2+} binds to Syt-1 at two cytoplasmic Ca^{2+} binding C_2 domains, the C_2A domain at the N-terminal and the C_2B domain at the C-terminal which are homologous to Ca^{2+} binding domains of protein kinase C (PKC). (Perin et al., 1990; Brose et al, 1992; Geppert et al., 1994; Fernández-Chacón et al., 2001). These domains are separated by a flexible nine residue linker region that is essential for the proper functioning of the protein. (Sutton et al., 1999, Bai et al., 2004) Exactly where and when the C_2A and C_2B domains bind is still up for debate (Betke et al., 2012). However, the C_2B domain appears to play a more dominant role in exocytosis (Nishiki and Augustine, 2004a). The C_2B domain interacts with anionic phospholipids and partially insert into the cytoplasmic monolayer of the plasma membrane while one or both of the C_2 domains interacts with the C-terminal of syntaxin-1 and the 9 C-terminal amino acids of SNAP-25 in SNARE complexes; this results in a dimpled plasma membrane due to lipid mixing that leads to membrane buckling as well as physical stress applied to the SNARE complex (Bennett et al.,1992; Davletov and Südhof, 1993; Chapman et al., 1995; Xu et al.,1998; Martens et al., 2007; Lai et al, 2011; Kyoung et al., 2011; Zhou et al., 2015). The C-terminal of SNAP-25 is essential for the tight zippering of the SNARE complex, if the final 9 C-terminal residues are removed, the resulting fusion pore is abnormal resulting in reduced conductance (Fang et al., 2008). This, coupled with the C-terminals importance in Ca^{2+}-Syt-1 binding suggests that Syt-1 may assist in this final tightening of the SNARE zipper that leads to exocytosis.

Although fast synchronous Ca^{2+} dependent release is mediated by Syt-1, ablation of Ca^{2+}-Syt-1 interaction does not affect the size of the RRP, nor does it negatively impact the slower asynchronous Ca^{2+}-dependent release that relies on different calcium sensors (Geppert

et al., 1994; Fernandez-Chacon et al., 2001; Voets et al., 2001). In fact, asynchronous Ca^{2+}-dependent release increases in Syt-1 knock outs (KOs) (Nishiki and Augustine, 2004b). Likewise, spontaneous Ca^{2+}-independent release increases when Syt-1 and its homolog Syt-2 are mutated (Littleton et al., 1993; Kochubey and Schneggenburger, 2011). These findings suggest that, not only does Syt-1 act as a critical Ca^{2+} sensor for fusion it also acts as a regulator of asynchronous and synchronous release and may act as a clamp on unevoked release. Recently it has been shown that for 10-50ms after an action potential, Syt-1 holds unfused vesicles in a tightly primed state via the action of the C_2B domain with the plasma membrane, thus increasing the likelihood of fusion during subsequent stimulation (Chang et al., 2018).

1.1.5   Voltage Gated Calcium Channels

1.1.5.1 Morphology of Voltage Gated Calcium Channels

Depending on the synapse, it has been estimated it only takes between one and five VGCCs opening to trigger release (Stanley, 1993; Shahrezaei et al., 2006; Bucurenciu et al., 2008) There are two main classes of VGCC, high voltage activated (HVA) and low voltage activated (LVA) channels (Armstrong and Matteson, 1985; Bean, 1985). Both HVA and LVA channels have a pore forming $Ca_v\alpha1$ subunit, which confers VGCC subtype. Only HVA channels contain the ancillary subunits $Ca_v\beta$, which is responsible for gating of $Ca_v\alpha1$ and trafficking to the cell membrane, and $Ca_v\beta2\delta$, which attaches to the extracellular membrane and may modulate release probability (Catterall et al., 2008, Hoppa et al., 2012; Simms and Zamponi 2014). The $Ca_v\alpha1$ subunit is made up of four transmembrane domains each with six individual membrane spanning helices, S1-S6. S4 confers voltage sensitivity, while the cation pore is formed from S5, S6 and the membrane bound P-loop between them (Yu et al., 2005). In

addition, the membrane domains have large linker regions that show diverse protein-protein interactions depending on channel subtype.

VGCCs that incorporate the $Ca_v\alpha 1$ subunit, $Ca_v 1$, are L-type channels which are gated in a slow voltage dependent manner and tend to appear postsynaptically - although they have been found to contribute to synaptic release at ribbon synapses as well as playing a critical role in Ca^{2+} dependent endocytosis (Perissinotti et al., 2008, Tippens et al., 2008; Rosa et al., 2012). VGCCs with the $Ca_v\alpha 1$ subunit, $Ca_v 2$, are P/Q ($Ca_v 2.1$), N ($Ca_v 2.2$), and R ($Ca_v 2.3$) type channels which all participate in fast evoked synaptic transmission requiring strong depolarization (Tsien et al., 1991; Simms and Zamponi, 2014). Of the channels associated with presynaptic terminals, N-type channels have the largest single channel conductance which allows them to generate large and fast Ca^{2+} transients, they, alongside P/Q-type are most common in typical synapses (Catterall, 2000; Weber et al., 2010). VGCCs with the $Ca_v\alpha 1$ subunit $Ca_v 3$ are T-type channels which are LVAs and thus are involved in low-threshold release events (Simms and Zamponi, 2014).

1.1.5.2 <u>Subtype Prevalence</u>

Although synaptic transmission in certain cell-types is governed by strictly one VGCC subtype, oftentimes release is controlled by a mix of N, P/Q and R-type channels with one subtype dominating over the others (Stanley, 1993; Wheeler et al., 1994; Mintz et al., 1995; Wu et al., 1999; Bucurenciu et al, 2008). In lamprey reticulospinal axons, all HVA channel subtypes except for L have been shown to participate in neurotransmitter release; with N-type channels dominating in adults and R-type dominating in ammocoetes (Krieger et al., 1999; Photowala et al., 2005). Experiments that attempt to elucidate single subtype participation in release have shown that blocking one subtype does not always have a linear effect on release,

suggesting that release at a given site can be governed by the compounding Ca^{2+} transient from multiple subtypes (Takahashi and Momiyama, 1993). The spatial relationship of the different VGCC subtypes may have substantial relevance to how their individual contributions control release.

1.1.5.3 <u>Modulation of Calcium Entry through Voltage Gated Calcium Channels</u>

Prolonged high intracellular $[Ca^{2+}]$ is toxic (Stanika et al., 2012). VGCCs have several inactivation pathways to prevent Ca^{2+} building to toxic levels. All VGCCs show voltage-dependent inactivation to protect the cell during prolonged depolarization, although how this mechanism works is not yet well understood (Simms and Zamponi, 2014).

VGCCs also show Ca^{2+}-dependent modulation under repetitive stimulation mediated by pre-associated calmodulin (CaM) binding to $Ca_{v}\alpha 1$ (Lee et al., 1999; Erickson et al., 2001; Mochida et al., 2008; Tadross et al., 2008; Minor et al., 2010; Nanou et al., 2016). Ca^{2+}/CaM-dependent regulation of VGCCs is highly variable depending on endogenous Ca^{2+} buffers, density and location of VGCCs, as well as the size and shape of neurons. CaM causes the inactivation of L-type channels through local Ca^{2+} transients, whereas P/Q channel deactivation appears to require global rises in $[Ca^{2+}]$ (Zamponi, 2003). P/Q channels have also shown Ca^{2+}-dependent facilitation by the action of calmodulin regulated by local transients (DeMaria et al., 2001; Lee et al., 2003; Chaudhuri et al., 2007). Ca^{2+}-dependent inactivation of P/Q channels has been observed in the calyx of Held and in overexpression assays, but is absent in Purkinje cells and superior cervical ganglion (SCG) neurons (Forsythe et al., 1998; Lee et al., 1999; Chaudhuri et al., 2005; Mochida et al., 2008). The open probability of N-type channels is modulated by a balance of the phosphatase calcineurin Aα (CNAα) and the kinase cyclin-

dependent kinase 5 (CDK5), which in turn is a determinant of release probability at individual synapses (Su et al., 2012; Ryan and Kim, 2013).

Syntaxin-1A and SNAP-25 are involved in the regulation of Ca^{2+} influx through P/Q and N-type channels by lowering the inactivation voltage of VGCCs (Bezprozvanny et al., 1995; Wiser et al., 1996; Zhong et al., 1999). Syt-1 is also capable of binding P/Q and N-type channels. As $[Ca^{2+}]$ increases syntaxin-1 tends to release from the VGCCs and associate with Syt-1 (Sheng et al., 1996,1997).

It has recently been shown that the waveform of an action potential is not uniform across a neuron and can be locally modulated (Hoppa et al., 2014; Rowan et al., 2014, 2016). This is relevant to Ca^{2+} influx as the reversal potential for Ca^{2+} influx is about 50 mV (Llinás 1991). At cooler temperatures, much of the Ca^{2+} influx occurs during the falling phase of the action potential in the absence of modulation (Llinás 1991). However, at warmer temperatures the amplitude of the action potential is reduced allowing Ca^{2+} influx to occur during the upstroke and peak of the action potential (Sabatini and Regehr, 1996). It has been shown that the depolarizing waveform is greatly attenuated by local potassium channels, which allows for earlier Ca^{2+} influx (Hoppa et al., 2014; Rowan et al., 2016). Due to the ability of potassium channels to effect the amplitude of an action potential, the presence and modulation of these channels will have profound effects on the movement of Ca^{2+} ions directly as well as through voltage dependent inactivation of VGCCs.

1.1.5.4 <u>Localization of Voltage Gated Calcium Channels to Active Zones</u>

Less than a millisecond after the onset of a presynaptic action potential, Ca^{2+} enters the presynaptic cell through VGCCs and triggers exocytosis which garners a response in the postsynaptic cell (Sabatini and Regehr, 1996). Because diffusion and signaling cascades are relatively slow and there are many endogenous Ca^{2+} buffers that could sequester

free Ca^{2+}, the tight temporal coupling of action potential and release implies that at least some Ca^{2+} channels are located in close proximity to the SNARE complex and that Ca^{2+} interacts directly with the fusion machinery (Schneggenburger and Neher, 2000; Bornschein and Schmidt, 2019).

The hypothesis that tight coupling leads to rapid release is bolstered by the recent discovery that the number of VGCCs seems to increase as the size of the synapse and RRP increase (Miki et al., 2017). However, not all VGCCs are tightly coupled to the release machinery. By utilizing the Ca^{2+} buffers EGTA (ethylene glycol-bis(2-aminoethylether)-N,N,N',N'-tetraacetic acid) and BAPTA (1,2-bis(2-aminophenoxy)ethane-N,N,N',N'-tetraacetic acid) populations of VGCCs can be identified that are either tightly coupled to the release machinery or located more distally (Bornschein and Schmidt, 2019). While the two chelators have similar affinity as represented by K_D, BAPTA's association rate (K_{ON}) is about 40 times greater than EGTAs (Naraghi and Neher, 1997; Neher, 1998). This means that BAPTA will quickly sequester incoming Ca^{2+} and prevent neurotransmitter release when VGCCs are tightly coupled. With its relatively slow K_{ON}, at moderate concentrations EGTA takes longer to buffer Ca^{2+} and is therefore unable to prevent neurotransmitter release at tightly coupled release sites. However, EGTA will prevent neurotransmitter release that is triggered by Ca^{2+} entry triggered at distal VGCCs (Neher, 1998). These studies confirm the presence of both proximal and distal populations of VGCCs in relationship to the fusion machinery.

Electron micrographs (EMs) at frog neuromuscular junctions show proteins, suspected to be Ca^{2+} channels, within 20 nm of synaptic vesicles (Harlow et al., 2001). In subsequent studies, this distance has ranged from 10-130 nm across different cell types with the distance between VGCCs and fusion machinery having physiological effects on release probability (P_r) and short-term synaptic plasticity (STP) (Bucurenciu et al., 2008; Schmidt et al., 2013; Arai and Jonas, 2014; Vyleta and Jonas, 2014; Nakamura et al., 2015; Pangrsic et al., 2015, Bohme et al., 2016). Release sites purely governed by distal VGCCs require more channels to evoke

release than release sites with tightly-coupled channels (Wang et al., 2009). There is emerging evidence that the coupling of VGCCs tightens as synapses mature, as well as evidence that coupling distance is subject to use-dependent modulation (Nakamura et al., 2015; Midorikawa and Sakaba, 2017).

The organized spatial localization of VGCCs and fusion machinery requires a number of protein interactions that target Ca^{2+} channels to active zone scaffolding. There appears to be large redundancy between active zone scaffolding proteins, knocking out any one protein usually does not have a large impact on synaptic transmission (Ghelani and Sigrist et al., 2018). This has made it more difficult to study the individual roles of proteins in trafficking VGGCs to release sites. However, a number of proteins that may be involved in this process have been identified.

The first protein discovered to position VGCCs was Bruchpilot (BRP) in flies (Kittel et al., 2006). However, its closest mammalian homologue ELKS, which binds the β subunit of VGCCs, does not appear to be as important for VGCC targeting (Liu et al., 2014). As mentioned earlier, RIM forms an active zone protein scaffold with Munc-13 and $\propto$-liprins which is essential for SV docking and priming (Aravamudan et al., 1999; Augustin et al., 1999; Richmond et al.,1999; Zhen and Jin, 1999; Schoch et al., 2002) In addition, RIM interacts with the C terminals of N and P/Q-type Ca^{2+} channels and is crucial for targeting VGCCs to active zones (Kaeser et al., 2011). RIM continues its role in localizing VGCCs by mediating channel density in an activity-dependent manner (Han et al., 2011). N and P/Q-type channel interactions with RIM-binding Protein (RBP) play a direct role in coupling evoked Ca^{2+} influx to neurotransmitter release (Hibino et al., 2002; Acuna et al., 2015). Extracellularly, the positioning of VGCCs may be influenced by their own subunit, $\alpha2\delta$, by interactions with neurexin (Hoppa et al., 2012; Wu et al., 2016; Tong et al., 2017).

In addition to these interactions, N and P/Q type channels interact with syntaxin-1 and SNAP-25 directly via synprint domains (Bennet et al, 1992; Sheng et al., 1994,1996; Rettig et eal.,1996) However, the synprint domain does not seem to traffic VGCCs to active zones; mutants lacking the synprint domain as well as invertebrates which naturally lack VGCCs with synprint domains are still able to localize VGCCs near SNAREs (Kaneko et al., 2002, Spafford et al., 2003; Rajapaksha et al., 2008). Instead, the synprint domain appears to be important for the close coupling of VGCCs to SNAREs after they've already been localized to active zones (Rettig et al., 1996). VGCC synprint domain binding of syntaxin-1 and SNAP-25 is modulated by phosphorylation via protein kinase (PKC) and Ca^{2+}/calmodulin-dependent protein kinase II (CaMKII) (Yokoyama et al., 1997). This may inhibit steady-state syntaxin-mediated inactivation of N-type channels (Jarvis and Zamoponi et al., 2001; Yokoyama et al., 2005; Catterall and Few, 2008)

1.1.5.5 The Role of Calcium Channels in Release Probability

The likelihood of SV release for a given action potential is related to $[Ca^{2+}]$ (Dodge and Rahamimoff, 1967; Heinemann et al., 1994). Ca^{2+} dependent evoked release of a single SV can occur with the opening of as few as one or two VGCCs with a peak local $[Ca^{2+}]$ transient in the range of tens of μM, however this peak is short lived (Schneggenburger and Neher, 2000; Shahrezaei et al., 2006). Synaptotagmin has a relatively low affinity for Ca^{2+} so the influx of Ca^{2+} is likely to activate Syt-1 without saturating it before Ca^{2+} diffuses or binds to additional endogenous Ca^{2+} buffers such as calbindin and parvalbumin (Schwaller et al., 2010; Walter et al., 2018). Synaptic strength increases as the number of VGCCs at the presynaptic terminal increases (Sheng et al., 2012). These findings suggest that the physical location of VGCCs in relationship to the fusion machinery can have profound effects on neurotransmission.

This can be seen in the ability for spatial relationships between VGCCs and SNAREs to effect P_r. VGCCs clustered within nanometers of the release machinery tend to increase initial P_r and display fast temporal coupling to action potentials, whereas Ca^{2+} entry through VGCCs at micrometer distance from the release machinery is more vulnerable to endogenous calcium buffers and may play a role in synaptic plasticity (Meinrenken et al., 2002; Buccurenciu et al., 2008; Ahmed and Siegelbaum, 2009; Christie et al., 2010; Goswami et al., 2012; Williams et al., 2012). Modeling has shown that, in the absence of additional downstream targets of Ca^{2+}, high frequency stimulation increases short term facilitation (STF) at synapses with distal VGCCs much more than it effects STP at synapses with tight spatial coupling to VGCCs (Böhme et al., 2018). This suggests that even without endogenous buffers, coupling-distance of VGCCs to SNAREs alone will confer physiologically relevant synapse heterogeneity.

Different synapses show different P_r evoked by a single action potential. Synapses with high initial P_r quickly exhaust the RRP after a single action potential and subsequent action potentials may show decreased neurotransmission, known as short term depression (STD), however some synapses are quickly able to recruit new SVs from the reserve pool to the release face, reducing STD (Dittman et al., 2000; Saviane and Silver, 2006; Hallermann et al., 2010a, 2010b). On the other hand, synapses with low initial P_r do not immediately deplete their RRP and often display STF during subsequent action potentials (Abbott and Regehr, 2004). Synapses with low initial P_r act as a filter favoring repetitive stimulation, while synapses with high initial P_r and subsequent STD favor intermittent stimulation (Atluri and Regehr, 1996; Rose and Fortune, 1999).

The rise in $[Ca^{2+}]$ increases subsequent P_r through a variety of mechanisms. It is tempting to credit this to increased $[Ca^{2+}]$ having increased action with Syt-1. However, diffusion and Ca^{2+} buffering quickly eliminates hyperlocal Ca^{2+} transients, making simple compounding of Ca^{2+} from a train of APs unlikely to increase Syt-1 interaction and therefore P_r. There are several additional proposed mechanisms for STF; high $[Ca^{2+}]$ aids in the recruitment of

additional SVs to the active zone, saturates endogenous Ca^{2+} buffers resulting in higher free

Ca^{2+} at active zones, as well as interacts with other slowly binding Ca^{2+} sensors such as Syt-7

that facilitate vesicle fusion and eventually gene transcription (Katz and Miledi, 1968; Atluri and

Regehr, 1996; Abbott and Regehr, 2004; Blatow et al., 2003; Millar et al., 2005; Simms and

Zamponi 2014; Vyleta and Jonas, 2014; Jackman et al., 2016; Jackman and Regehr, 2017; Miki

et al., 2017). In addition to a diacylglycerol-dependent effect on STP, Munc-13 may play an

important role in this Ca^{2+}-dependent STP. Munc-13 interacts with Ca^{2+} at Ca^{2+}/calmodulin and

Ca^{2+}/PIP_2 binding domains, the abrogation of which has dramatic effects on short-term synaptic

function (Rhee et al., 2002; Junge et al., 2004; Shin et al, 2010). Additionally, Munc-13 has

been shown to directly regulate Ca^{2+} influx on its own by inactivating VGCCs through its C_2B

domain (Calloway, et al., 2015).

It has been shown that even after the traditionally defined RRP has been depleted by 1s

of high frequency stimulation, it is still possible to evoke release via uncaging of intracellular

calcium (Wadel et al., 2007). This is most simply explained by these "reluctant" vesicles sitting

farther away from VGCCs and therefore not receiving the necessary high Ca^{2+} transient

necessary for release. It is also possible that the "reluctant" vesicles are tightly coupled to

VGCCs that have been inactivated through one of the afore-mentioned pathways. Indeed, in the

Calyx of Held and SCG neurons transfected with P/Q channels, rapid STD was inhibited when

VGCC modulation was disrupted (Mochida et al., 2008; Leal et al., 2012). It is likely that the

compounded effects of spatial organization as well as channel inactivation, endogenous

buffering of Ca^{2+}, and additional modulatory Ca^{2+} pathways all play a role in STP.

1.1.5.6 Calcium Influx through Single Channels

Work in our lab by Shankar Ramachandran on lamprey reticulospinal

axons (published in his thesis), showed that single Ca^{2+} channel conductance was extremely

low and that the probability of any given channel opening was likewise very low regardless of subtype. At a given synapse the average number of channels present was 51 (6 N-type, 6 P/Q-type, 12 R-type and 10 L-type), with a maximum of 68. For any given stimulus only 1-4 channels of each subtype open, however this was observed by alternative blocking of different subtypes. It is possible that physiological channel opening has different characteristics. However, peak $[Ca^{2+}]$ in response to a stimulus measured using Ca^{2+} dyes as chelators for entering Ca^{2+} was a paltry 2.2nM, which corroborates the notion of few channel openings. It is important to note that in the lamprey, these release sites are univesicular (Bourne et al., 2006, Brodin and Shupliakov, 2006; Schwartz et al., 2007). These findings suggest there is a high degree of redundancy in channels available to evoke release of a single vesicle. However, thus far, presynaptic Ca^{2+} transients observed with line-scanning confocal microscopy have appeared stable, but only short periods of recording were possible before either movement or photobleaching prevented further recording (Photowala et al., 2005). In addition, in single channel recordings with a 100ms step pulse, voltage-dependent and calcium-dependent inactivation were not observed. As this method only activates a single terminal, and thus does not produce a large intracellular Ca^{2+} transient, this implies the importance of global $[Ca^{2+}]$ for VGCC modulation.

1.1.6   Kiss and Run Fusion

Typically, the amount of neurotransmitter released for a given signal is quantal, meaning that a single quantum of neurotransmitter is loaded into synaptic vesicles and completely unloaded upon stimulation, the amplitude of the signal then directly relates to the number of vesicles that have undergone fusion (Heuser et al., 1979). However, it has been shown that vesicles throughout the total releasable pool (TRP) can make transient contact with the membrane (less than 0.9 s), forming a smaller fusion pore which only allows partial release of neurotransmitter before the fusion pore closes without undergoing classical clathrin-mediated

endocytosis (Klyachko and Jackson, 2002; Aravanis, 2003; Gandhi and Stevens, 2003; Ryan, 2003; Harata et al., 2006).

This type of fusion, known as kiss and run, lowers the concentration of neurotransmitter released into the cleft, but does not diminish the probability of release (Zakharenko et al 2002; Schwartz et al., 2007). The rate at which vesicles repetitively undergo kiss-and-run fusion also increases with higher frequency stimulation (Harata et al., 2006) However, even as the speed of kiss-and-run events increases, the overall type of vesicle fusion trends away from transient kiss and run fusion towards full fusion under high frequency stimulation (Harata et al., 2006, Zhang et al., 2009). The tendency for kiss and run fusion to predominate at low frequency stimulation may exist as a way to ensure there are a large number of vesicles primed and ready for release if and when a large demand for neurotransmitter release occurs. High frequency stimulation then allows for rapid and large release of neurotransmitter via full fusion. Although this will quickly deplete the RRP, it may be that this sacrifice is worth it in order to adequately respond to important signals.

Dynamin, typically associated with clathrin-mediated endocytosis, may act in such a way that prevents the full collapse of a kiss-and-run vesicle (Holroyd et al., 2002; Xu et al., 2008; Van Hook and Thoreson, 2012). Dynamin may not only prevent full collapse during transient fusion, it may also have an additional role in the closure of the fusion pore. Indeed, it has been shown in large dense core vesicles that dynamin is necessary for transient fusion pore closure (Chiang et al., 2014). However, this may not be applicable to synaptic vesicles as synaptic vesicles and large dense core vesicles do not transition through the same intermediary steps for pore closure (Klyachko and Jackson, 2002).

1.1.7   <u>G Protein Coupled Receptors</u>

Overstimulation of synapses can result in a depletion of vesicles and loss of neuronal transmission. In order to prevent this from happening a number of proteins act as inhibitors of unwanted release. One such class of inhibitors are inhibitory Gi/o-coupled G protein coupled receptors (GPCRs). (Betke et al., 2012). GPCRs are a class of protein with seven α-helical transmembrane domains whose extracellular N-terminal domains interact with specific ligands resulting in the activation of heterotrimeric guanine-nucleotide binding proteins (G proteins) by the intracellular C-terminal domains (Clapham and Neer, 1997). These G proteins are made up of α, β, and γ subunits which each have a number of isoforms (in humans: 27, 5 and 13 respectively). Regardless of which isoforms are present the β and γ units always exist as a dimer, functioning physiologically as a monomer. (Smrcka, 2008; Betke at al., 2012).

The action of inhibitory GPCRs is complex. The Gα subunit contains a GTPase as well as a binding domain for the G$\beta\gamma$ subunit (Betke et al., 2012). The GTPase on the Gα subunit uses the exchange of GDP to GTP in order to fuel the disassociation of itself from the G$\beta\gamma$ subunit which allows both subunits to go on to interact with their effectors (Oldham and Hamm, 2008). The Gα subunit isomers are grouped into four categories based on their function, $G_{12/13}$, $G_{i/o}$, G_q and G_s (Simon et al., 1991). Several of the Gα subunits are involved in regulation of exocytosis by triggering a cytoplasmic signaling cascade that results in the phosphorylation of important components of exocytotic machinery (Brown and Sihra, 2008). There is large heterogeneity in the number and type of G$\beta\gamma$ isoforms different cell types produce. This suggests that the isoforms of G$\beta\gamma$ have specificity but it is not yet clear how different isoforms achieve this specificity (Betke et al., 2014). The actions of G$\beta\gamma$ and Gα are modulated by G protein coupled receptor kinases (GRKs) which phosphorylate GPCRs, acting in a negative feedback loop, resulting in the inability of G$\beta\gamma$ and Gα to interact with its downstream effectors (Lodowski et al., 2003).

Postsynaptically, GPCRs have modulatory effects on synaptic transmission through G-protein activated inward rectifying potassium channels (GIRKs). Upon binding of neurotransmitter to the relevant GPCR, $G\beta\gamma$ activates GIRKs resulting in K^+ efflux which hyperpolarizes the postsynaptic cell and decreases its sensitivity to subsequent stimulation (Luscher et al., 1997). Presynaptic GIRKs are also activated by $G\beta\gamma$ (Meer and Buchanan, 1992; Ladera et al., 2008). However, under voltage clamping, inhibition by 5-HT is still observed (Van Hook et al., 2017). Indicating there are additional presynaptic inhibitory actions mediated by $G\beta\gamma$ such as inhibition of VGCCs and a direct action of $G\beta\gamma$ on fusion machinery (Clapham and Neer, 1993).

Presynaptic GPCRs distal to the active zone are not likely to directly affect proteins at the active zone, and are more likely to activate signaling cascades, however GPCRs located near the active zone can have direct effects on active zone proteins. In lamprey reticulospinal axons, 5-HT inhibition via $G_{I/o}$-coupled-$G\beta\gamma$ at active zones is thought to work by shifting the mode of fusion events from full fusion towards kiss and run by a direct interaction of $G\beta\gamma$ with SNAREs (Blackmer et al., 2001; Gerachshenko et al., 2005). It is important to note that in many systems, $G\beta\gamma$ binds to VGCCs and reduces Ca^{2+} entry during excitation, however this effect has not been observed in lamprey reticulospinal giant synapses which is the sole organism and synapse used for this work (Hille, 1994; Ikeda and Dunlap, 1999; Dolphin, 2003; Gerachshenko et al., 2005).

1.1.8 5-hydroxytryptamine Mediated Inhibition

Presynaptic activation of 5-HT_{1B}-$G_{i/o}$-coupled receptors causes severe reduction in postsynaptic EPSCs (Buchanan and Grilner, 1991). The inhibitory effects of 5-HT are rapid (within 20 ms of application) which suggests the inhibition is not due to activating one of many

GPCR signaling cascades, but rather through direct manipulation of active zone proteins (Gerachshenko et al., 2005). This decrease in synaptic transmission is caused by the binding of the G$\beta\gamma$ subunit to the C-terminal end of SNAP-25 disrupting Ca^{2+}-Syt-1 binding, resulting in a change of the fusion mechanism towards kiss and run (Blackmer et al., 2001, 2005; Gerachschenko et al., 2005 Photowala et al., 2006,. Schwartz et al., 2007). This has the physiological effect of reducing fictive motion in lamprey, playing a role in noradrenaline's nociceptive pathway, as well as being involved in inhibition at ribbon-type synapses such as cone photoreceptors (Schwartz et al., 2005; Delaney et al., 2007, Van Hook et al., 2017). In addition to these effects in the nervous system, the G$\beta\gamma$ inhibition of signaling appears to occur in non-neuronal cell types such as pancreatic β cells (Komatsu et al., 1995; Zhao et al., 2010). As intracellular $[Ca^{2+}]$ rises in response to just 3-5 action potentials at 50 Hz, Syt-1 outcompetes G$\beta\gamma$ for binding to the SNARE complex, relieving the G$\beta\gamma$ block (Yoon et al., 2007, Gerachshenko et al., 2009).

5-HT$_{1B}$ inhibition relies on particular spatial relationships with the SNARE complex. Typically, in hippocampal CA1 pyramidal neuron terminals, 5-HT activates 5-HT1b receptors to directly inhibit neurotransmitter release without altering Ca^{2+} entry, however, when SNARE complexes are disrupted by cleaving syntaxin with BoNT/C the specificity of G$\beta\gamma$ for the C-terminal of SNAP-25 is eliminated and subsequent 5-HT application results in inhibition of Ca^{2+} influx (Hamid et al., 2014). This coupled with the fact that modulation of VGCCs by G$\beta\gamma$ is membrane delimitated suggests it is not a lack of G$\beta\gamma$-VGCC binding capability that prevents the inhibition of VGCCs in lamprey, but rather there is a similar physical barrier provided by the SNARE complex itself as seen in hippocampal slices (Tedford and Zamponi, 2006).

1.2   <u>**The Lamprey as a Model**</u>

Lamprey (*Petromyzon marinus*) possess the most primitive vertebrate nervous system which makes them enticing for study of highly conserved neuronal mechanisms (Xu et al., 2016). The lamprey giant axon has been a key tool used by researchers to improve our understanding of exo-endocytotic processes, from early EM studies by Wickelgren to recent and continuing work from Brodin, de Camilli etc. Lamprey are an ideal model system for studying synaptic transmission due to the large, easily accessible giant reticulospinal axons they possess. The giant axons possess many *en* passant glutamatergic synapses with postsynaptic motor neuron targets throughout the entire spinal cord (Rovainen, 1974; Buchanan et al., 1987; Brodin et al, 1998; Gustafsson et al., 2002). Physiologically, these synaptic connections between reticulospinal axons and motor neurons provide rapid activation of trunk movements as well as displaying phasic bursting important for locomotion (Brodin and Shupliakov, 2000; Zelenin, P.V., 2011)

These axons run the length of the ventromedial and lateral columns. It is relatively simple work to excise the spinal cord and cut it into sections. The axons survive this procedure and seal up at the severed ends retaining their proper intracellular environment and function for days after being isolated (Buchanan, 2001). Throughout the spinal cord segments, reticulospinal axons do not branch, this coupled with their large diameter of 20-80μm makes them easily identifiable (Buchanan, 2001; Brodin and Shupliakov, 2006). Once the axons are identified they are also easy to manipulate. Their large size makes it simple to access the intracellular environment via micropipettes. In addition to providing stimulation, the micropipettes can serve as a vector for introducing peptides, toxins, dyes or other small soluble materials (Gustafsson et al., 2002; Brodin and Shupliakov, 2006).

Each postsynaptic neuron makes approximately 5-12 synaptic connections with presynaptic terminals along the surface of the reticulospinal axon (Photowala et al., 2005; Bleckert et al., 2012). Active zones are well separated making it easy to study them individually

(Gustafsson et al., 2002). Simple active zones with single release sites dominate in these axons, making up 80% of the total population (Bourne, 2005). The remaining active zones are deemed complex with multiple points of contact with the dendritic field, these active zones can either share a vesicle pool or each maintain distinct pools with vesicle size averaging 50nm (Gustafsson et al., 2002). Typical release events in the lamprey release one vesicle at a time (Schwartz et al., 2007).

Ca^{2+} transients in response to stimulation have been shown to occur at discrete hot spots throughout the reticulospinal axons by the use of Ca^{2+} sensitive dyes. These Ca^{2+} hotspots have been shown to be located at active zones by observing the overlap with phalloidin-labeled filamentous actin (F-actin) as well as seeing localization of FM 1-43 loaded vesicles (Photowala et al., 2005; Bleckert et al., 2012). Ca^{2+} influx at hotspots has a very quick baseline to peak rise time of 6 ms whereas the Ca^{2+} transients throughout the axon have a delayed onset of their peak concentration, with a relatively slow rise time and long decay demonstrating diffusion and buffering of Ca^{2+} within the axon (Photowala et al., 2005).

In the lamprey, presynaptic activation of $5\text{-HT}_{1B}\text{-G}_{i/o}$-coupled receptors by saturating doses of 5-HT causes a profound reduction in postsynaptic EPSCs to an amplitude ~20% of control without affecting the docking and priming of synaptic vesicles or Ca^{2+} influx. (Buchanan and Grilner, 1991; Blackmer et al., 2001; Takahashi et al. 2001; Gerachshenko et al., 2005). This is in part due to decreases in afterspike hyperpolarization (AHP) caused by 5-HT mediated inhibition of presynaptic GIRKs as well as the effect of $G\beta\gamma$'s competitive interaction with Syt-1 (Meer and Buchanan, 1992; Blackmer et al., 2001; Gerachshenko et al., 2005). In the lamprey 5-HT does not inhibit VGCCs as it does in other systems (Hille, 1994; Ikeda and Dunlap, 1999; Dolphin, 2003; Gerachshenko et al., 2005).

2. METHODS

2.1   Lamprey Sacrifice

"Experiments were performed on isolated spinal cords or spinal cords and brainstems of

lampreys. The animals were anesthetized with tricaine methanesulfonate (100 mg/l; Sigma-

Aldrich) and sacrificed by decapitation, and the spinal cord was dissected in an ice-cold saline

solution (Ringer's) of the following composition: 100 mM NaCl, 2.1 mM KCl, 2.6 mM CaCl2, 1.8

mM MgCl2, 4 mM glucose, and 5 mM HEPES, adjusted to a pH of 7.60. For patch clamp

experiments a thin layer of tissue was sliced from the ventral surface of the ventral horn using a

vibrating tissue slicer (Vibraslice). Slicing was performed in saline cooled by a Peltier effect

device on the slicing chamber. The tissue was transferred to a cooled and superfused recording

chamber." (Wells et al. 2012)

2.2   Electrophysiology

"Paired cell recordings were made between reticulospinal axons and neurons of the

spinal ventral horn. Axons of reticulospinal neurons were recorded with sharp microelectrodes

containing 1 M KCl, 5 mM HEPES buffered to pH 7.2 with KOH, and a SNAP-25 mutant protein

and BoNT/E mixture as defined below. Electrode impedances ranged from 20 to 50 MΩ.

Postsynaptic neurons were recorded with a patch clamp in voltage-clamp conditions. Patch

electrodes contained 102.5mM cesium methane sulfonate, 1 mM NaCl, 1 mM MgCl2, 5 mM

EGTA, and 5 mM HEPES, pH adjusted to 7.2 with CsOH. BoNt/E and proteins were pressure

microinjected through presynaptic microelectrodes using a Picospritzer II (Parker Hannifin,

Hollis, NH). Presynaptic recordings were made within 100 μm of the synaptic contact to ensure

protein diffusion to the region of the terminal, and this was confirmed by injection of

fluorescently tagged SNAP-25 protein in separate experiments. Light-chain BoNT/E (65g/ml;

List Biological Laboratories Inc., Campbell, CA) was stored at 20°C in 20 mM HEPES, 50 mM

NaCl, and 0.015 mM bovine serum albumin at pH 7.4. The buffered toxin was diluted as 5 μl

with 20 μl of 2 M KMeSO4 and 5 mM HEPES and 20 μl of solution containing one of three

different variants of SNAP-25. SNAP-25 proteins were stored at 20°C in a buffer containing 25

mM HEPES-KOH, pH 8.0, 150 mM KCl, 5 mM 2-mercaptoethanol, 0.5% n-octylglucoside, 1 mM

EDTA, and 10% glycerol. The buffered protein mixed with BoNT/E where appropriate was

diluted 1:5 with 2 M KMeSO4 and 5 mM HEPES. Microinjections of buffer solutions do not affect

the synaptic response or 5-HT inhibition." (Wells et al. 2012)

2.3   Imaging

Widefield fluorescence imaging was performed on an Olympus BXW 50 microscope with

an Olympus LUMPFL 40x 0.8 NA lens with a 3.2 mm working distance. Images were captured

via an air cooled Cooke sCMOS PCO.edge camera driven through a dual camera port Active

Silicon acquisition board at up to 100 Hz. An LED with peak emission at 594nm, with a band

pass filter narrowing the excitation bands to within 20 nm of the LED peak, was used to evoke

fluorescence excitation. LED intensity was controlled through current controlled linear power

supplies. Timing of LED illumination was controlled by TTL pulses generated by an Arduino

signaling solid state relays. Emission was detected through dichroic mirrors in the Olympus

BXW 50 band by band pass emission filters on a computer controlled filter wheel (Sutter

Instruments). The camera, emission and excitation paths were controlled using MicroManager

(Edelstein et al., 2010) and ImageJ (Schneider et al., 2012) software.

LLSM fluorescence imaging was performed on a microscope adapted from the Janelia

farms design (Chen et al., 2014). The light path for illumination is described at

https://www.aicjanelia.org/llsm-techspecs. Adaptations were made to the system to allow for

intact tissue recording. This includes a chamber that allows a cooled saline solution (Ringer's) to

be continuously perfused and allows access for a stimulating electrode. An in depth description of the microscope, including all adaptations can be found at https://lattice.anat.uic.edu/facilities.html.

Recordings were taken at rates of up to 1 kHz with a 50x50 μm field of view. Fluorescence excitation was evoked by a 560 nm solid state 300 mW MPB fiber laser. The beams were shaped through a spatial light modulator and mask projected through a Special Optics water dipping 0.65 NA lens with a 3.74 mm working distance. Emission was detected through a Nikon CFI Apo LWD 25x water dipping 1.1 NA lens with 63x magnification and a 3 mm working distance.

2.4   <u>Animal Treatment Compliance</u>

All experiments were performed per institutional guidelines of the University of Illinois at Chicago. These conform to guidelines of the Association for Assessment and Accreditation of Laboratory Animal Care (Appendix A).

3: IDENTIFICATION OF CRITICAL RESIDUES ON SNAP-25 for G$\beta\gamma$-MEDIATED INHIBITION OF EXCOYTOSIS

3.1   <u>**Introduction**</u>

As detailed in the previous sections, exocytosis is a complex, highly regulated process.

Initially, it requires the carefully orchestrated process of docking and priming by accessory

proteins as well as the core SNAREs. Once this has occurred, in order for fusion to take place,

VGCCs and additional ion channels as well as Ca^{2+} sensors such as syt-1 also must be present

and functioning properly. This sets the foundation for exocytosis but is still further regulated by

GPCRs. These then activate heterotrimeric G-protein complexes causing the dissociation of the

G$\beta\gamma$ subunit form the Gα subunit, which in turn acts on various effectors resulting in regulation

of synaptic transmission. (Clapham and Neer, 1997; Gautam et al., 1998; Vanderbeld and Kelly,

2000; Cabrera-Vera et al., 2003; Blackmer et al., 2005; Gerachshenko et al., 2005; Smrcka,

2008)

As discussed earlier, in many presynaptic systems one of the effectors of G$\beta\gamma$ are

VGCCs themselves, which in turn directly affect neurotransmission, however, we do not see 5-

HT mediated inhibition of VGCCs in the lamprey giant synapse. (Hille, 1994; Cochilla and

Alford, 1998; Ikeda and Dunlap, 1999; Takashi et al., 2001; Dolphin, 2003; Gerachshenko et al.,

2005) The ability of G$\beta\gamma$ to bind with the secretory machinery, particularly with the ternary

SNARE complex itself, has been well studied. Unlike the disparity in VGCC interaction with G$\beta\gamma$

between other organisms and the lamprey, lamprey G$\beta\gamma$ seems to interact with ternary SNARES

and result in inhibition of synaptic transmission as predicted biochemically as well as in

chromaffin cells, pancreatic cell and neurons. (Blackmer et al., 2001, 2005; Gerachshenko et

al., 2005; Betke et al., 2012., Photowala et al., 2006; Delaney et al., 2007; Yoon et al., 2007,

2008; Zhao et al., 2010; Zhang et al., 2011).

One of the primary candidates for G$\beta\gamma$ regulation of synaptic transmission is the C-

terminal end of SNAP-25. Nine residues from the C-terminal of SNAP-25 are cleaved by

BoNT/A (Schiavo et al., 1993; Binz et al., 1994). When botulinum neurotoxin A (BoNT/A) is

applied to reticulospinal axons, the ability for those axons to participate in 5-HT mediated inhibition is impaired (Blackmer et al., 2001; Gerachshenko et al., 2005). In addition to this evidence, Gβγ-mediated inhibition was also impaired by a 14-amino acid peptide that mimicked SNAP-25s C terminal (Blackmer et al., 2005; Gerachshenko et al., 2005). The 5-HT mediated inhibition involving Gβγ was confirmed to be at least in part due to an interaction of Gβγ with SNAP-25 by assays that showed Gβγ had reduced binding with SNAP-25 cleaved by BoNT/A compared to its binding with untreated SNAP-25 (Yoon et al., 2007; Zhao et al., 2010). However, SNAP-25 is not the only SNARE target of Gβγ. It has also been shown to bind directly to the ternary SNARE complex as a whole, the t-SNARE dimer, as well as the individual SNARE proteins: syntaxin-1A and synaptobrevin (Yoon et al. 2007)

The full-length sequence of SNAP-25 was scanned for binding interaction with $G\beta_1\gamma_1$ by cumulatively examining peptides 15 amino acids long. This resulted in the identification of eight residues that were important for $G\beta_1\gamma_1$-SNAP-25 binding. The importance of these residues was confirmed when fluorescently labeled $G\beta_1\gamma_1$ had decreased interaction with full length SNAP-25 mutated at these eight sites. In addition, experiments in lamprey reticulospinal axons showed that the mutated SNAP-25 did not participate in 5-HT mediated inhibition.

3.2   Experimental Results

3.2.1   Identifying Gβγ Interaction with Specific SNAP-25 Peptides

The C-terminus of SNAP-25 is critical for binding Gβγ (Yoon et al., 2007). The C-terminus of SNAP-25 is also crucial for interactions with Ca^{2+}-synaptotagmin during exocytosis (Xu et al., 1998). We sought to create a mutant SNAP-25 that did not bind Gβγ , but was still able to maintain normal interaction with synaptotagmin, in order to investigate Gβγ's role in normal synaptic transmission.

SNAP-25 was screened in short increments of 15 residues in order to investigate all binding interactions with G$\beta\gamma$. The full 192 residue sequence of SNAP-25 was broken down into this series of peptides by the peptide synthesizer, ResPep SL. The peptides were created on a membrane and subsequently exposed to G$\beta_1\gamma_1$. After G$\beta_1\gamma_1$ was washed off, a Gβ-specific antibody and a secondary chemiluminescent antibody conjugated with horseradish peroxidase (HRP) were introduced to the membrane (Fig. 1A)

Fig. 1B shows a representative image of this membrane once exposed to G$\beta_1\gamma_1$. Each spot on the membrane contained one of these 15 residue sequences. As opposed to creating a peptide of 1-15 and the next being 15-30, each peptide sequence was shifted only 3 residues from the previous sequence to ensure all functional zones would be captured. Peptides were generated in this way for the entirety of SNAP-25. Each individual peptide (1-64 in Fig. 1B) was tested three times for binding of G$\beta_1\gamma_1$. In addition, we performed our assay on four known G$\beta\gamma$ binding peptides [SIRK (SIRKALNILGYPDYD) (Scott et al., 2001), QEHA (QEHAQEPERQYMHIGTMVEFAYALVGK) (Weng et al., 1996), βARK (WKKELRDAYREAQQLVQRVPKMKNKPRS) (Koch et al., 1993)], (GID site: KSPLDAVLKRAATKKSRNDLI) (De Waard et al., 2005).] Gβ_1's extreme C-terminus was the epitope of the primary antibody and served as an additional positive control (positive controls shown individually in Fig. 1B) (Mazzoni et al., 1991). As a negative control, five spots on the membrane (65-69 in Fig. 1B) were left underivatized in order to show binding of the primary antibody to the membrane itself or G$\beta_1\gamma_1$'s nonspecific binding.
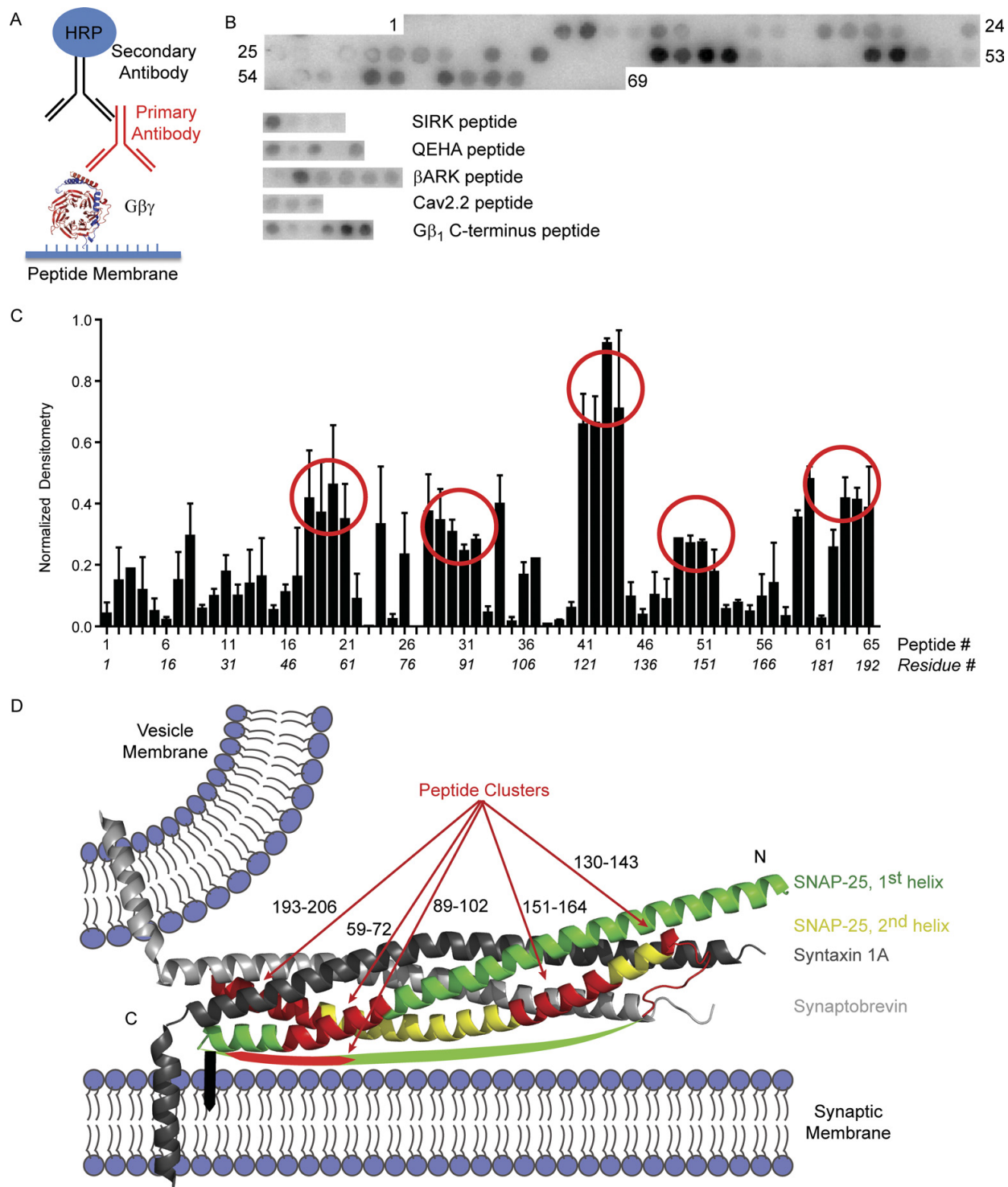
Figure 1. Screening of SNAP-25 peptides for interaction with $G\beta_1\gamma_1$. The premise of the antibody screen as a cartoon. Image of a membrane exposed to $G\beta_1\gamma_1$. Densitometry of the average of three membranes. The x-axis reflects both the peptide number according to B as well as the residue number of the first residue in each respective peptide. Representation of the peptides of interest (red) mapped onto the X-ray crystallography of the SNARE complex. Adapted with permission from Wells et al., 2012 (Appendix B).

We were able to determine several regions of SNAP-25 that could bind $G\beta_1\gamma_1$ by performing densitometry on images of the membranes. By normalizing these results to the brightest signal, we observed a clustering of binding over several adjacent peptides in the overlapping sequence of SNAP-25 we created, highlighted by the red circles in Fig.1B. Fig. 1D shows the location of these regions of interest on a model of a docked and primed vesicle with a representation of the quaternary structure of SNAP-25, syntaxin-1A, and synaptobrevin (Sutton et al., 1998). It is shown in this state because it is at this point in the life of a synaptic vesicle that $G\beta\gamma$ is expected to exert its inhibition on exocytosis (Blackmer et al., 2005; Yoon et al., 2007). Within SNAP-25, the $G\beta\gamma$ binding peptide sequences are shown in red. Three of these sequences of interest are clustered at the C-terminus near the transmembrane domains of the SNARE proteins, one of the C-terminal regions of interest is near the palmitoylation site of SNAP-25 on an unstructured arc. Two additional sequences are located on the N-terminus of the second helix of SNAP-25.

We subjected the sequences of interest to alanine-scanning mutagenesis and compared the resulting mutant peptides ability to bind $G\beta\gamma$ with that of wild type(WT)-SNAP-25. For each peptide in Fig 2A. each spot indicates the $G\beta\gamma$ binding capacity for that mutation. The first spot in each row indicates the WT sequence and each subsequent spot represents the mutation of one residue of the sequence to alanine beginning with the 1st residue and proceeding sequentially to the 14th. Residues that impaired the binding of $G\beta\gamma$ compared to WT were identified by averaging the results of three trials and performing densitometry normalized to the brightest spot (Fig 2B).
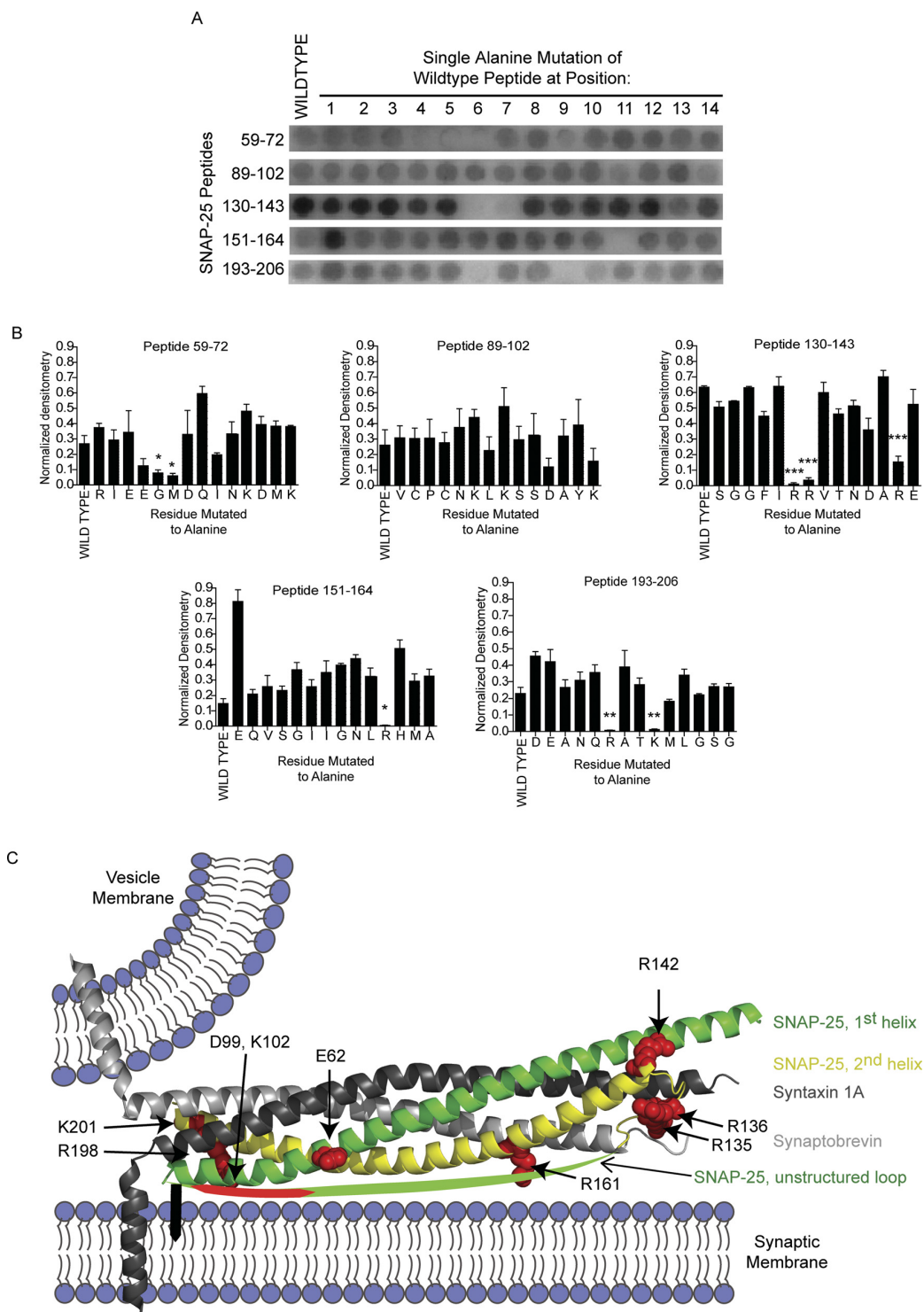
Figure 2. Alanine mutagenesis screening of SNAP-25 peptides that bind Gβγ. Representative image of the alanine screening for SNAP-25 peptides synthesized on a membrane. Densitometry across three membranes Means ± S.D. are displayed for each peptide and its mutants. (Student's *t* test; * *p* < 0.05; * * *p* < 0.01; * ** *p* < 0.001). On the X-ray crystal structure, residues in red are those that displayed a reduction in Gβγ binding when mutated to alanine. (PDB 1SFC). Adapted with permission from Wells et al., 2012 (Appendix B).

We were able to identify nine point-mutations (Table 1, mutated residues in boldface) that impaired Gβγ binding, seven lose a positively charged residue by this mutation and the remaining two lose a negatively charged residue.

TABLE I
SNAP-25 PEPTIDES FOUND IN SCREENING[a]

PEPTIDE	PEPTIDE SEQUENCE
59-72	RIE**E**GMDQINKDMK
89-102	VCPCNKLKSS**D**AY**K**
130-143	SGGFI**RR**VTNDA**R**E
151-164	EQVSGIIGNL**R**HMA
193-206	DEANQ**R**AT**K**MLGSG

[a] Adapted with permission from Wells et al., 2012 (Appendix B).

These nine peptides cluster in areas of known interest. It is known that Gβγ interacts with the C-terminus of SNAP-25, so it is parsimonious to find a cluster of these impaired residues occurring at this same region (Yoon et al., 2007). These residues are Arg198, Lys201, Asp99 and Lys102. The first two residues are located very near the end of the C-terminus, while the latter two are near the palmitoylation site of SNAP-25 in the linker region between the two helical domains.

Another cluster of residues (Gly63, Met64) that significantly impaired binding of Gβγ was identified in the first helix of SNAP-25 in the region where SNAP-25 interacts with syntaxin-1A and synaptobrevin. However, as we believe Gβγ interacts with the SNARE complex after

docking and priming have occurred and these residues would not be accessible at this stage,

we did not consider these residues to be good candidates for mutation of the full-length SNAP-

25.

3.2.2   <u>Adapting Point-mutations on Partial Peptides to Full Length SNAP-25</u>

Next, we sought to determine if the mutations in the partial peptides of SNAP-25

were able to similarly effect G$\beta\gamma$ binding in the full length peptide. As previously mentioned, the

two residues Arg198 as well as Lys201 have previously been implicated in the interaction of G$\beta\gamma$

with SNAP-25 and syntaxin (Yoon et al., 2007). As such, mutation of these two residues was

our first priority and the full length version of SNAP-25 after this mutagenesis was dubbed

SNAP-25(2A). We then began expansion of this mutation as detailed in Table 2.

TABLE II
SNAP-25 ALANINE MUTANTS[a,c]

Mutant Name	Residues of SNAP-25 Mutated	Log EC$_{50}$	EC$_{50}$	Max[b]
WT	Not Applicable	-6.45 ($\pm$ 0.20)	3.5×10^{-7}, (2.2×10^{-7}-5.6×10^{-7})	100 ($\pm$ 15)
2A	R198A, K201A	-6.18 ($\pm$ 0.13)	6.6×10^{-7}, (4.9×10^{-7}-8.9×10^{-7})	96 ($\pm$ 10)
3A	**E62A**,R198A, K201A	-5.93 ($\pm$ 0.12)	1.2×10^{-6}, (8.9×10^{-7}-1.5×10^{-6})	122 ($\pm$ 16)
4A	E62A, **D99A**, R198A, K201A	-6.12 ($\pm$ 0.13)	7.6×10^{-7}, (5.6×10^{-7}-1.0×10^{-6})	71 ($\pm$ 8)
5A	E62A, D99A, **K102A**,R198A, K201A	-6.08 ($\pm$ 0.15)	8.3×10^{-7}, (5.9×10^{-7}-1.7×10^{-6})	70 ($\pm$ 9)
6A	E62A, D99A, K102A, **R135A**, R198A, K201A	-5.97 ($\pm$ 0.08)	1.1×10^{-6}, (7.4×10^{-7}-1.2×10^{-6})	88 ($\pm$ 8)
7A	E62A, D99A, K102A, R135A, **R136A**, R198A, K201A	-6.12 ($\pm$ 0.09)	7.6×10^{-7}, (6.2×10^{-7}-8.9×10^{-7})	33 ($\pm$ 3)
8A	E62A, D99A, K102A, R135A, R136A, **R142A**, R198A, K201A	-5.87 ($\pm$ 0.12)	1.3×10^{-6}, (1.02×10^{-6}-1.8×10^{-6})	20 ($\pm$ 8)
9A	E62A, D99A, K102A, R135A, R136A, R142A, **R161A**, R198A, K201A	-6.36 ($\pm$ 0.23)	4.4×10^{-7}, (2.6×10^{-7}-7.4×10^{-7})	25 ($\pm$ 4)
N4A	R135A, R136A, R142A, R161A	-6.69 ($\pm$ 0.14)	2.0×10^{-7}, (1.5×10^{-7}-2.8×10^{-7})	44 ($\pm$ 3)

[a] Adapted with permission from Wells et al., 2012 (Appendix B).

[b] Max F1/F0 of the nonlinear regression, normalized to the max F1/F0 for wild-type SNAP-25.

[c] Data are means $\pm$ S.E.

We incorporated the additional C-terminal residues that effected G$\beta\gamma$ binding to create

the mutant SNAP-25s: 3A, 4A and 5A. Next we mutated the key N-terminal residues identified

via alanine mutagenesis on top of the C-terminal mutations to create the mutant SNAP-25s: 6A,

7A, 8A and 9A. Lastly a mutant with only N-terminal mutations was created: N4A. In Table 2,

the specific residue changes are listed for each SNAP-25 mutant we created, the boldface residues represent the additional residue targeted for each sequential mutant.

In order to determine the ability of these mutant SNAP-25 proteins to bind $G\beta_1\gamma_1$ we utilized the fluorescent probe MIANS (2-(4′-maleimidylanilino) naphthalene-6-sulfonate) which shows increased fluorescence when the environment becomes more hydrophobic as would be expected when levels of protein-protein interaction increase. $G\beta_1\gamma_1$ was purified and then labeled with MIANS. While keeping the MIANS- $G\beta_1\gamma_1$ concentration (20 nM) fixed we introduced sequentially higher concentrations of WT-SNAP-25. MIANS-$G\beta_1\gamma_1$ fluorescence increased with an EC_{50} of 0.35μM (Fig3A, Table2) while the C-terminal mutants 2A, 3A, 4A and 5A showed comparatively decreased affinity. Mutations 6A, 7A, 8A and 9A show a slight enhancement of baseline fluorescence but not to the degree of WT-SNAP-25. The N4A mutant with mutations limited to the N-terminal also showed impaired binding of $G\beta_1\gamma_1$ (EC_{50} 0.20μM) implying that there is an interaction between the N-terminal of SNAP-25 and $G\beta_1\gamma_1$, however, this is distinct from the interaction of $G\beta_1\gamma_1$ with the C-terminus.
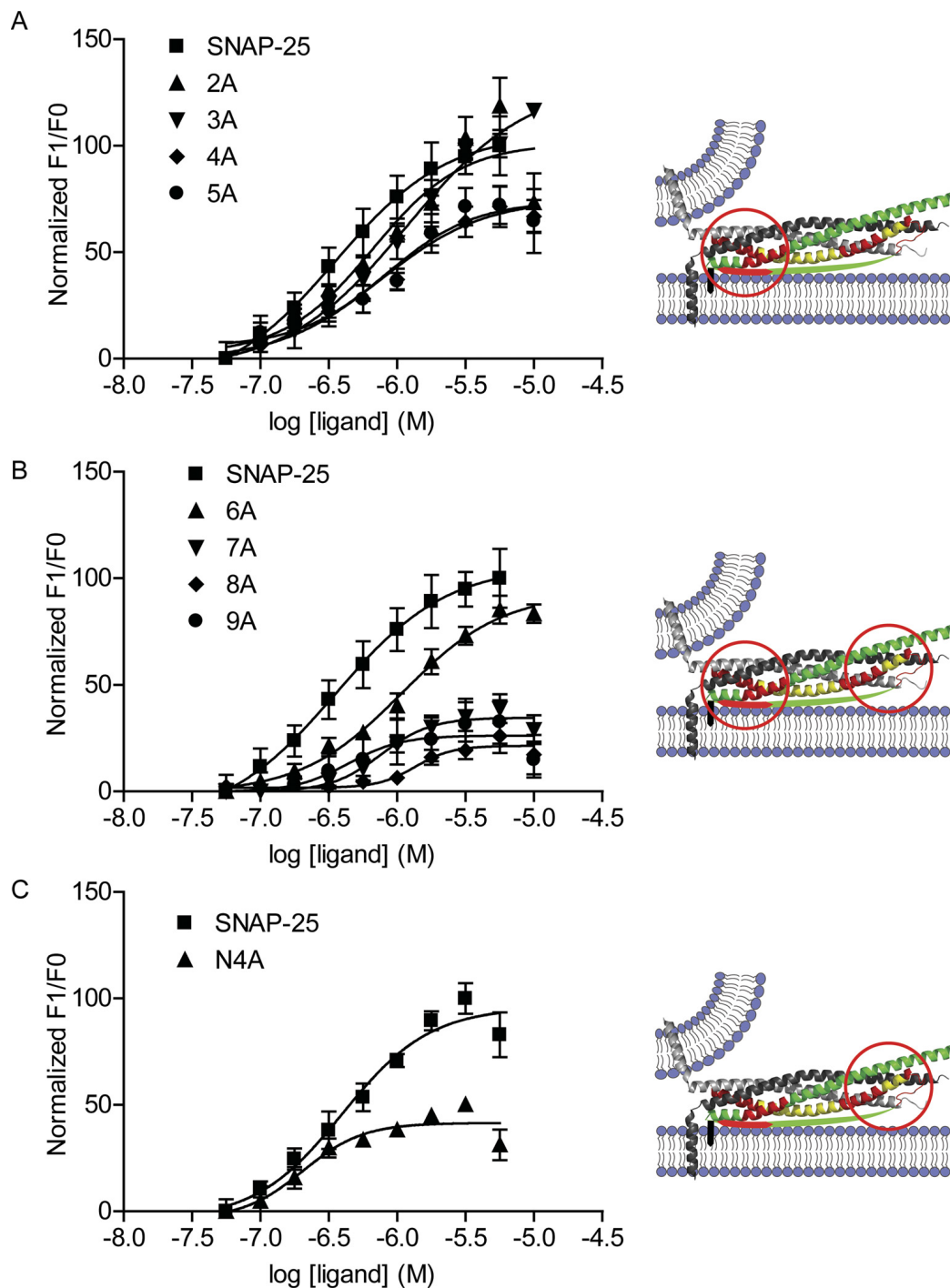
Figure 3. Binding of SNAP-25 and its alanine mutants to MIANS-labeled G$\beta\gamma$. Dose response curves for MIANSG G$\beta_1\gamma_1$ binding to SNAP-25. F1/F0 is the ratio of fluorescence of G$\beta_1\gamma_1$ in the presence of SNAP-25, corrected for intrinsic fluorescence of SNAP-25 and normalized to the highest fluorescence of WT SNAP-25-G$\beta_1\gamma_1$ binding. The red circle in the adjacent cartoons denotes the area on the SNARE complex where these mutated residues are located. Adapted with permission from Wells et al., 2012 (Appendix B).

3.2.3 G$\beta\gamma$ Interaction with SNAP-25 is Inhibited by a C-Terminal Peptide of SNAP-25

It is clear from these data that the binding of G$\beta\gamma$ to SNAP-25 is complex, not only occurring at the known C-terminal end but also interacting with N-terminal residues. Therefore, it is necessary to confirm which residues are essential with multiple approaches. We utilized short peptide sequences from WT-SNAP-25 at a constant concentration of 0.3μM alongside 20nM G$\beta_1\gamma_1$ labeled with MIANS. This tested the ability of these peptide sequences (1.5 mM) to inhibit G$\beta_1\gamma_1$ binding, of the five sequences tested, only SNAP-25(193-206), the peptide shown to be involved in 5-HT mediated inhibition, was able to reduce the binding efficacy of G$\beta_1\gamma_1$ to the full-length WT-SNAP-25 (Garachshenko et al., 2005). We mutagenized this peptide sequence with the R198A and K201A mutations and found that it did not prevent G$\beta_1\gamma_1$ from binding to full-length WT-SNAP-25, thus confirming our previous results (Fig. 4).

SNAP-25 Peptides (1.5 mM)
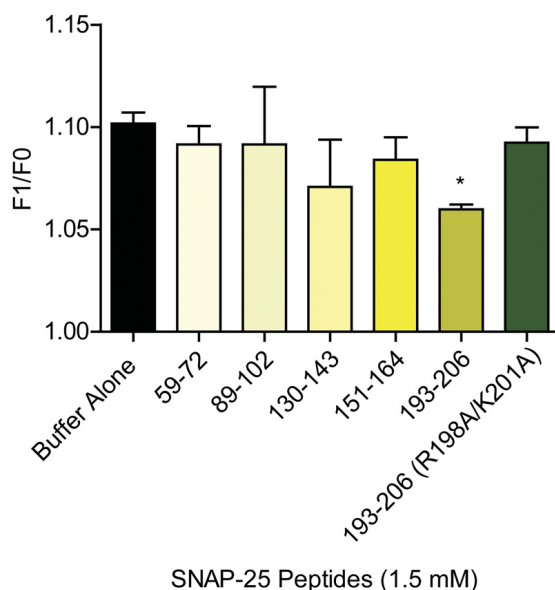
Figure 4. Inhibition of G$\beta\gamma$-SNAP-25 binding by SNAP-25 peptides. Only the unmutated C-terminal residue significantly inhibited binding (Student's *t* test, $p < 0.01$; *n* = 3). The mutated C-terminal residue with R198A and K201A no longer showed this effect (Student's *t* test, $p < 0.05$; *n* = 3). Adapted with permission from Wells et al., 2012 (Appendix B).

3.2.4   Synaptotagmin Interaction with Mutant SNAP-25

As discussed in the preliminary section of this work, synaptotagmin binds to the C-terminal end SNAP-25 in a Ca^{2+} dependent manner and triggers synchronous release of neurotransmitter. In order to ensure our mutations did not negatively impact this interaction, the glutathione S-transferase (GST) tagged WT-SNAP-25 as well as five GST-tagged mutant SNAP-25s (5A, 6A, 7A, 8A and 9A) were adhered to glutathione-Sepharose beads. Syt-1- C_2AB was then introduced to this preparation for one hour with either Ca^{2+} in the form of 1 mM $CaCl_2$ or with 2 mM EGTA which acts as a Ca^{2+} buffer. The EGTA condition allows us to test if the Ca^{2+}-independent binding of t-SNARES with synaptotagmin (Gerona et al., 2000; Mahal et al., 2002; Rickman and Davletov, 2003; Nishiki and Augustine, 2004) is effected by our mutations. Our assay shows the expected result of Ca^{2+} causing an increased binding between WT-SNAP-25 and syt-1 (Fig 5A). As evidence that our mutations did not disrupt the Ca^{2+}-dependent interaction between synaptotagmin and SNAP-25, we saw no reduction in the binding of the two proteins in the presence of $CaCl_2$ (Student's t test, $p < 0.05$) (Fig. 5B). The Ca^{2+}-independent interaction between syt-1 and SNAP-25 was partially reduced in some of our mutants. SNAP-25(6A) and SNAP-25(9A) had a reduction in binding of syt-1 compared to wt-SNAP-25 (Student's t test, $p < 0.05$ and $p < 0.01$ respectively). Arg161 is the residue mutated only by SNAP-25(9A), and since this mutant showed such a dramatic reduction in Ca^{2+}-independent binding of syt-1, this residue may mediate binding of the two proteins.

We made a mutant SNAP-25 with only the R161A mutation to test this theory. Densitometry normalization of a Western blot using syt-1-C_2AB for a pulldown assay showed that the R161A mutation significantly reduced the Ca^{2+}-independent binding of syt-1 (Student's t test, $p < 0.01$)(Fig. 5C). This residue does not appear to be critical for the Ca^{2+}-dependent binding of syt-1 and SNAP-25, as the results for the single R161A mutant were not significantly different than those of the entire SNAP-25 9A mutant (Fig. 5D).

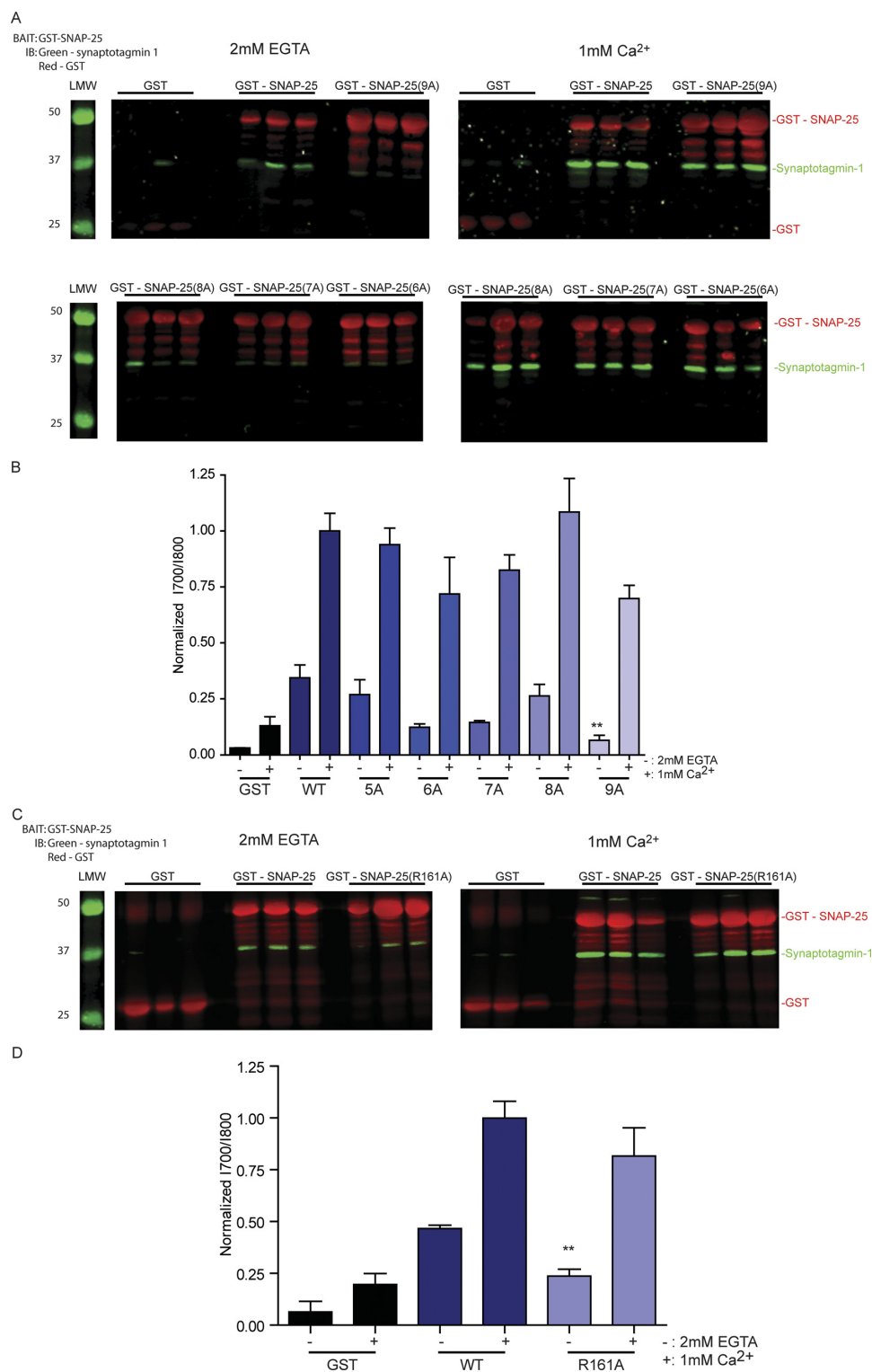Figure 5. Binding of SNAP-25 mutants to synaptotagmin-1 by GST pulldowns. Representative blots imaged with Odyssey for simultaneous quantitation of synaptotagmin-1 (green) and GST (red) signal intensity. IB = immunoblot; LMW = low molecular weight. The ratio of normalized synaptotagmin-1: GST signals averaged over three samples. ($^{**}p < 0.01$, Student's t test). Adapted with permission from Wells et al., 2012 (Appendix B).

3.2.5   **G$\beta\gamma$ Binding is Reduced When t-SNARES are Formed with SNAP-25(8A)**

In vitro, G$\beta\gamma$ binds not to SNAP-25 alone, but to the t-SNARE complex of SNAP-25 and Syntaxin-1A (Zurawski et al., 2019b). It was necessary to see if the impaired binding of mutants to SNAP-25 alone was repeated when binding the t-SNAREs as a unit. Once again using the MIANS-G$\beta_1\gamma_1$ assay, we showed that increasing WT- t-SNARE concentration increased G$\beta_1\gamma_1$ binding with an EC_{50} of 0.13 μM (*n*=4; 95% CI 0.067–0.26 μM) (Fig. 6). Full-length SNAP-25(8A) was produced with a single reaction in a vector that also contained WT-syntaxin-1A. By using this subcloning strategy that expresses both proteins at once, the efficient formation of t-SNAREs is promoted. The t-SNARE that is formed with SNAP-25(8A) (t-SNARE(8A)) showed identical fluorescence patterns to the WT-t-SNAREs (Fig. 6). However, it's affinity for G$\beta_1\gamma_1$ as tested by the MIANS assay was reduced to a level 4-times lower than that of WT (EC_{50} of 0.58μM) (n=4; 95% CI 0.47–0.70 μM).
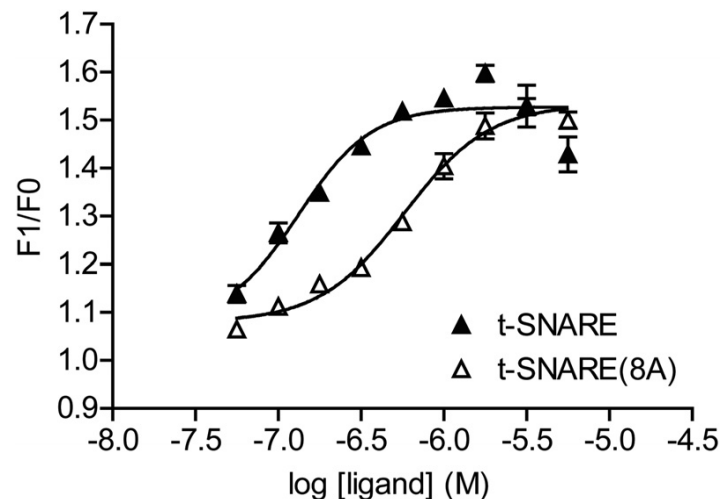

Figure 6. Binding of wild-type t-SNARE and SNAP-25 (8A) t-SNARE to MIANS-labeled G$\beta\gamma$. Adapted with permission from Wells et al., 2012 (Appendix B).

3.2.6   <u>Gβγ Mediated Inhibition is Reduced When SNAP-25(8A) is Incorporated into</u>

<u>SNARE Complexes</u>

We now wanted to investigate if the reduced affinity these mutants have for Gβγ

would result in a reduction of 5-HT mediated inhibition, as it has been shown that this serotonin

inhibition requires the Gβγ interaction we are studying (Blackmer et al., 2001; Gerachshenko et

al., 2005). I developed a novel approach for studying mutant SNAP-25 proteins. BoNT/E

cleaves the 26 C-terminal amino acids of SNAP-25 (Schiavo et al., 1993). A mutant version of

SNAP-25 with the Asp179Lys (SNAP-25(D179K)) mutation resists this cleavage by botulinum

toxin (Zhang et al., 2002). I tested if it was possible to inject this BoNT/E resistant peptide

directly into a lamprey reticulospinal axon and incorporate it into SNARE complexes.

Upon acquiring a paired reticulospinal axon and a postsynaptic ventral horn target

neuron, synaptic responses were generated by giving brief depolarizing presynaptic currents

(2ms, 1-3nA) at 30s intervals. After a baseline was established with at least ten responses, the

presynaptic cell was given a train of 300 stimuli at 1 Hz. This ensures that all vesicles that are

already docked and primed undergo exocytosis (Gerachshenko et al., 2005). The axon was

allowed to recover for 5 minutes after which EPSCs were recorded to ensure the pair was still

functioning. At this point, injecting BoNT/E completely eliminated the chemical component of

synaptic transmission, the remaining response is electrical (Fig. 7A). I then asked if it was

possible to rescue this loss of synaptic transmission by pressure pulse injection of the BoNT/E

resistant SNAP-25(D179K). A fluorescently labeled version of SNAP-25 confirmed that the

pressure injection successfully distributed SNAP-25 into the axons (data not shown).

Remarkably, this injection of mutant SNAP-25 was able to partially restore synaptic

transmission (Fig. 7B), implying that SNAP-25(D179K) is capable of replacing the endogenous

SNAP-25 in SNARE complexes after treatment with BoNT/E. A wash in of 1μM 5-HT inhibited

the postsynaptic response to 24 ± 13% of control. Therefore the mutation that instills BoNT/E

resistance to SNAP-25 has no effect on 5-HT-Gβγ-mediated inhibition.
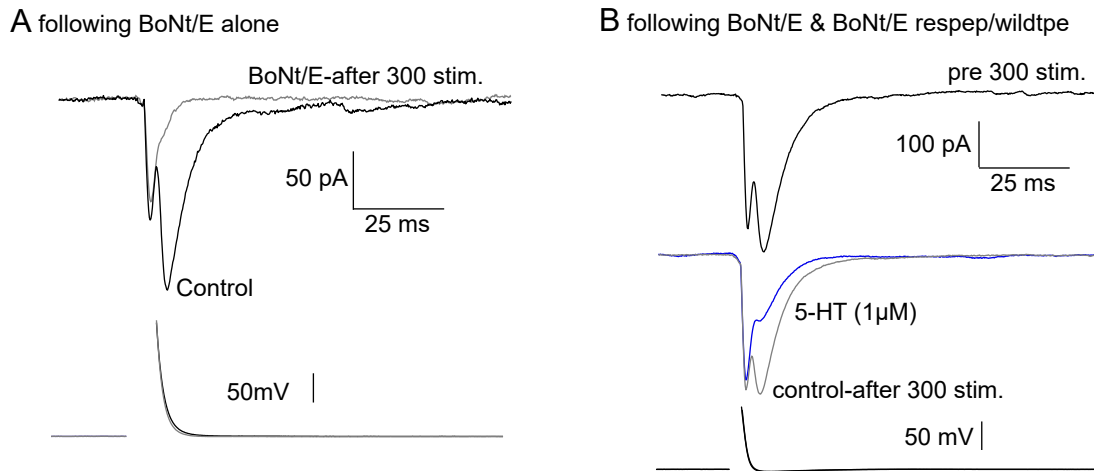
Figure 7. Injection of mutant BoNT/E resistant SNAP-25 rescues synaptic transmission after cleavage of endogenous SNAP-25. Each recording shown is the mean of at least 10 sequential EPSCs from before (black), after 300 stimuli (1 Hz, gray), and after addition of 5-HT (1μM, blue). The author of this thesis performed these experiments. Adapted with permission from Wells et al., 2012 (Appendix B).

A BoNT/E resistant version of SNAP-25(8A) (SNAP-25(D179K)(8A)), was pressure

injected in a reticulospinal axon following the same protocol to cleave endogenous SNAP-25

and exhaust the readily releasable pool. SNAP-25(D179K)(8A) rescued EPSC amplitude to 73 ±

9% of control (n = 5) (Fig. 8). This shows that SNAP-25(D179K)(8A) forms t-SNAREs with

endogenous syntaxin and supports vesicle fusion. However, unlike SNAP-25(D179K), 5-HT

mediated inhibition was significantly affected by replacing endogenous SNAP-25 with SNAP-

25(D179K)(8A) (EPSC amplitude 76 ± 5% of the pre-5-HT amplitude, p < 0.01 compared to

control inhibition) (Fig. 8). We conclude that the reduced affinity of Gβγ for SNAP-25(8A) directly results in the loss of 5-HT mediated inhibition by decreasing the action of the Gβγ subunit.
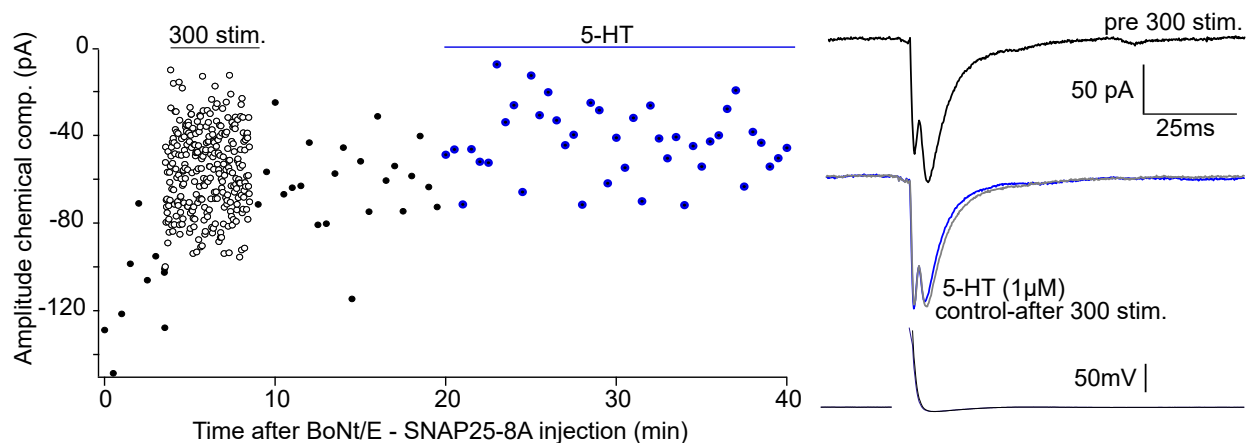
Figure 8. Effect of SNAP-25 (8A) on presynaptic inhibition in lamprey with 5-HT. Each recording shown is the mean of at least 10 sequential EPSCs from before (black), after 300 stimuli (1 Hz, gray), and after addition of 5-HT (1μM, blue). The author of this thesis performed these experiments. Adapted with permission from Wells et al., 2012 (Appendix B).

3.3   Discussion

We delineated several key residues on the C-terminal of SNAP-25 involved in the binding of Gβγ and through their mutation produced a version of SNAP-25 with reduced Gβγ affinity that did not disrupt the normal Ca^{2+}-dependent interaction with synpatotagmin-1. From injection of the protein into lamprey giant axons, it is also clear that versions of SNAP-25 that do not allow GPCR and Gβγ mediated inhibition (SNAP-25 (8A)) can fully support synaptic transmission. Combining injection of BoNT/E resistant mutants of these mutant SNAP-25s with BoNT/E provides extremely strong evidence that it is the interaction between SNAP-25 and Gβγ that mediates presynaptic inhibition.

We defined residues on the N-terminal of SNAP-25 that showed an affinity for G$\beta\gamma$, as well as a single residue that participates in the binding of syt-1 in a Ca^{2+}-independent manner. This large array of G$\beta\gamma$ domains implies there is more to the interaction of G$\beta\gamma$ and SNAP-25 than we previously thought. We have confirmed that G$\beta\gamma$ plays a regulatory role in the release of neurotransmitter from presynaptic vesicles. Experiments in lamprey reticulospinal axons showed that SNAP-25(D179K)(8A) is able to reconstitute SNARE complexes *in vivo* and participate in exocytosis. Serotonin inhibition of post-synaptic responses was dramatically relieved by SNAP-25(D179K)(8A), this result alongside the fact that t-SNARE(8A) showed a 4-fold reduction in G$\beta\gamma$ affinity confirms the crucial role SNAP-25 plays in G$\beta\gamma$-mediated inhibition of exocytosis.

It has previously been shown that G$\beta\gamma$ binding to the C-terminus of SNAP-25 has an important role to play in the regulation of synaptic transmission (Blackmer et al., 2005; Gerachshenko et al., 2005; Yoon et al., 2007; Zhao et al., 2010). This regulatory role of the G$\beta\gamma$ subunit of the GPCR-coupled 5-HT receptor can been abolished by the cleaving of endogenous SNAP-25 with BoNT/A (Gerachshenko et al., 2005). SNAP-25 whose nine C-terminal residues have been cleaved shows decreased affinity for G$\beta_1\gamma_1$ and the removal of the larger, 26 residue, end of SNAP-25 ablates G$\beta_1\gamma_1$ binding entirely (Yoon et al., 2007). In this study, we confirmed the critical role of SNAP-25's C-terminus by showing isolated peptides from that region were able to decrease binding of G$\beta_1\gamma_1$ to WT-SNAP-25 whereas the isolated peptides from the N-terminus were unable to reduce WT binding of G$\beta_1\gamma_1$ (Fig. 4).

The mechanism for G$\beta\gamma$'s inhibition of synaptic transmission has been shown to be a competition for binding to SNAP-25 with the C$_2$AB domain of synaptotagmin-1 (Blackmer et al. 2005; Yoon et al. 2007) Syt-1 has an increased ability to outcompete G$\beta\gamma$ for SNAP-25 binding when SNARE complexes are composed of SNAP-25 missing 9 C-terminal amino acids (Yoon et al., 2007). We identified the C-terminal residues Arg198 and Lys201 as important components

of this interaction. We also identified two additional residues, Asp99 and Lys102, that are close

to the C-terminal as well, but are not in the same domain as the previous two residues. When

these residues in addition to the first helical residue Glu62 (Fig. 2) are mutated to alanine in the

SNAP-25(5A) mutant the affinity for G$\beta\gamma$ sharply declines from 0.35 to 0.83 μM (Fig. 3).

In addition to the well-studied importance of the C-terminal of SNAP-25 for G$\beta\gamma$ binding,

we have shown there may be an additional region close to the N-terminal of SNAP-25 that are

also important for binding G$\beta\gamma$ (Fig. 3). As opposed to the reduced affinity caused by C-terminal

mutations, mutations at the four N-terminal residues identified by our screen lead to increased

affinity for G$\beta\gamma$ of 0.20 μM compared to 0.40 μM for WT with a decrease in maximal

fluorescence (Fig. 3C). When substitutions are made in both the C and N terminals, as in the 9A

mutant, affinity for G$\beta\gamma$ is once again reduced and the decrease in maximal fluorescence is

maintained (Fig. 3B).

When [Ca^{2+}] rises, the inhibition by G$\beta\gamma$ is relieved presumably because Ca^{2+}-

synaptotagmin has such a high affinity for SNAP-25 that it outcompetes G$\beta\gamma$ for binding (Yoon

et al., 2007). Interestingly, Ca^{2+}-synaptotagmin binding to SNAP-25 is not disturbed when the

G$\beta\gamma$ binding residues are mutated (Fig. 5). The residues on SNAP-25 necessary for syt-1

binding are also on the C terminus, but have been shown to be different than the residues we

have shown interact with G$\beta\gamma$ (Zhang et al., 2002). This may mean that the competition between

syt-1 and G$\beta\gamma$ is spatial rather than direct competition for the same binding sites. We were able

to reduce the Ca^{2+}-independent binding of syt-1 to SNAP-25 by mutating a single arginine

residue on the C-terminus of SNAP-25, this mutation had no effect on the Ca^{2+}-dependent

binding of syt-1 (Fig. 5).

The N and C-terminal G$\beta\gamma$ binding domains we discovered are approximately 90Å apart

whereas the length of G$\beta\gamma$ is no more than 70Å, therefore it does not seem that a single dimer of

G$\beta\gamma$ would be capable of binding to both the N and C-terminal of SNAP-25 at once (Sondek et

al., 1996; Sutton et al., 1998). It is possible that two individual Gβγ's bind to SNAP-25 at the same time, it is also possible that a single dimer bound at a low-affinity site will switch to the high-affinity site under certain conditions. It is also possible that Gβγ undergoes a conformational change while binding that causes it to lengthen beyond the 70Å that has been shown thus far and that additional length allows it to occupy both SNAP-25 binding domains simultaneously. Although no studies have been done on the crystal structure of Gβγ and SNAREs, studies on other SNARE proteins have not shown conformational changes when bound to various proteins (Sutton et al.,1998; Chen et al., 2002; Pobbati et al., 2004; Kümmel et al., 2011).

The alanine SNAP-25 mutants we created were able to form t-SNAREs with syntaxin-1A however, these mutant t-SNAREs were not able to bind Gβγ as well as unmutated t-SNAREs, confirming that SNAP-25 is an important component of Gβγ binding to the t-SNARE complex as a whole (Fig. 6). In addition, ternary SNARE complexes formed with mutant SNAP-25 in lamprey reticulospinal axons did not fully participate in serotonin mediated inhibition (Fig. 8).

We have shown that decreasing SNAP-25 affinity for Gβγ has functional consequences. However, to fully understand the role of Gβγ we must consider the complex protein-protein interactions known to occur at SNARE complexes. There are many modulators of SNAREs that organize and regulate the process of exocytosis such as complexin, Munc-18, and tomoysn (Hatsuzawa et al., 2003; Tang et al., 2009; Smyth et al., 2010). There is evidence that SNAREs alongside Gβγ are involved in modulation of other proteins, such as VGCCS (Jarvis et al., 2000; Davies et al., 2011). The discovery of an N-terminal binding domain on SNAP-25 suggests there may be an additional role for Gβγ besides competition with synaptotagmin. As an avenue for further study, we postulate that Gβγ may prevent conformational changes in SNARE proteins required for exocytosis. Syntaxin-1A itself exists in a closed position at rest and requires the action of accessory proteins to open the protein into a conformation that can form SNARE

complexes (Dulubova et al., 1999; Hammarlund et al., 2007; Gerber et al., 2008). In addition, a docked vesicle that is located in close proximity to the plasma membrane must become fully primed before it can undergo fast synchronous release, this requires zippering of SNARE motifs, and we propose this may be a good candidate for further study of Gβγ interaction (Rickman and Davletov, 2003; Nishiki and Augustine, 2004; Pobbati et al., 2006; Wu et al., 2012).

We have shown that our technique readily identifies residues on SNAP-25 that bind Gβγ and have a functional role in modulation of exocytosis. We will be able to utilize this same peptide screening to identify binding domains for Gβγ on the remaining SNARE proteins to further characterize Gβγ's role in this process. We will also be able to further study the mutant SNAP-25s we have created to examine the role of these residues in other protein-protein interactions.

In this study we identified two clusters of previously uncharacterized Gβγ binding residues on SNAP-25. Gβγ binding was reduced when we mutated these sites to alanine. With a novel technique for introducing mutant SNAP-25 directly to an axon via pressure pulse, I was able to show that the reduced affinity for Gβγ in SNAP-25(8A) led to a reduction in 5HT-mediated inhibition. This directly shows that Gβγ is crucial in the modulation of exocytosis mediated by the Gi/o-coupled-Serotonin receptor and provides strong evidence of its target on the SNARE protein SNAP-25.

4:   5-HT MEDIATED INHIBITON REQUIRES THE ACTION OF Gβγ ON THE EXTREME C-TERMINUS OF SNAP-25

4.1   <u>Introduction</u>

The Ca^{2+} dependent binding of Syt-1 to the plasma membrane as well as SNARE complexes is essential to overcome the spatio-kinetic barrier for fusion (Zhang et al., 2002; Bai et al., 2004; Lai et al., 2011). This interaction of Ca^{2+}-Syt-1 with SNAP-25 involves residues near the C-terminus (Zhang et al., 2002). We delineated in the previous chapter a novel binding region on the N-terminal of SNAP-25 as well as confirmed and further described $G\beta\gamma$ binding residues on the C-terminus (Gerachshenko et al., 2005; Yoon et al., 2007; Wells et al., 2012).

I utilized the BoNT/E resistant SNAP-25(D179K)(8A) mutant in *in vivo* paired cell recordings in order to show the lowered $G\beta_1\gamma_1$ affinity correlated to a decrease in 5-HT mediated inhibition when endogenous SNAP-25 was cleaved with BoNT/E (Wells et al., 2012). Through this work, I have helped to characterize the molecular interaction between $G\beta\gamma$ and SNAP-25 as well as begin to understand the functional implications of that interaction. However, the full physiological effects of Gi/o-coupled GPCRs and $G\beta\gamma$ inhibition is still not well studied. Although drugs targeting presynaptic GPCRs have been used to treat schizophrenia and anxiety, it is not known how this modulation actually relieves disease conditions (Swanson et al., 2005; Patil et al., 2007).

In order to broaden our studies on $G\beta\gamma$ to pathophysiology, it is crucial for us to generate an organism that has reduced 5-HT mediated inhibition while maintaining otherwise normal synaptic transmission. Knocking out $G\beta_1\gamma_1$ itself is not feasible as there are a total of 17 different subunits of $G\beta$ and $G\gamma$ (Betke et al., 2012). Therefore, the knockout of just one type of these proteins will most likely end in a redundant protein taking its place. Betke et al. (2014) have been able to identify which $G\beta$ and $G\gamma$ subunits are present in the human brain, and thus interesting for pathophysiological studies, it is still unclear which of these subunits specifically interact with SNAP-25 as we have studied. We also do not know all of the effectors of $G\beta\gamma$ so it would be difficult if not impossible to ascribe any abnormalities we saw to the loss of $G\beta\gamma$

binding to SNAREs. If we instead take the converse approach and knockout SNAP-25, we end up with a mutation that is lethal to neonates (Washbourne et al., 2002). It would then appear that the obvious candidate for a transgenic line of mice would be the previously studied SNAP-25(8A) mutant. However, each of the eight residues identified to be relevant for $G\beta\gamma$ binding is on a separate exon which makes creation of this mutant impractical if not unfeasible (Oyler et al., 1989). Due to these complications, it was necessary for us to find an additional SNAP-25 mutant that has reduced affinity for $G\beta\gamma$, results in reduction of 5-HT mediated inhibition, and is more conducive to mutation.

4.2   Experimental Results

4.2.1   Alphascreen Assay for $G\beta\gamma$ to SNAP-25

We developed the Alphascreen assay, which allowed us to use less material as well as increased the resolution of recombinant mouse SNAP-25 and $G\beta\gamma$ binding (Fig. 9). $G\beta_1\gamma_2$ (170nm) tagged with histidine was extracted from baculovirus treated Sf9 cells. These subunits then interact with SNAP-25 (20nM) that has been nonspecifically biotinylated. This biotinylation allows SNAP-25 to attach to a streptavidin-conjugated donor bead, and the histidine tag allows $G\beta\gamma$ to attach to a Ni-nitrilotriacetic acid (Ni-NTA) acceptor bead. 680 nm light causes dye associated with the donor bead to produce singlet oxygen. If the acceptor bead is in close proximity to the donor bead, the singlet oxygen will cause the acceptor bead to produce light in the 520-620nm range which can be detected by the plate reader. Due to the random distribution of beads, a small but negligible fluorescence is observed when 680nm of light is shone on beads containing no protein. Additionally, when the beads are alternatively conjugated with proteins that do not interact with SNAP-25 or $G\beta\gamma$ ($G_{\alpha i}$-GDP(170nm) or GST(20nm) respectively)

there is again negligible fluorescence. Thus, when the beads are conjugated with SNAP-25 and

G$\beta\gamma$ the intensity of 520-620nm light is directly related to the affinity of SNAP-25 for G$\beta\gamma$ (Fig. 9).
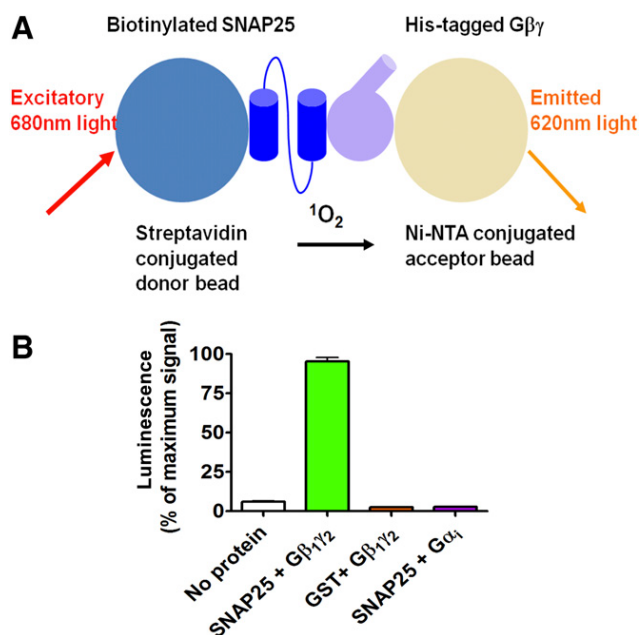
Figure 9. The Alphascreen G$\beta\gamma$-SNAP25 protein-protein assay. Cartoon of the assay and nonspecific binding controls for the Alphascreen assay (n = 3) presented as the mean $\pm$ S.E.M. Adapted with permission from Wells et al., 2012 (Appendix B).

4.2.2   SNAP-25(2A) Rescues Synaptic Transmission but Fails to Maintain 5-HT Mediated Inhibition

Although SNAP-25(8A) is not a good candidate for creating a transgenic mouse

model due to all mutations existing on separate exons, we do know it effectively reduces the

ability for G$\beta\gamma$ to mediate 5-HT-mediated inhibition of exocytosis. Therefore, it is logical to look

for a subset of these eight mutations that exhibits a similar reduction in 5-HT mediated inhibition

but are better candidates for creation of a transgenic mouse. We previously created a mutant

SNAP-25 (SNAP-25(2A)) that mutated only two of the C-terminal residues on SNAP-25(8A) (R198 and K201). This mutant had nearly half the affinity for G$\beta\gamma$, with no reduction in Syt1 binding (Wells et al., 2012).

To test if SNAP-25(2A) impaired the ability of G$\beta\gamma$ to inhibit synaptic transmission in the presence of 5-HT we created a BoNT/E resistant version (SNAP-25(D179K)(2A)). As described previously, a baseline was established in paired cell recordings prior to injection. I insured that BoNT/E was present in the axon by co-injecting 1mM Alexa 594 (Fig. 10A, 10Bi) and observing the resultant fluorescence throughout the axon including the synapses recorded from with the paired postsynaptic pipette. After injection and allowing 5 min for BoNT/E cleavage of endogenous SNAP-25 the RRP was depleted by a 1Hz train of 300 stimuli ensuring all remaining endogenous SNAP-25 is cleaved by BoNT/E (Gerachshenko et al., 2005; Wells et al., 2012). Subsequent presynaptic stimulation confirms that synaptic transmission is abolished (Fig 10Bii). I previously showed that after cleavage with BoNT/E, synaptic transmission could be recovered with BoNT/E resistant SNAP-25 and continue to participate in 5-HT mediated inhibition (Chapter 3, Wells et al., 2012). Injection of SNAP-25(D179K)(2A) rescued EPSCs abolished by BoNT/E to 81 $\pm$ 2% of control amplitude (*n*=5) (Fig. 10C). This implies SNAP-25(D179K)(2A) is able to reconstitute t-SNAREs for normal synaptic transmission. However, when 1μM 5-HT was applied to this preparation EPSCs were reduced to 33 $\pm$ 5% of the rescued amplitude (69 $\pm$ 4% of control amplitude, *n* = 4) (Fig. 10C). This is unlike what I saw with the 8A mutant, whereas SNAP-25(D179K)(8A) did not participate in 5-HT mediated inhibition, the 2A mutant still does. The affinity of SNAP-25(2A) for G$\beta\gamma$, while reduced compared to WT, was not as heavily impacted as the affinity for SNAP-25(8A) which may explain these results (Wells et al., 2012).
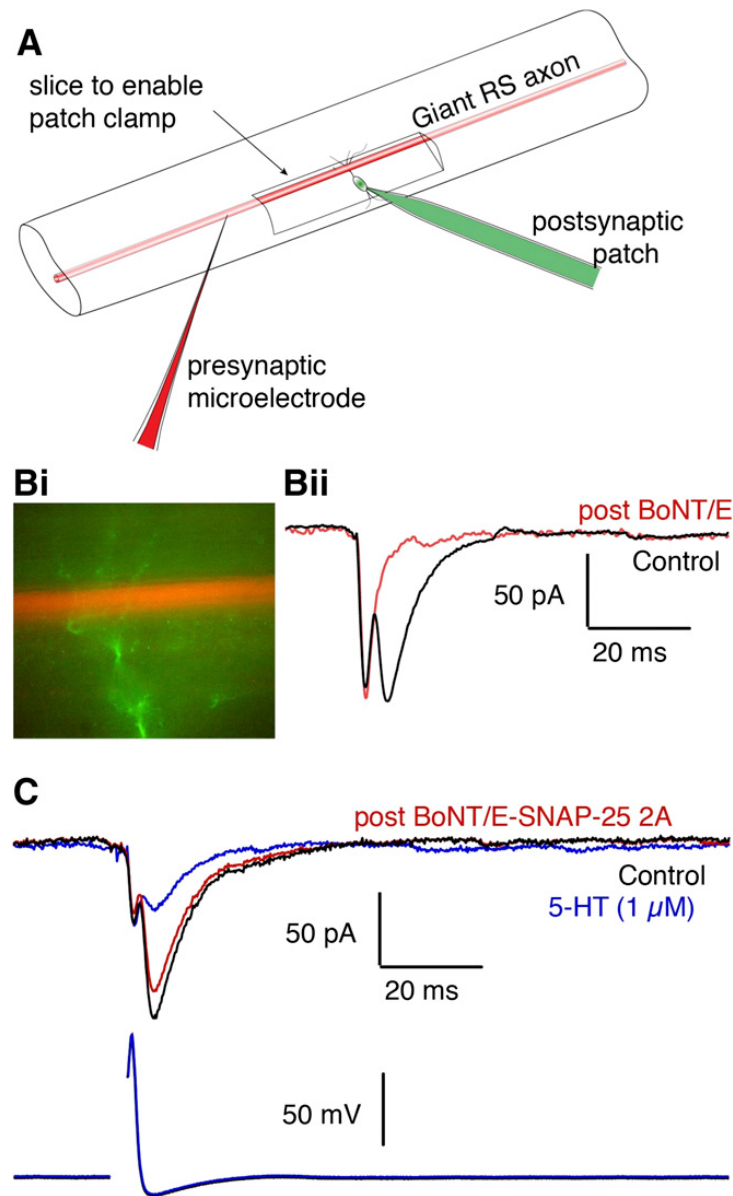
Figure 10. The SNAP25 2A mutant supports the inhibitory effect of 5-HT on glutamate release in lamprey spinal neurons. Diagram of assay principle. Image with the presynaptic terminal dyed red (Alexa 594) and postsynaptic dyed green (Alexa 488). Evoked EPSCs recorded from the postsynaptic cell before (black), after BoNT/E and depletion of RRP (red), and after addition of 5-HT (1μM) The author of this thesis performed these experiments. Adapted with permission from Wells et al., 2012 (Appendix B).

4.2.3 SNAP-25(2E) Fails to Rescue Synaptic Transmission

The mutated residues of the 2A mutant are both positively charged in the WT protein (Wells et al., 2012). We attempted a charge reversal on these same residues by substituting the negatively charge glutamic acid instead of the electrostatically neutral alanine in order to further disrupt the binding of G$\beta\gamma$. We dubbed this mutant SNAP-25(2E) and confirmed with the Alphascreen assay that this mutation negatively impacted G$\beta_1\gamma_2$ affinity (EC$_{50}$ = 116nm, 95% CI: 56-81nM compared to WT EC$_{50}$ = 67nm, 95% CI: 90-150nm) (Fig. 11A). This dramatic reduction in binding prompted us to create a BoNT/E resistant version of the mutant (SNAP-25(D179K)(2E)).
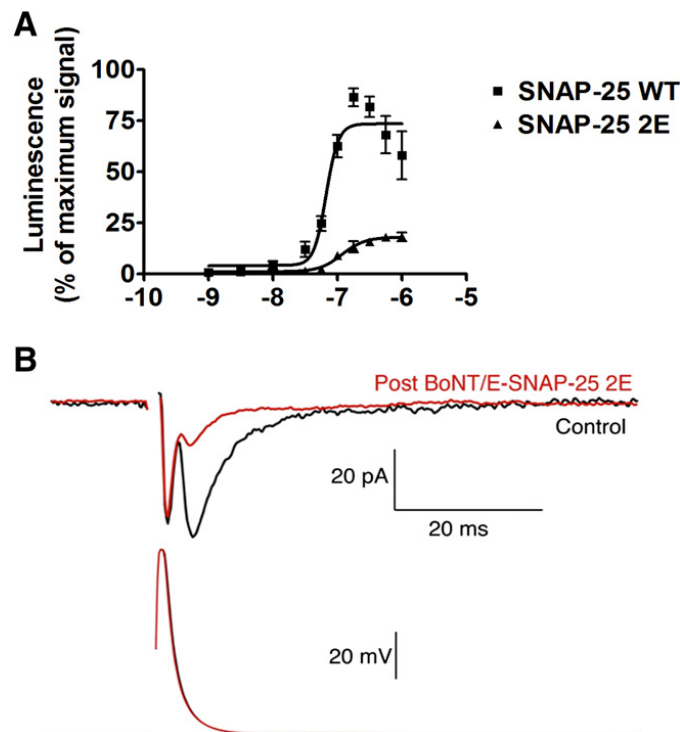
Figure 11. The SNAP25 2E mutant exhibits inhibited G$\beta\gamma$ -SNARE binding and inhibited neurotransmission. Alphascreen concentration-response curves normalized to the maximum luminescence signal obtained in each experiment. Example trace of paired recording showing the chemical portion of the EPSC is reduced. The author of this thesis performed the experiments in B. Adapted with permission from Wells et al., 2012 (Appendix B).

Using the same protocol as I did for the 8A and 2A mutants, I directly injected SNAP-25(D179K)(2E) into reticulospinal axons, depleted the RRP and cleaved endogenous SNAP-25. Unlike the previous two mutants, SNAP-25(D179K)(2E) was unable to significantly restore synaptic transmission (peak amplitude $23 \pm 10\%$ of control, $n = 2$)(Fig. 11B). The charge reversal at these two residues may have altered the binding characteristics of SNAP-25 as a whole and interfered with the regular Ca^{2+}-dependent binding of Syt-1 to the C-terminal of SNAP-25, thus resulting in the loss of synaptic transmission I have shown here.

We tested the interaction of SNAP-25(2E) and the Ca^{2+}-Syt1 by repeating the GST pulldown assay described in the previous chapter. In the presence of the C_2AB domain of Syt-1 (400nm), $5\mu g$ GST-WT-SNAP-25 and GST-SNAP-25(2E) were incubated for 1hr on glutathione-sepharose beads. As before, these preparations were done in either 1mM $CaCl_2$ or 2mM EGTA. Western blots and densitometry analysis show that, as expected, the Ca^{2+}-dependent binding of SNAP-25(2E) was significantly reduced, while the Ca^{2+}-independent binding was unperturbed (Student's t test, $p<0.001$ and $P<0.076$ respectively) (Fig. 12).
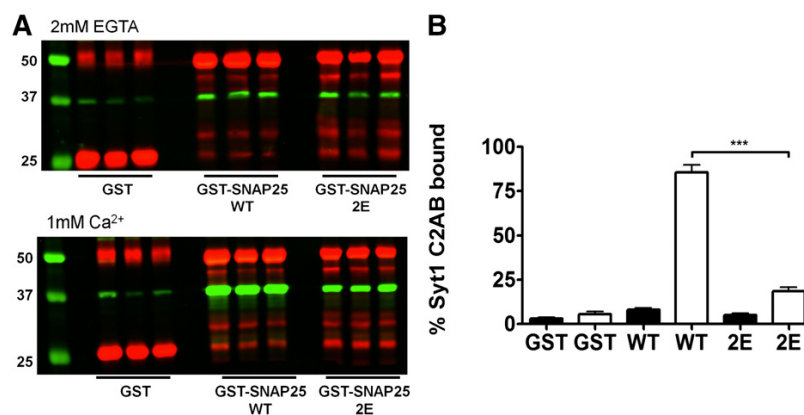
Figure 12. SNAP-25(2E) inhibits syt-1 Ca^{2+}-dependent binding. Western blot images of GST or GST-SNAP25 (red) and Syt1 C_2AB (green). In B, densitometry: each bar is the ratio of Syt1 C_2AB: GST or GST-SNAP25 present normalized to WT. White bars = 2mM EGTA, black bars = 1mMCa^{2+} represented as mean ± S.E.M. (two-tailed student's t test, ***$P <0.001$; $n = 3$) Adapted with permission from Wells et al., 2012 (Appendix B).

4.2.4   SNAP-25Δ3 Rescues Synaptic Transmission While Reducing 5-HT
Mediated Inhibition

It is possible that our initial method of using short peptide sequences to identify crucial residues for Gβγ binding to SNAP-25 failed to identify residues that may only show an effect in the full length protein. At this point we looked to previous research performed by Yoon et al. (2007) that identified a mutant SNAP-25 with the final 9 C-terminus residues cleaved (SNAP-25Δ9) which had reduced affinity for Gβγ and impaired 5-HT-mediated inhibition. However, this mutation also resulted in impaired zippering of SNARE complexes, which is undesirable for our purposes (Fang et al., 2008). We looked for a smaller truncation of SNAP-25 that would preserve normal synaptic transmission while still showing decreased affinity for Gβγ. SNAP-25Δ3 is one such smaller truncation that does not impair synaptic transmission (Criado et al., 1999; Gil et al., 2002). However, it's Gβγ binding properties have not previously been studied. By utilizing the Alphascreen assay we have shown that the maximum binding of SNAP-25Δ3 for $G\beta_1\gamma_2$ was reduced by a factor of 2, as well as well as displaying reduced $G\beta_1\gamma_2$ affinity (EC_{50} = 89nM, 95% CI: 75-105nM compared to EC_{50} = 76nM, 95% CI: 64-91nM) (Fig. 13A).

When a BoNT/E resistant version of SNAP-25Δ3 was injected into lamprey reticulospinal axons as before, SNAP-25Δ3 rescued synaptic transmission to a greater degree than any other mutant tested with EPSCs returning to 99±4% of control amplitude. When 1μM 5-HT was applied to the bath, the inhibition on EPSC amplitude was reduced, only impairing them to 48±11% of control (n = 3) (Fig. 13B).
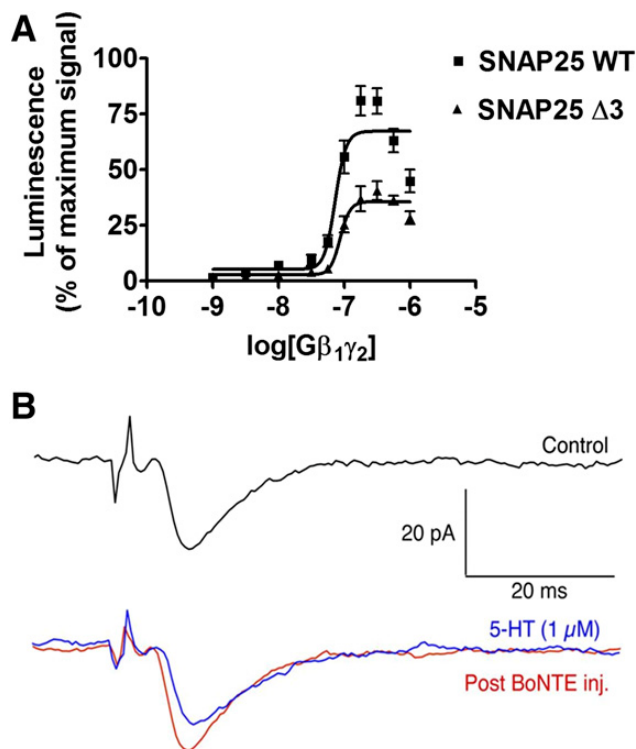
Figure 13. The SNAP-25Δ3 mutant shows impaired Gβγ binding and impaired inhibitory effect of 5-HT. (A) Alphascreen concentration-response curves normalized to the maximum luminescence signal obtained in each experiment. (B) Example trace of presynaptically evoked EPSCs before (black), after BoNT/E and depletion of RRP (red), and after application of $1\mu M$ 5-HT. The author of this thesis performed the experiments in B. Adapted with permission from Wells et al., 2012 (Appendix B).

Although SNAP-25Δ3 has not been shown to impair synaptic transmission in previous work (Criado et al., 1999; Gil et al., 2002) and was able to rescue transmission in our assay (Fig. 13), when we repeated the GST-pulldown assay with SNAP-25Δ3, Ca^{2+}-dependent binding of Syt-1 showed a 1.4-fold decrease (Fig 14). Ca^{2+}-independent binding of Syt1 was unaffected ($P = 0.065$). The Ca^{2+}-dependent binding of Syt-1 was also reduced in GST pulldown assays for SNAP-25Δ9 (1.8 fold reduction, Student's t test, $p < 0.001$) While the Ca^{2+}-independent binding of Syt-1 was once again unaffected ($P = 0.065$)
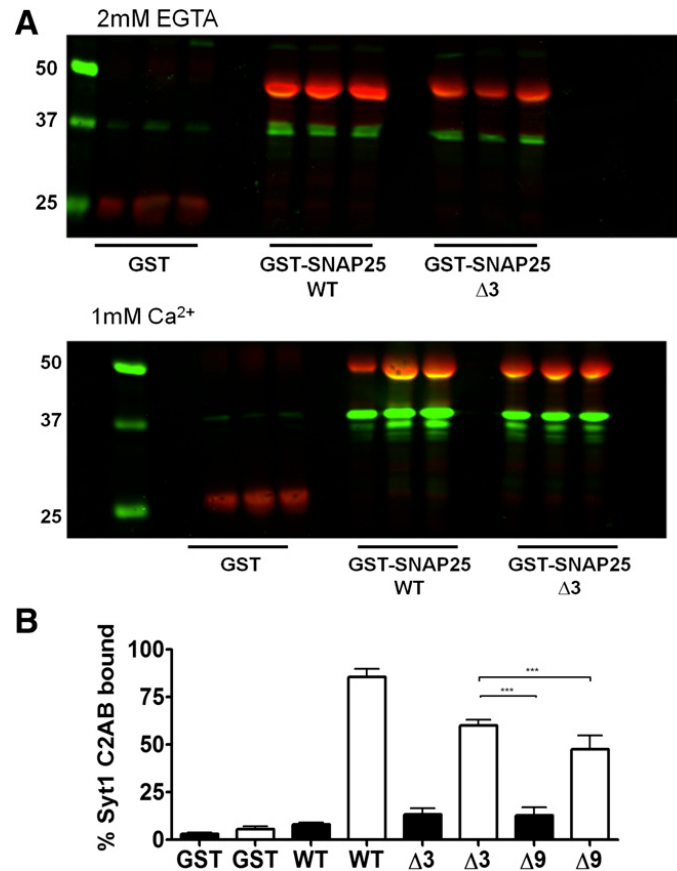
Figure 14. Syt1 calcium-independent binding is slightly reduced in the SNAP-25Δ3 mutant. Western blot images of GST-pulldown assay as in Fig. 12. SNAP25Δ9 immunoblot is not shown. In B, Densitometry for Syt1 C_2AB pulled down by GST-SNAP25 WT, Δ3, or Δ9 in the presence of 2mM EGTA (white bars) or 1 mM Ca^{2+} (black bars). Measured by two-tailed Student's t test (*$P < 0.05$; **$P < 0.01$; ***$P < 0.001$; $n = 3$). Adapted with permission from Wells et al., 2012 (Appendix B).

4.3   Discussion

Our initial results from SNAP-25(2E) suggested that R198 and K201 were important for Ca^{2+}-dependent Syt1 binding, however, the change of residues from positively charged to negatively charged may affect the entire C-terminal's binding capabilities. This is evidenced by the less extreme mutation of these residues to alanine in the 8A mutant not showing a reduction in Ca^{2+}-dependent Syt-1 binding (Wells et al., 2012). Although I was unable to show R198 and K201 were crucial for 5-HT mediated inhibition with alanine mutations, and the 2E mutation

almost completely abolished exocytosis. As an alternative, we could produce single mutations at R198 and K201 to glutamic acid to determine the role these residues play since the double mutation causes such a drastic reduction in Gβγ affinity (Fig. 11). However, R198E, R198Q, and K201E mutants have been studied and exhibit a reduction in the frequency and kinetics of exocytosis as well as lengthening the amount of time the fusion pore remains open (Gil et al., 2002; Sorensen et al., 2006; Fang et al., 2015). We were able to offer a possible explanation for these deficiencies by performing GST-pulldown assays of SNAP-25(2E) and the Ca^{2+} binding domain of Syt-1 that showed reduce binding between the mutant protein and Syt-1. These previous studies as well as our own research tells us that a mutant made with R198E and/or K201E would likely result in defects in synaptic transmission and thus would not be appropriate for our purposes as we require our transgenic animal to exhibit normal exocytosis.

M202 and L203 have also been shown to have relevance in exocytosis but were not identified in our screen for Gβγ binding (Criado et al., 1999; Gil et al.,2002). M202 is important for fast synchronous release and L203 plays a role in the latter stages of exocytosis (Gil et al., 2002; Sorensen et al.,2006) The SNAP-25Δ3 mutant leaves these key residues intact as well as the residues important for exocytosis that were mutated in the 2E mutant (R198 and K201)(Fang et al., 2015). I confirmed previous studies that showed the final 3 C-terminal residues, truncated in SNAP-25Δ3, are not required for normal synaptic transmission (Criado et al., 1999). However, I also demonstrated that SNAP-25Δ3 reduced 5-HT mediated inhibition compared to WT, likely due to its reduced affinity for Gβγ and therefore reduced Gβγ competition with Ca^{2+}-Syt1 for binding. BoNT/A truncates SNAP-25 by 9 C-terminal residues and reduces 5-HT mediated inhibition (Schiavo et al., 1993). The SNAP-25Δ9 mutant which mimics the action of BoNT/A, shows decreased Ca^{2+}-dependent binding of Syt1, and a reduction in neurotransmitter release (Gerona et al., 2000; Gil et al., 2002; Tucker et al., 2004) In addition, the 9 C-terminal residue truncation removes a phosphorylation site involved in

exocytosis and a residue involved in forming SNARE complexes (Schiavo et al., 1993; Shimazaki et el., 1996). SNAP-25Δ3 maintains these important residues. For these reasons, SNAP-25Δ3 is a good candidate for obtaining a mutant that would allow us to study the role of Gβγ binding *in vivo*. We can generate this mutant by using CRISPR/Cas9 to introduce the Δ3 mutation into the WT-SNAP-25 transcript.

However we do not settle on SNAP-25Δ3 without reservations. The residues truncated in this mutant were not shown to be important for Gβγ binding in our previous work (Wells et al., 2012) A downfall of alanine-scanning-mutagenesis is that it can overlook residues with similar properties to alanine. In addition, our use of short peptide sequences to probe for Gβγ binding may miss Gβγ binding domains that require higher order structure. In addition, this model will not allow us to explore the previously identified N-terminal binding site of Gβγ that we discovered in earlier work but have not studied electrophysiologically (Wells et al., 2012). SNAP-25(8A) mutated residues at both the N and C-terminal resulting in the highest degree of interference with 5-HT mediated inhibition of the mutants tested (Wells et al., 2012). It can be inferred that the full action of 5-HT mediated inhibition may require both N and C-terminal residues. The action of Gβγ on N-terminal SNAP-25 residues may be involved in synergistic inhibitory interactions with VGCCs by assisting Gβγ binding to the N-terminal of syntaxin-1A (Stx1A) and thereby mediating Ca^{2+} entry through these channels (Jarvis et al., 2002). While rat and lamprey neurons both confirm BoNT/A ablation of 5-HT mediated inhibition, in the lamprey, Gβγ has not been shown to inhibit entry of Ca^{2+} through VGCCs in this manner (Gerachshenko et al., 2005; Hamid et al., 2014). It is possible that evolutionarily, Gβγ's action on inhibition through its interaction with SNAP-25 came first and the synergistic inhibition of Ca^{2+} entry through VGCCs developed later. The extension of our work to a mammalian model is necessary to further understand these Gβγ binding domains.

Previous experiments in mammalian neurons have shown G$\beta\gamma$ inhibition of synaptic transmission mediated by α2 adrenergic receptors, 5-HT$_{1b}$ receptors as well as group II metabotropic glutamate receptors (Delaney et al., 2007; Zhang et al., 2011; Hamid et al., 2014). However, these studies relied on either botulinum toxins to cleave endogenous SNAREs or G$\beta\gamma$ scavengers to prevent G$\beta\gamma$ binding. Both of these techniques can have confounding effects on synaptic transmission beyond the G$\beta\gamma$-SNAP-25 interaction. This study directly led to the successful creation of a transgenic animal that expresses SNAP-25Δ3, with which the G$\beta\gamma$-SNAP-25 interactions can be studied without reliance on botulinum toxins or G$\beta\gamma$ scavengers. These transgenic animals exhibit systemic defects resulting from the loss of G$\beta\gamma$-SNAP-25 interactions (Zurawski et al., 2019a).

5. QUANTIFICATION OF CALCIUM TRANSIENT VARIABILITY WITH HIGH SPATIO-TEMPORAL RESOLUTION

5.1   <u>Introduction</u>

5.1.1   <u>Background</u>

Following an action potential, Ca^{2+} influx through 1-4 VGCCs triggers neurotransmitter release via SV fusion (Stanley, 1993; Shahrezaei et al., 2006; Bucurenciu et al., 2010). [Ca^{2+}] at the active zone is directly related to neurotransmitter release, with a concentration in the tens of μM sufficient for release (Dodge and Rahamimoff, 1967; Heinemann et al., 1994; Schneggenburger and Neher, 2000). [Ca^{2+}] is regulated by endogenous buffers, which quickly reduce free [Ca^{2+}] after an action potential, thus causing tight temporal coupling of neurotransmitter release to action potentials (Walter et al., 2018). The P_r of a given synapse is highly dependent on Ca^{2+} signaling as discussed previously in this work. However, the probability of VGCC opening in response to a given action potential and the impact on fluctuating channel opening on presynaptic Ca^{2+}transients is not well studied. Imaging studies of presynaptic Ca^{2+} transients in lamprey RS axons have shown these transients to be stable over short periods of stimulation of 4 to 10 stimuli (Photowala et al., 2005). However, single Ca^{2+} channel conductance is low and the probability of any given channel opening is likewise low regardless of subtype (Ramachandran, S., dissertation). If the probability of VGCC opening is low, even with large redundancy in available channels we would expect to see variability in Ca^{2+} transients.

I utilized new advances in imaging to corroborate the variability of Ca^{2+} influx in response to a single action potential. The influx of Ca^{2+} through VGCCs is modulated by [Ca^{2+}] (discussed in greater detail in section **1.1.5** of this work). I observed Ca^{2+}-dependent attenuation of Ca^{2+} transients, however, this was variable across different active zones. In adult lamprey reticulospinal axons, all VGCC subtypes aside from L-type contribute to neurotransmitter release with N-type channels being the most prevalent (Krieger et al., 1999; Photowala et al., 2005). I found all subtypes possessed variable Ca^{2+} transients and exhibited deactivation over a train of stimuli with the profile of deactivation varying between subtypes.

5.1.2   High Speed Calcium Imaging Supplies Preliminary Evidence for Calcium Transient Variability

Preliminary experiments with wide field high-speed imaging garnered promising results, however, there were inherent issues in our methodology. Segments of lamprey spinal cord were backfilled with the calcium sensitive dye Calcium Green Dextran (3000 MW). The dye was allowed to diffuse through the tissue for a minimum of 12 hours (Fig. 15A). Although this backfill produced highly illuminated axons, the tissue's health was variable. If the tissue survived the procedure, it was stimulated by a bipolar electrode in the bath every 10s and the resulting Ca^{2+} transients were captured. This technique allowed us to capture Ca^{2+} transients at multiple active zones within a single segment of lamprey spinal cord at once (Fig. 15B). This had not been possible with previous techniques. However, the images were gathered through a large focal plane, capturing noise from both above and below the axon resulting in a low signal to noise ratio. These transients were fit with a decay to account for bleaching of the dye during experimentation which introduced additional error into the results. Hotspot transients (Fig. 15C, Black) were isolated by subtracting the global rise in $[Ca^{2+}]$ (Fig. 15C, Blue) from the local rise (Fig. 15C, Red).
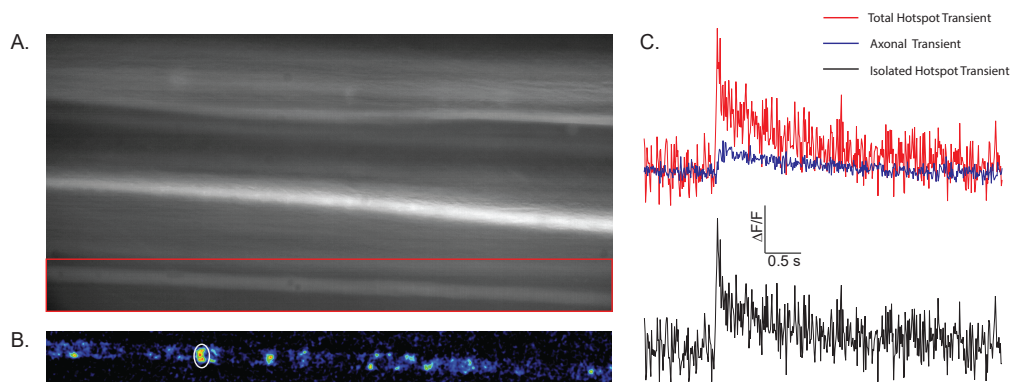
Figure 15. Wide field high speed imaging captures calcium transients. A, section of tissue backfilled with Calcium Green Dextran. B, $\Delta F/F$ of an axon within the red rectangle in A during stimulation. C, Example subtraction resulting in an isolated hotspot Ca^{2+} transient.

I found that the signal to noise ratio was too low to be able to make well supported arguments about Ca^{2+} influx. However, when looking at the transient captured, I was able to discern variability within individual hot spots. Fig. 16 displays four Ca^{2+} transient traces from a single hotspot with variable amplitude. When comparing the variability in peak amplitude, to the variability in noise, 38% of all hotspots (n = 29) showed variability beyond that which could be attributed to noise. However, due to the noise, it was difficult to make any further claims aside from noting that there was variability.

Figure 16. Variability in calcium transients from a single hot spot. Four example traces of isolated hot spot Ca^{2+} transients

We sought to explore VGCC subtype Ca^{2+} transient variability. I acquired preliminary data regarding this issue by washing in saturating doses of ω-Conotoxin MVIIC (50 μM) and

SNX-482 (20 μM) in 0.1% Bovine Serum Albumin (BSA) to block P/Q, R and N type channels.

In some cases, a small Ca^{2+} transient remained (Fig. 17, blue trace). Although L-type channels
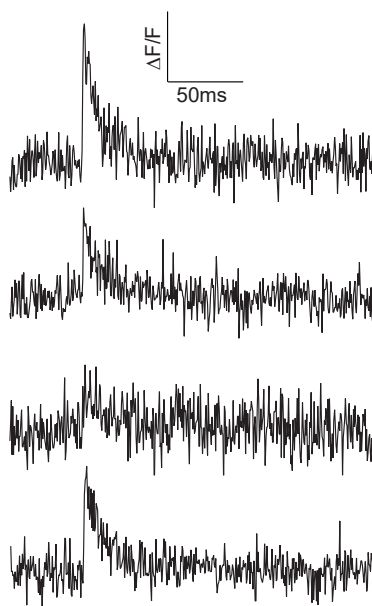
have not been shown to be involved in adult lamprey RS axonal transmission (Krieger et al.,

1999), it is possible that L-type channels compensate when all other types have been blocked.

The remaining Ca^{2+} transient after P/Q, R and N-type VGCCs were blocked could be eliminated

with the L-type VGCC blocker, Nimodipine (20 μM) (Fig. 17, red). The Nimodipine effect was

reversible by wash out (data not shown). The traces shown in Fig. 17 have been smoothed for

illustrative purposes and do not accurately reflect the noise in these recordings.

In addition to the large Ca^{2+} transients observed due to VGCC opening, direct stimulation

of axons results in Ca^{2+} influx via NMDA receptors (Cochilla and Alford, 1999). However, distal

stimulation of RS axons, as done throughout this work, tends not to cause discernable Ca^{2+}

influx through NMDA receptors (Cochilla and Alford, 1999). Additionally, any rise in $[Ca^{2+}]$ by

influx through NMDA receptors tends to be global rather than in distinct puncta and would thus

be subtracted with the total axonal rise in Ca^{2+}. The complete loss of measurable Ca^{2+}

transients when all VGCCs are blocked assures us that the Ca^{2+} influx we measure via this

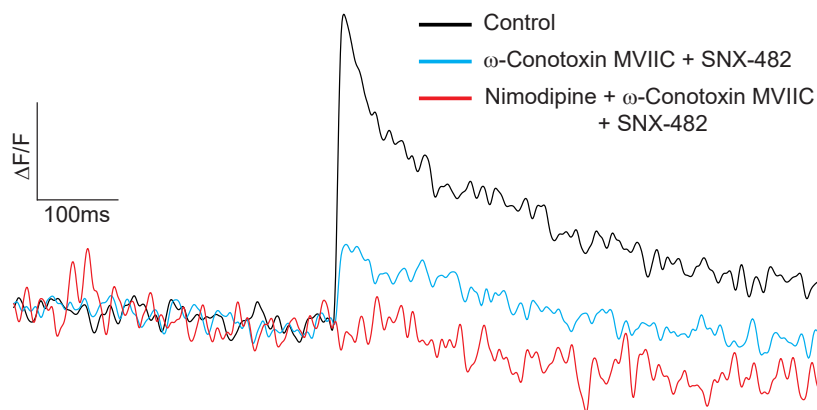method is indeed through VGCCs and not NMDA receptors (Fig. 17).

Figure 17. Block of all calcium channels by a cocktail of toxins shown by representative traces.

5.1.3   <u>Increased Resolution and Decreased Noise with Lattice Light Sheet</u>
<u>Microscopy</u>

In order to image Ca^{2+} transients we need both high spatial and high temporal resolution. In response to an action potential VGCCs remain open for less than a millisecond (Augustine et al., 1991). While $[Ca^{2+}]$ rises throughout the cell during this time, we are specifically interested in the acute rise in $[Ca^{2+}]$ at active zones where VGCCs are tightly coupled to the fusion machinery. The lamprey giant synapse is uniquely suited for this study due to having simple active zones with a small number of channel openings and a large axon into which Ca^{2+} can disperse enabling us to resolve Ca^{2+} responses from single active zones (Gustafsson et al., 2002; Bourne, 2005). This was observed with high speed wide-field imaging, however, I found that the signal to noise ratio was too low to be able to make well supported arguments about Ca^{2+} influx (Fig. 15,16). The fluorescent noise and pigment bleaching that occurred in our wide-field experiments can be avoided by traditional confocal imagery, however, this form of imaging has its own drawbacks.

Confocal imagery either limits the temporal resolution of recording, or at high-speed with line-scanning drastically limits our field of view. The likelihood of capturing more than one active zone per line is not very high and the odds of keeping it within the correct z and x planes even worse. Confocal imaging also requires high light intensity meaning increased bleaching and photodamage. This becomes relevant when we are trying to asses if failures or variation in the amplitude of Ca^{2+} influx are due to a failure in triggering an action potential, or an actual function of the VGCCs themselves. If we capture more than one active zone, as we were able to with the wide field approach, we can confirm triggering of an action potential by comparative analysis of multiple hotspots. Another consequence of the limited field of view of a confocal microscope is that searching for spots inherently leads to bias. If we observe a Ca^{2+} transient in the wide field view of an axon, for confocal imagery with line scanning we then narrow our focus to that one spot. This results in the selection of large, robust hot spots that are easy to find. Smaller spots

that are less consistent may be disregarded. If there is any heterogeneity of Ca^{2+} between these subpopulations of hotspots, we are unlikely to observe it.

To overcome these limitations, I made use of the newly constructed Lattice Light Sheet Microscope (LLSM) (Chen et al. 2014). Exposing live tissue to fluorescence imaging with most techniques results in irradiated tissue to such a degree that it hinders the proper functioning of the tissue in addition to photobleaching. In order to limit this photo damage, an approach that requires lower light intensity and images at a higher speed is desirable. This can be achieved through traditional light sheet microscopy which utilizes a sheet of light to illuminate a single plane within the tissue which is then observed orthogonally with a second objective (Jones et al., 2011). Unfortunately, this method has limited penetrative ability due to the refractive nature of tissue causing the light sheets to rapidly disperse. In order to limit this refraction, the LLSM uses a convergent lattice of Bessel beams to form a plane of light that self-reinforces as it passes through the tissue. (Gao et al, 2014; Chen et al., 2014). Like with traditional light sheet microscopy, the tissue is viewed orthogonally to the light source which allows for rapid viewing of the illuminated tissue at low light intensity which limits photobleaching. Although Bessel beams are able to penetrate live tissue with much higher fidelity than a traditional light sheet, they will still refract if they pass through tissue beyond $100\mu m$ resulting in degraded images, but for our purposes this is not an issue. (Chen et al., 2014)

The LLSM provides a volumetrically accurate imaging approach similar in outcome to confocal microscopy. However instead of only imaging one line through tissue we are able to image an entire plane. This gives us the same advantages as wide field imaging, in that we can record Ca^{2+} transients at multiple active zones at once, without the downsides of significant background noise and photobleaching.

5.2   <u>Results</u>

5.2.1   <u>Quantal Variation in Calcium Transients Induced by a Single Action</u>
<u>Potential</u>

Lamprey RS axons were labeled by pressure injecting the calcium

sensitive dye Calcium Green Dextran (3000 MW) via a sharp micropipette. The tissue was

stimulated by a bipolar electrode in the bath every 10s at a stimulation intensity of up to 50 μA.

Utilizing an adapted LLSM I imaged Ca^{2+} transients at rates of up to 1kHz in single planes

across multiple hotspots in a single axon. Images were processed in ImageJ by dividing the

average of two to three frames at the time of stimulation by the pre-stimulus average. This

allowed for clear identification of hotspots (Fig.18A). Fig. 18B outlines the isolation of the portion

of the Ca^{2+} transient attributable to a single hotspot (red trace) by subtracting the axonal

transient (gray trace) from the total Ca^{2+} transient at the hotspot (black trace). If this subtraction

did not show a clear remaining signal at any stimulation the hotspot was thrown out.

Additionally, if any stimulation failed to increase Ca^{2+} transients throughout the entire axon, the

stimulation was not included in the analysis, as it cannot be determined if the failure was due to

a physiological condition or an external failure to generate an action potential.

The isolated Ca^{2+} transients varied independently between hotspots within the same

axon, a portion of which were fairly consistent while other hotspots displayed variation in

amplitude. Fig. 18C shows the peak of hotspot transients from the axon shown in Fig. 18A over

multiple stimuli. Each line corresponds to transients recorded at the matching colored hotspot in

A. An amplitude ≤ 0 indicates that the local transient was not higher than the background axonal

transient, therefore any increase in fluorescence at this spot for this stimulation can be attributed

to diffusion of Ca^{2+} away from the site of stimulation or to a small degree from secondary

sources of Ca^{2+}, such as internal stores (Cochilla et al., 1998). Thus this indicates a local failure

of Ca^{2+} entry through local VGCCs at that active zone. Fig. 18D shows three example traces for

the hotspot highlighted in red showing the variation that can occur at a single hotspot.
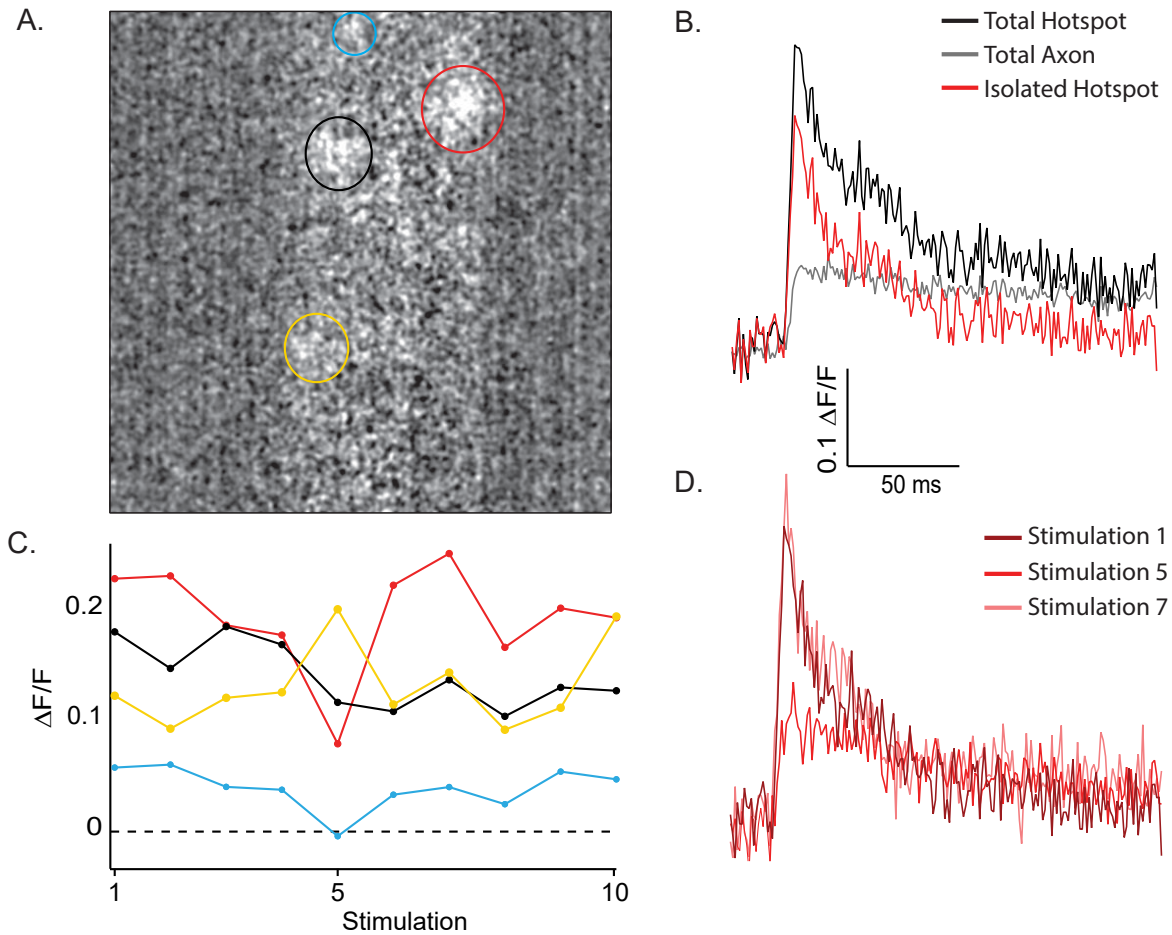
Figure 18. Calcium transients at multiple hotspots in a single axon show variation over multiple stimulations. Widefield image with highlighted hotspots. Representative traces showing axonal transient subtraction. Transients for separate hotspots within a single active zone, one spot is then highlights to show variation in representative traces.

For the purpose of normalization, an average transient for each hotspot was obtained by excluding failures as well as the maximum and minimum value for each spot. Individual Ca^{2+} transients (n = 1783 over 93 hotspots, average stimuli per hotspot = 19) were divided by these averages and displayed as a histogram well fit by 6 Gaussians (Fig.19 A). Failures (n = 83) are included as a bar at 0 but not fit by the Gaussians. Failures were observed in 25% of hotspots

(n=21) with the majority of hotspots that exhibited this phenomenon showing more than one

failure (n=17). This quantal variation suggests that a given hotspot has several VGCCs

available to open, but not all open during each stimulation.

The histogram for individual transients is useful for showing quantal variation, but fails to

characterize how individual hotspots behave. In order to show this variability, I calculated the

range of the normalized transients for each hotspot (Fig.19B). A range close to zero for a given

hotspot suggests the same number of channels are opening during each stimulation. The

variation in Ca^{2+} transient for most hotspots is nearly equal to the average total Ca^{2+} transient at

that hotspot (represented as a value of 1.0 on the histogram). Although there could be multiple

reasons for this, the recent evidence that there are only 1-4 VGCCs at a single hotspot (Stanley,

1993; Bucurenciu et al, 2010) coupled with this large fluctuation in Ca^{2+} transient suggests that

we are observing the failure of a small number of channels, possibly even one, to open in

response to stimulation (Stanley, 1993).

Several hotspots showed larger as well as smaller ranges in Ca^{2+} transient amplitude

(Fig. 19B). A fluctuation to amplitudes much larger than the average transient may suggest that

there are many VGCCs at that particular hotspot. However, it does not necessarily mean there

are more VGCCs than at hotspots with less variation, because factors in the recording approach

other than Ca^{2+} channel numbers can substantially affect the amplitude of the recorded

transients; it only tells us that the VGCCs present show a higher degree of variability in their

response to stimulation. Likewise, a smaller range does not confirm there are fewer VGCCs at a

particular hotspot, it only tells us that the hotspot does not display a high degree of variability of

VGCC opening.

Our data shows that Ca^{2+} transients at individual active zones have a variable nature,

sometimes failing to allow Ca^{2+} entry altogether, with some active zones having a higher degree

of instability than others even within the same axon. This would likely have a profound effect on

evoked release of neurotransmitter although we have not yet been able to use the LLSM to

observe Ca^{2+} transients at an active zone in a paired protocol with EPSPs. Even under a paired

protocol it may be difficult to discern the effects of a single active zone as neurons make

multiple *en passant* synapses with a single RS axon (Gustafsson et al., 2002).
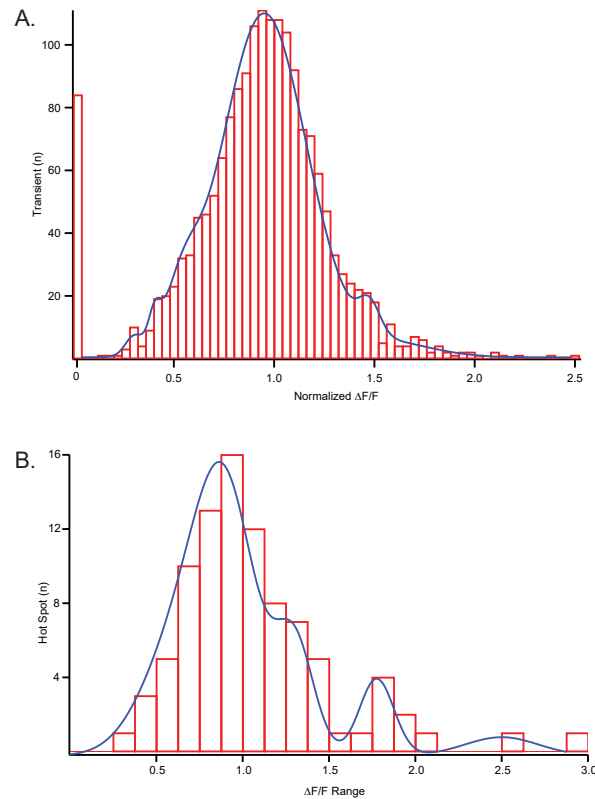
Figure 19. Quantal fluctuation and variation in calcium transients shown by 6 Gaussians fit to all transients, as well as 4 Gaussians fit to the range of transients at individual hotspots.

5.2.3 <u>Paired Pulse Effects on Calcium Transients Differ Between Active Zones</u>

As discussed in the introductory portion of this work, [Ca^{2+}] effects STP.

Rising [Ca^{2+}] increases P$_r$. Local [Ca^{2+}] after an action potential is rapidly reduced by Ca^{2+}

buffering agents and diffusion. With a sufficiently high [Ca^{2+}] local buffers may become

saturated allowing for increased interactions with Syt-1 as well as slower acting Ca^{2+} sensors (Jackman and Regehr, 2017). $[Ca^{2+}]$ may also play a role in STD as many VGCCs exhibit Ca^{2+} dependent inactivation (Simms and Zamponi, 2014). Therefore, under repetitive stimulation these inactivated VGCCs may prevent further Ca^{2+} influx, resulting in a decrease of P_r. It is possible that the size of Ca^{2+} transients varies based on repetitive stimulation. Previous studies have shown mixed results regarding facilitation of Ca^{2+} influx in response to repetitive stimulation, however no previous study has been able to directly examine use-dependent Ca^{2+} entry through VGCCs at high spatio-temporal resolution evoked by stimulation (Jackman and Regehr, 2017).

Following the observation that Ca^{2+} transients at active zones were highly variable, with some hotspots showing higher degrees of variation and failures than others, I sought to determine how this variability would express itself under a paired pulse protocol. Following the same dye injection and stimulation protocol as previously described, I gave the tissue two shocks 20ms apart. Reticulospinal action potentials are capable of firing repetitively at 50Hz during locomotor behavior (Sirota et al., 2000). Thus, this stimulation duration was chosen in order to be physiologically relevant to the lamprey while giving enough time between stimulations to separate the two peak Ca^{2+} transients.

Fig. 20A shows the time course of a Ca^{2+} transient throughout an axon showing Ca^{2+} entry at active zones and subsequent diffusion from those sites. Before stimulation there is no discernable Ca^{2+} signal above the noise. At the first stimulus, hotspots appear where VGCCs are located. The second stimulus is more diffuse as it shows the compounding increase of $[Ca^{2+}]$ throughout the axon via diffusion as well as the local increase of $[Ca^{2+}]$ through VGCCs. Post-stimulation, the Ca^{2+} signal continues to diffuse throughout the axon until it approaches pre-stimulus levels. When the diffusional Ca^{2+} component is subtracted, we are able to resolve two peak Ca^{2+} transients. In Fig. 20B three separate traces from a single hotspot are overlaid to show typical variation over multiple paired pulse recordings. Note that individual paired pulses

can have different effects on the same hotspot, varying between facilitation and depression of Ca^{2+} influx.

Peak Ca^{2+} fluorescence was calculated by subtracting the peak $\Delta F/F$ (taken from an average of 2-3 points) from either the average of the pre-stimulus baseline or from the decay of the 1st transient. Paired Pulse Ratios (PPRs) were calculated for each pair of stimuli at every hotspot by dividing the 2nd transient by the 1st (n = 1465 paired pulses over 73 hotspots). The average PPR across all hotspots was .80 $\pm$ 30, with an average median PPR at each hotspot of .70 $\pm$ 26. This indicates a high degree of variability in the behavior of active zones. A histogram of all PPRs across all hotspots shows notable clusters around PPRs of 0 (indicating a complete loss of the second transient) and 0.5 suggesting the inactivation of some or all VGCCs after the first stimulus (Fig. 20C). Another cluster of PPR occurs at 1, which indicates a number of events that did not result in facilitation or inhibition of Ca^{2+} influx (Fig. 20C). A less clustered population of events that resulted in a PPR $\geq$ 1.25 (~ 11%, n = 168, 24 events are beyond the scope of Fig. 20C with a maximum PPR of 6.6) was observed, demonstrating facilitation of Ca^{2+} influx in a paired pulse.

Different hotspots within the same axon showed varying responses to paired pulses, indicating that the activity of VGCCs at different active zones within a single axon can behave independently from one another. This is shown in Fig. 20D. Solid circles represent peak transients of the first pulse, open circles represent the peak transient of the 2nd pulse.
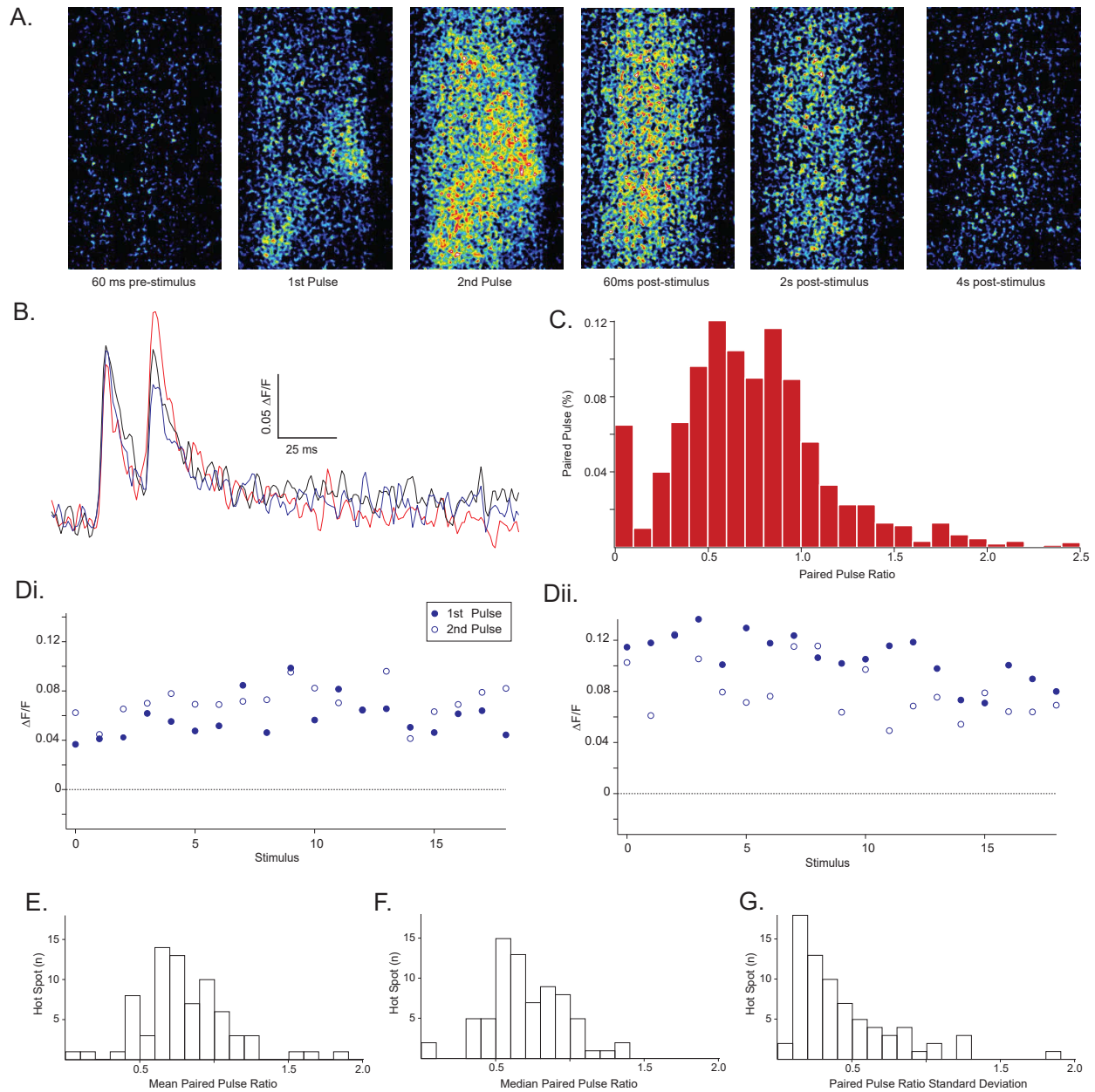
Figure 20. Paired pulse stimulation has varying effects on calcium transients. Fluorescence imaging of a single axon during one paired pulse stimulation. Example traces of one hotspot over 3 paired pulse stimulations. Histogram of all PPRs. Example hotspot transients over multiple paire pulses. Histogram of mean, median, and variance in PPR at each hotspot.

Within one axon, in response to the same stimuli, two separate hotspots displayed paired pulse potentiation of Ca^{2+} transients (Fig. 20Di) as well as paired pulse inhibition of Ca^{2+} transients

(Fig. 20Dii). Histograms of the mean and median PPRs at each hotspot (Fig.20 E,F) show the majority of hotspots display a tendency for the 2nd transient to be less than or equal to the first, while only 4 hotspots (~5%) had an average PPR $\geq$ 1.25. The variance of PPR at a given hotspot was relatively high with 77% of hotspots exhibiting a standard deviation greater than 20%, including 6 hotspots (~7%) with a standard deviation greater than 100% (Fig. 20G). This tells us, that while some hotpots are relatively consistent from paired pulse to paired pulse, other hotspots do not exhibit a standard PPR and rather show different behavior for each paired pulse. Together, the mean, median and variance of active zones suggests that the population of VGCCs at any given active zone have variable responses to paired pulses that would likewise have variable effects on STP.

VGCCs display both Ca^{2+} dependent and voltage dependent inactivation, it is likely that both of these mechanisms are partially responsible for the reduction of Ca^{2+} transients at the second pulse (Mochida, 2019). The fact that some hotspots display a second Ca^{2+} transient larger than the first suggests that there may be additional VGCCs present at hotspots that do not always open during the first stimulation. The large variance in a hotspot's response to paired pulses may be due in part to channel open time, or the probability of VGCC opening as observed in our single pulse experiments.

5.2.4   Calcium Transients at 50 Hz Stimulation Maintain Variability

The paired pulse experiments showed us that both inactivation of VGCCs and probability of channel opening are at play during repeated stimulation. In order to further elucidate how repetitive stimulation effects Ca^{2+} transients, and to further tease out quantal representation of VGCCs, I subjected axons filled with the low affinity calcium dye, Fluo-5F, to a 5 pulse train at 50Hz via a bipolar electrode adjacent to the tissue with a 10 second pause between each train. These experiments used Fluo-5F as opposed to the relatively high affinity

Calcium Green Dextran in order to prevent dye saturation due to the high $[Ca^{2+}]$ that may build up over the course of the train. As before, hotspots were identified in ImageJ by dividing the frames during pulses by the frames before stimulation. $[Ca^{2+}]$ builds throughout the axon over the course of the train (Fig. 21A), however, it is still possible to distinguish distinct local transients (black) at each of the five stimulations by subtracting the axonal Ca^{2+} transient (blue) from the hotspot transient (red) as before (Fig. 21B).
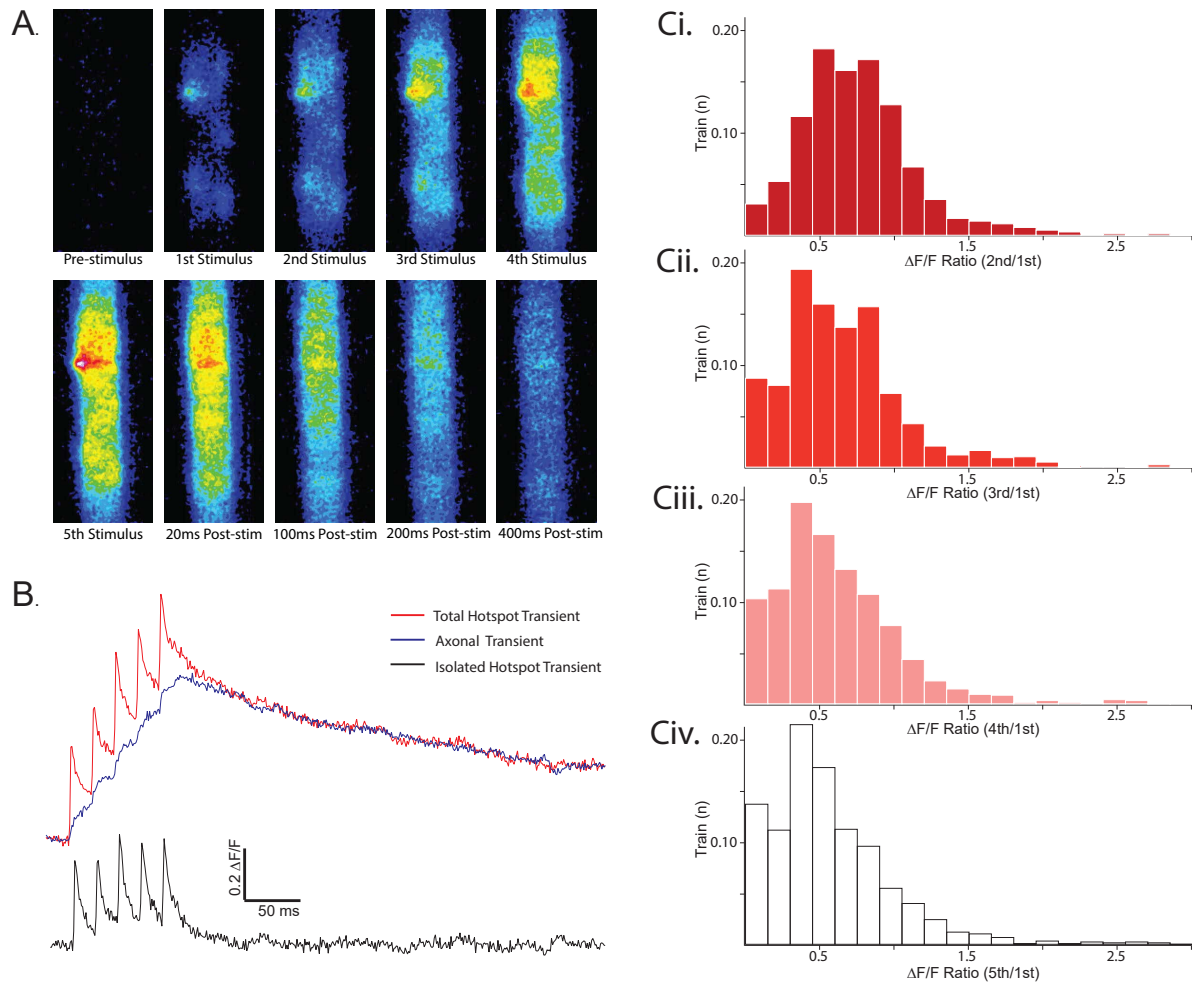

Figure 21. Calcium Transients in response to a 50 Hz train of 5 stimuli. Fluorescence imaging of calcium transients at a single axon. Example traces of the raw ΔF/F from the hotspot and axon, as well as the isolated hotspot transients. All transients from all hot spots represented by histograms of the ratios of the 2nd, 3rd, 4th and 5th stimulus (respectively) to the 1st stimulus.

Ca^{2+} transient amplitude was determined by subtracting either the pre-stimulus $\Delta F/F$ or the decay of previous stimulations from the average of 2-3 points at the time of stimulation. Peaks were measured as an average to minimize the effects of noise on the results. Each Ca^{2+} transient was translated into a ratio by dividing the stimulus in question (2nd, 3rd, 4th and 5th) by the 1st transient in that specific train. If, however, the 1st stimulus failed to evoke a transient and subsequent stimuli did evoke a transient, the ratio was calculated by taking an average of all 1st stimulus transients in order to avoid dividing by zero and additionally to accurately depict the size of transients at subsequent stimuli. The ratios for each train recorded (n = 1162 trains over n =51 hotspots) are displayed as histograms in Fig. 21 Ci-iv. On average, the relative size of the Ca^{2+} transient decreases as the train progresses (ratios of 0.81 ± 0.30, 0.67 ± 0.27, 0.64 ± 0.29, and 0.61 ± 0.30 for the 2nd, 3rd, 4th and 5th stimulus respectively) with an increase in failures that would be expected with $[Ca^{2+}]$ dependent inactivation. However, even after 5 stimuli 13% of transients had ratios ≥ 1, indicating that $[Ca^{2+}]$ dependent inactivation is not uniform. Indeed, when looking at individual active zones, the behavior is more nuanced than when looking at all transients combined (Fig. 22).

The heat map in Fig. 22 displays the median $\Delta F/F$ ratio for all transients at a given hotspot ranging from dark red, indicating no Ca^{2+} entry, to dark green, indicating a 35% increase in Ca^{2+} transient amplitude. An individual hotspot is displayed in a single row made up of four rectangles that represent the stimuli ratios as compared to the first transient. The median was chosen as opposed to the average in order to show the most likely state for each hotspot and to avoid skewing the results when a hotspot exhibited a small number of very small or very large Ca^{2+} transients. When viewing the data this way, differing populations of hotspots become apparent. Hotspots that showed sharp reductions in the 2nd Ca^{2+} transient compared to the 1st (Fig. 22, left column) tended to maintain or increase this reduction throughout the train. Likewise, those hotspots that showed a potentiation of the 2nd Ca^{2+} transient compared to the

1st (Fig. 22, right column lower half) tended to maintain this potentiation throughout the train. The hotspots that displayed moderate reduction in the 2nd Ca^{2+} transient compared to the 1st (Fig. 22, middle column and upper half of right column) showed variable behavior throughout the remaining stimuli.
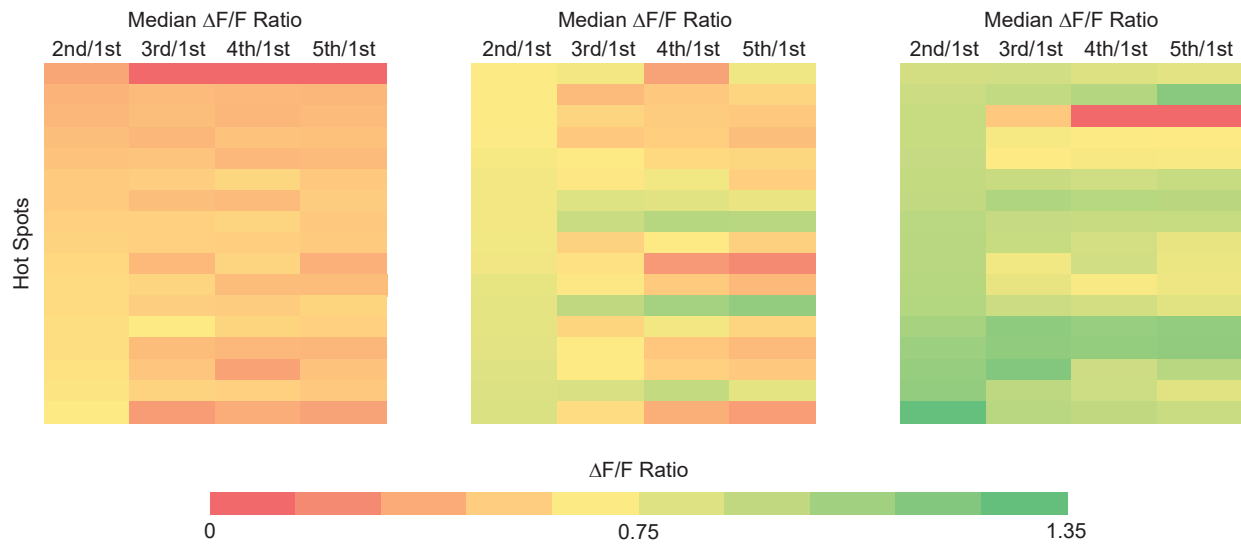
Figure 22. Heat Map of Calcium Transient Ratios over a 50Hz train of 5 stimuli. Each row in each of the 3 columns represents the median ΔF/F Ratio to the 1st Ca^{2+} transient for a given hotspot over the course of the train.

Although this gives us a good indication of how a hotspot responds over a large number of trains, it is not necessarily a good predictor of what any individual response will be. This is due to the large variance observed in the data. The average standard deviation in ΔF/F ratios was ± 38%, with 15 hotspots showing at least one transient with a standard deviation greater than ± 50%. This variation at a single hotspot is shown by example Ca^{2+} transients occurring during separate trains (Fig. 23A). Fig. 23B shows a representative example of a single hotspot's response to 80 individual trains resulting in the typical pattern of reduced transients over the

course of the train. Each circle represents the peak transient for one stimuli in the train, the
darkest circle is the 1st stimulus, ranging lighter until the open circle which represents the 5th
stimulus. Circles that have the same x-coordinate represent stimuli that occurred during the
same train. The data clusters around several ratios of ΔF/F (~0.6, ~0.4 and ~0.2) suggesting a
quantal nature in Ca^{2+} transients, with a trend towards fewer channel openings as the train
progresses. This is shown, by example, in the histogram of all ΔF/F ratios at one hotspot in Fig.
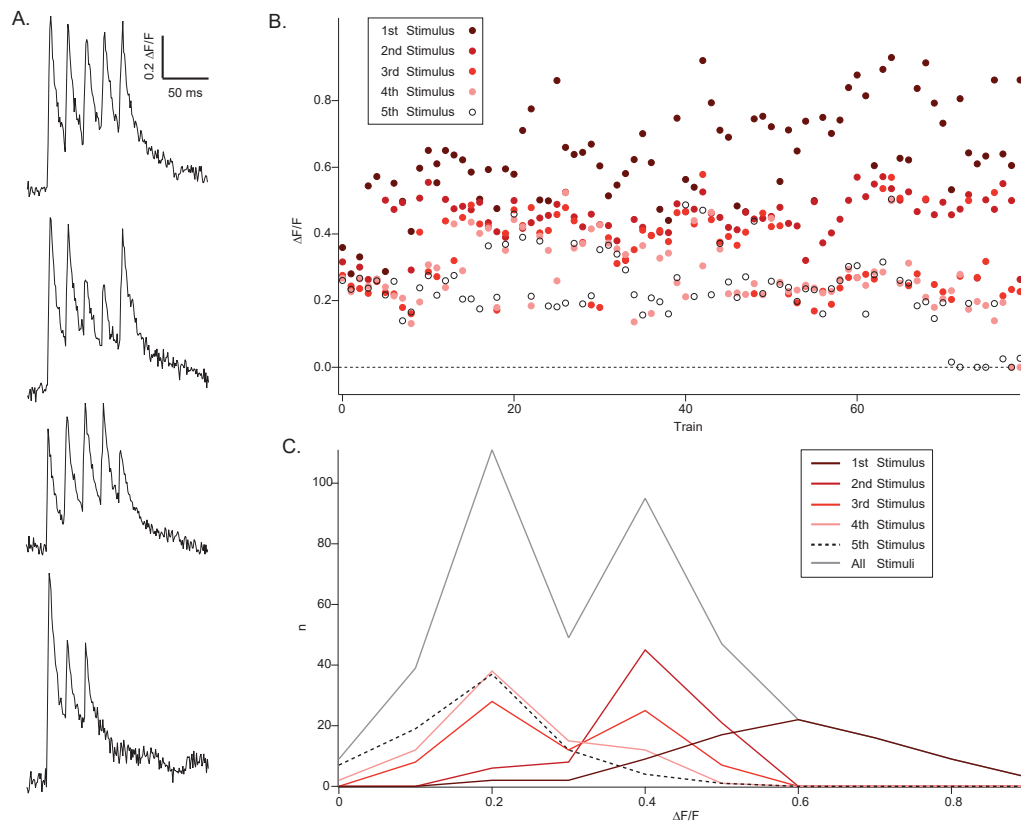23C.

Figure 23. Quantal nature of calcium transients in response to a 50Hz train of stimuli. Four
representative traces from a single hotspot. All transients from 80 trains at a single hotspot.
Histogram representing transients from each of the 5 stimuli in the train.

5.2.5 Calcium Transients in a 50Hz Train are Effected by Calcium Concentration

Ca^{2+} transients increase as external [Ca^{2+}] rises (Simms and Zamponi, 2014). Many VGCCs display Ca^{2+} dependent inactivation. To determine if our observation of VGCC inactivation under repetitive stimuli can be explained by an increase in [Ca^{2+}], I followed the protocol as before with a ringer solution containing either half or double normal [Ca^{2+}] (1.3mM and 5.2mM respectively) in tandem with a compensatory increase or decrease in [Mg^{2+}] (3.6mM and 0.9mM respectively). Each change in concentration was allowed to wash in for 10 minutes. Example traces with axonal Ca^{2+} subtracted are shown for the varying [Mg^{2+}] and [Ca^{2+}] at a single hotspot in Fig. 24A.
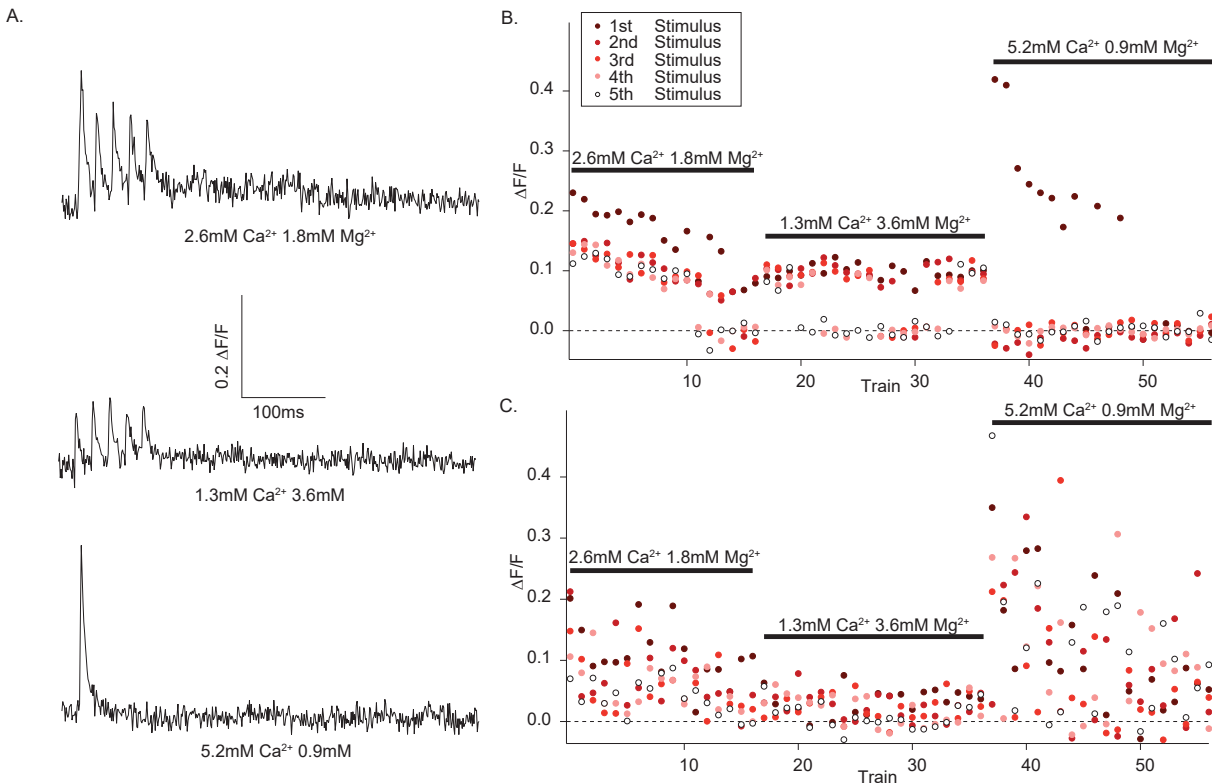

Figure 24. Calcium concentration effects calcium transients over a train in the majority of, but not all hotspots. Example traces at varying calcium and magnesium concentrations at a single hotspot. Examples of all transients for two hotspots that show differing behavior.

Example graphical representations (as described in Fig. 23) of all Ca^{2+} transients at two hotspots within the same axon are shown in Fig.24B. Hotspots displaying $[Ca^{2+}]$ dependent inactivation were abundant (n = 14) (E.g. Fig 24 A,B), however, some hotspots lacked this characteristic (n = 2) (E.g. Fig. 24C).

In low $[Ca^{2+}]$, the average $\Delta F/F$ ratio for the 2nd, 3rd, 4th and 5th stimuli compared to the 1st was 0.87 ± 0.41, 0.81 ± 0.43, 0.72 ± 0.48, and 0.60 ± 0.45 respectively, compared to control ratios of 0.54 ± 0.40, 0.48 ± 0.33, 0.47 ± 0.38, and 0.42 ± 0.29 (n = 16 hotspots) (Histogram in Fig. 25). This suggests that under low $[Ca^{2+}]$ we do not see a large initial effect of Ca^{2+} dependent inactivation but as $[Ca^{2+}]$ rises throughout the train, deactivation may be triggered resulting in continued decline of the Ca^{2+} transient. This differs from control conditions where the majority of deactivation occurs immediately. Interestingly, although the average $\Delta F/F$ ratio was larger for all transients under low $[Ca^{2+}]$, the frequency of events in which there was no Ca^{2+} entry increased (Fig. 25). These events are largely attributable to a subset of hot spots which can be seen in the heat map in Fig. 26.

Under high $[Ca^{2+}]$, the average $\Delta F/F$ ratio for the 2nd, 3rd, 4th and 5th stimuli compared to the 1st was 0.28 ± 0.92, 0.20 ± 0.51, 0.17 ± 0.52, and 0.25 ± 1.20 respectively. Note the large variance which is due to hotspots with some events in which there was no Ca^{2+} entry interspersed with events that displayed normal channel opening (Fig. 25). This lends support for the theory that the initial drop in Ca^{2+} transient peak amplitude during a train of stimuli is due to Ca^{2+} dependent inactivation, while variance after this inactivation is governed by other mechanisms. As we've seen throughout our experimentation, different hotspots behaved differently (Fig. 26). A population of hotspots (n = 2) did not exhibit any Ca^{2+} dependent inactivation (Fig. 26, E.g. Fig. 24C). While another population (n = 14) displayed strong Ca^{2+} dependent inactivation (Fig. 26, E.g. Fig. 24B). This may be due to varying VGCC subtypes at separate active zones.
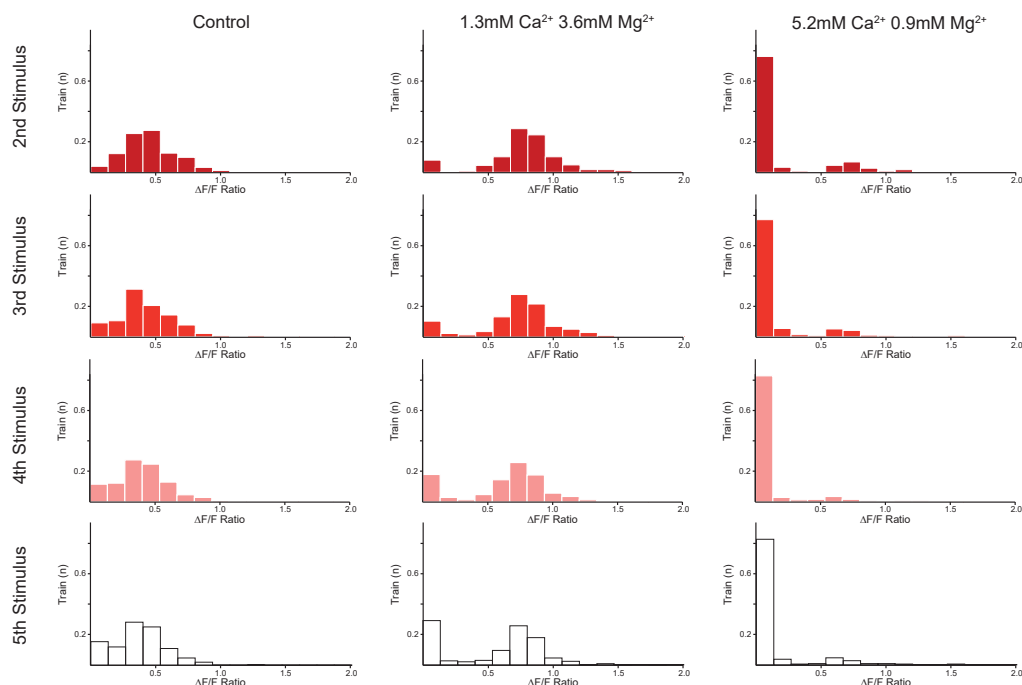
Figure 25. Histogram of all transients ∆F/F over all hotspots under varying calcium and magnesium concentrations.
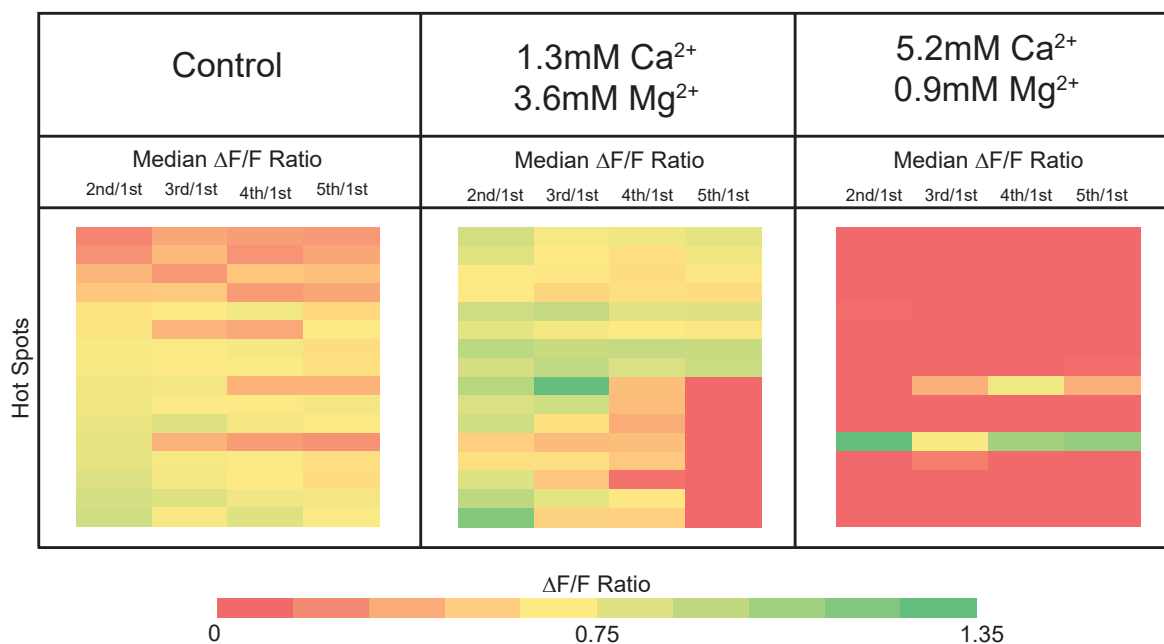

Figure 26. Heat Map of Calcium Transient Ratios over a 50Hz train of 5 stimuli across varying Calcium and Magnesium Concentration. Each row represents the median ∆F/F Ratio to the 1st Ca^{2+} transient for a given hotspot over the course of the train.

5.2.6   <u>Isolated Voltage Gated Calcium Channels have Distinct Calcium</u>
<u>Transient Characteristics</u>

We have observed that VGCCs localized to an active zone respond to stimuli with varying Ca^{2+} transient characteristics, independently from VGCCs at distal sites. This variable behavior may be due to the subtype of VGCCs at a given active zone. I washed in ω-Agatoxin IVA (P/Q-type VGCC blocker), ω-Conotoxin GVIA (N-type VGCC blocker) and SNX-482 (R-type VGCC blocker) in pairs at saturating doses (100nm, 100nm, and 20nm respectively) in 0.1% BSA for 20 minutes to ensure that only one channel subtype was active. The toxins were continually perfused as I altered the $[Ca^{2+}]$ as before with an additional wash in of 10 minutes for each change of solution. I followed the 5 pulse protocol as before. Due to the length of the experiment it was not feasible to hold a piece of tissue healthy and in focus through varying $[Ca^{2+}]$ both under control conditions and with VGCC blockers.

Example global Ca^{2+} transients are shown in control conditions and for each cocktail of blockers in Fig. 27A. Each cocktail of blockers reduced Ca^{2+} transients throughout the axon but never fully inhibited Ca^{2+} influx. This could be explained by most active zones having all channel types, or this could be due to a compensatory mechanism in which blocked VGCCs are replaced with functioning VGCCs. As show in in Fig. 17, we do know it is possible to block all VGCC function so we do not suspect the remaining transient is due to a partial block of VGCCs. Additionally, the remaining signal could be due to L-type channels, although L-type channels have not previously been shown to contribute to synaptic activity in lamprey reticulospinal axons (el Manira and Bussières, 1997; Photowala et al., 2005). In previous experiments blocking one VGCC subtype did not have a linear effect on release (Takahashi and Momiyama, 1993), we found the effect on Ca^{2+} transients was also non-linear when blocking multiple subtypes (Fig. 27). When only N-type channels were active, the 1st transient in the train was reduced to 76% $\pm$ 19 compared to control (E.g. Fig.27B, blue trace). For P/Q type channels, 2 of the 6 active

zones tested showed increased transients after blockers were applied (148% and 405% of control), lending support to the hypothesis that VGCCs might be replaced if they become blocked or that new VGCCs occupy VGCC slots that were previously unoccupied, in this case by VGCCs of higher channel conductance (Cao et al., 2004; Lübbert 2019). However, additional experiments would need to be performed to verify this theory. For the remaining P/Q type active zones, initial transients were reduced to 67% ± 16 compared to control (E.g. Fig.27B, red trace). A single hotspot with isolated R-type channels showed no reduction in transients, which may suggest this active zone initially only had R-type channels. For the remaining R-type active zones, initial transients were reduced to 70% ± 9 compared to control (E.g. Fig.27B, green trace).
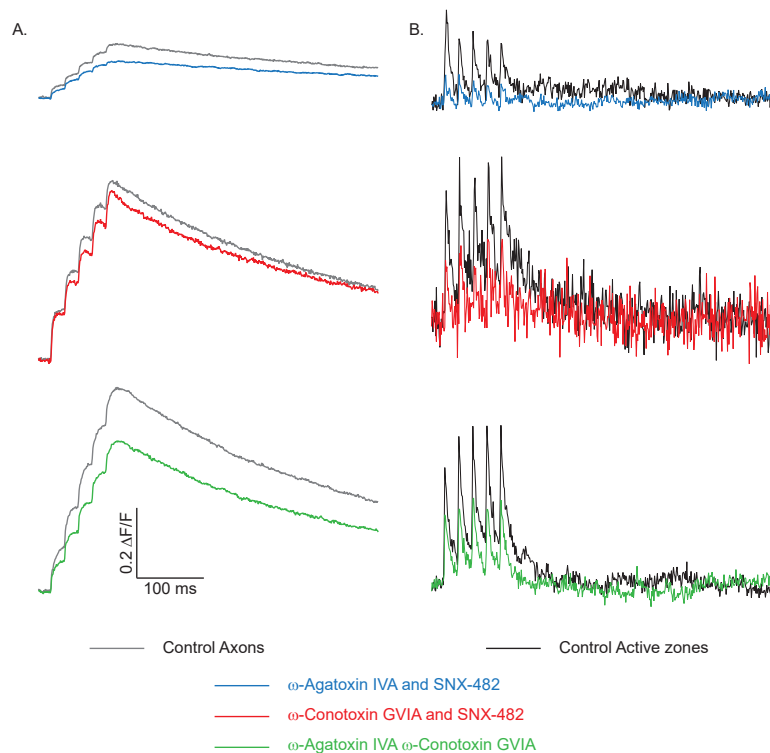

Figure 27. Blocking VGCC subtypes reduces calcium transients without eliminating them. Representative traces of axonal transients with and without blockers. Representative traces of hotspot transients with and without blockers.

A large degree of variability remains in the Ca^{2+} transient at each individual active zone. This may be due to additional morphological differences between active zones. It should also be noted that each drug application was only performed on a single animal, and it is possible that the active zones tested do not account for all varieties of active zone in lamprey reticulospinal axons. It is possible that a clearer pattern will emerge over a larger sample size. However, we were able to determine certain changes in characteristics as we isolated each subtype of VGCC.

N-type channels have the largest single channel conductance among HVA channels, and are the most prevalent in lamprey RS axons (Krieger et al., 1999; Catterall, 2000; Photowala et al., 2005; Weber et al., 2010). N-type channels were isolated by bath application of SNX-482 (20nm) and ω-Agatoxin IVA (100nm) (n = 8). Typical transients at a single hotspot over the course of the experiment are shown in Fig. 28A. After drug application, the average $\Delta F/F$ ratio shifted left for all stimuli in the train (Control median ratio = 1.20 ± 0.93, 0.94 ± 0.82, 0.87 ± 0.75 and 0.84 ± 0.74 ; isolated N-type ratio = 0.92 ± 0.60, 0.85 ± 0.63, 0.67 ± 0.56, and 0.64 ± 0.49 for the 2nd, 3rd, 4th and 5th stimuli respectively) suggesting that Ca^{2+} influx through N-type VGCCs is reduced during repetitive stimulation. Although several spots showed a pattern characteristic of $[Ca^{2+}]$ dependent inactivation (E.g. Fig. 28A), and indeed Ca^{2+} entry was greatly reduced over the course of the train, in high $[Ca^{2+}]$ (average high $[Ca^{2+}]$ $\Delta F/F$ ratio = 0.51 ± 0.55, 0.30 ± 0.41, 0.35 ± 0.43, and 0.36 ± 0.44 for the 2nd, 3rd, 4th and 5th stimuli respectively), there was also a decrease in Ca^{2+} entry throughout the train in low $[Ca^{2+}]$ similar to reductions at control $[Ca^{2+}]$ (Fig. 28b) (average low $[Ca^{2+}]$ $\Delta F/F$ ratio = 0.85 ± 0.60, 0.84 ± 0.67, 0.70 ± 0.58 and 0.54 ± 0.62 for the 2nd, 3rd, 4th and 5th stimuli respectively). This suggests that it is not only $[Ca^{2+}]$ dependent inactivation that causes Ca^{2+} entry to be attenuated through N-type VGCCs over a train of stimuli.

Figure 28. Example transients of calcium entry through isolated N-type VGCCs with 50hz stimulation and varying calcium and magnesium concentrations, in addition to histograms of all transients over all hotspots.

P/Q-type channels were isolated by application of SNX-482 (20nm) and ω-Conotoxin GVIA (100nm) (n = 6). Typical transients for a single hotspot after P/Q channel isolation are shown in Fig. 29A. After drug application, the initial reduction in Ca^{2+} transient was consistent over the remaining stimuli. (Control average $\Delta F/F$ ratio = 1.03 ± 1.05, 0.74 ± 0.56, 0.77 ± 0.63, and 0.77 ± 0.60; isolated P/Q-type ratio = 0.84 ± 0.89, 0.82 ± 0.86, 0.85 ± 0.73, and 0.89 ± 0.82 for the 2nd, 3rd, 4th and 5th stimuli respectively). In low $[Ca^{2+}]$, large reduction of the Ca^{2+} transient did not occur until the third stimulus and the average increased over the remaining stimuli (average $\Delta F/F$ ratio = 0.93 ± 0.86, 0.63 ±0.79, 0.69 ± 0.73, and 0.79 ± 0.79 for the 2nd, 3rd, 4th and 5th stimuli respectively). This reduction is due in large part to a high number of events that failed to produce any Ca^{2+} transients with the remaining successful transients shifting left throughout the course of the train (Fig. 29B). On average, in high $[Ca^{2+}]$, transients declined over the course of the train again due in large part to a number of events that failed to evoke Ca^{2+} entry while the remaining transients behaved similarly to control (Fig. 29B) (average $\Delta F/F$ ratio in high $[Ca^{2+}]$ = 0.63 ± 0.58, 0.55 ± 0.56, 0.56 ± 0.65 and 0.49 ± 0.63 for the 2nd, 3rd, 4th and 5th stimuli respectively).

P/Q channels have previously shown Ca^{2+}-dependent inactivation requiring a global rise in $[Ca^{2+}]$ (Zamponi, 2003). As the experiment continued, the number of failures increased. Although there was a wash in period for each change in concentration, and therefore global $[Ca^{2+}]$ concentrations should have returned to normal, it is possible that the large degree of stimulation could have had downstream effects that took minutes to be observed resulting in the increase of failures even in low $[Ca^{2+}]$. Although it hasn't been studied in lamprey, when local $[Ca^{2+}]$ increases P/Q channels have been shown to exhibit Ca^{2+}-dependent facilitation by the action of calmodulin (DeMaria et al., 2001; Lee et al., 2003; Chaudhuri et al., 2007). We did not observe this behavior, but it may have been masked by a global rise in $[Ca^{2+}]$
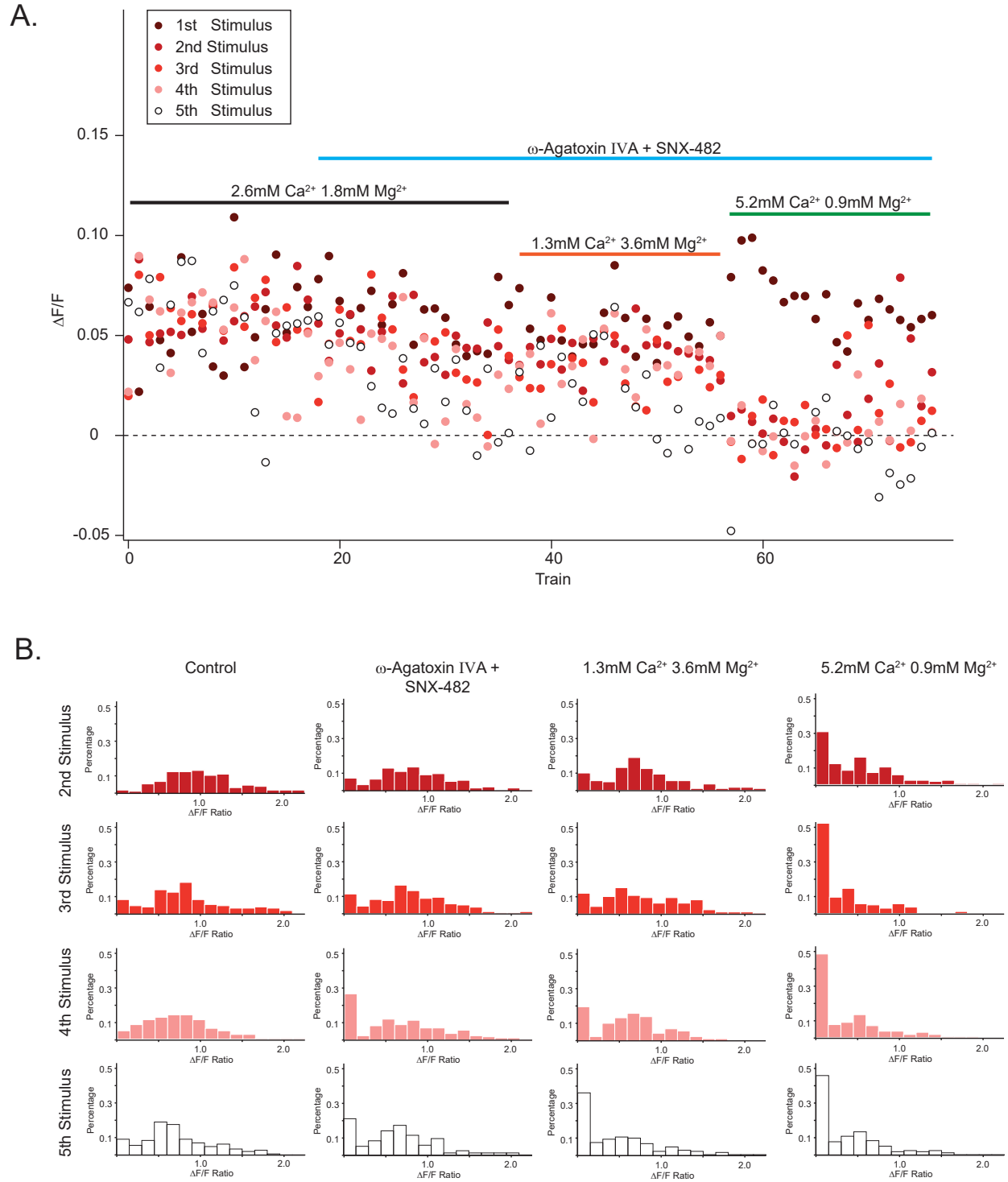
Figure 29. Example transients of calcium entry through isolated P/Q-type VGCCs with 50hz stimulation and varying calcium and magnesium concentrations, in addition to histograms of all transients over all hotspots.

R-Type VGCCs were isolated by application of ω-Agatoxin IVA (100nm) and ω-Conotoxin GVIA (100nm) (n = 7). Typical transients for a single hotspot after R-type VGCC isolation are shown in Fig. 30A. Before and after R-type VGCC isolation, the hotspots tested showed fairly consistent Ca^{2+} transients over the course of the train (Control average $\Delta F/F$ ratio = 0.94 $\pm$ 0.26, 0.95 $\pm$ 0.26, 0.93 $\pm$ 0.26 and 0.94 $\pm$ 0.29; isolated R-type ratio = 0.91 $\pm$ 0.23, 0.92 $\pm$ 0.29, 0.93 $\pm$ 0.27, and 0.97 $\pm$ 0.32 for the 2nd, 3rd, 4th and 5th stimuli respectively). Failure of a stimulus to produce a Ca^{2+} transient increased in low $[Ca^{2+}]$, but the remaining transients showed little reduction compared to control (Fig. 30B) (low $[Ca^{2+}]$ average $\Delta F/F$ ratio = 1.01 $\pm$ 0.76, 0.76 $\pm$ 0.64, 0.92 $\pm$ 0.79 and 0.98 $\pm$ 1.10 for the 2nd, 3rd, 4th and 5th stimuli respectively). In high $[Ca^{2+}]$, the 2nd stimuli had a dramatically reduced Ca^{2+} transient dominated by total lack of Ca^{2+} entry, with fewer failures at subsequent stimuli (Fig. 30B). When a Ca^{2+} transient was produced it had a $\Delta F/F$ ratio similar to control conditions (Fig. 30B) (high $[Ca^{2+}]$ average $\Delta F/F$ ratio = 0.49 $\pm$ 0.68, 0.88 $\pm$ 0.56, 0.88 $\pm$ 0.53 and 0.80 $\pm$ 0.67 for the 2nd, 3rd, 4th and 5th stimuli respectively). Suggesting that although there is an initial Ca^{2+}-dependent block, this block does not persist throughout the train as it does for N and P/Q type VGCCs.

In our initial experimentation, a population of hotspots exhibited a drop in the 2nd Ca^{2+} transient with a moderate recovery over the remaining stimuli (Fig. 22). Active zones with this behavior likely have R type channels present, as they were the only isolated VGCCs to show this characteristic (Fig. 30). However, many of the phenomena observed with all VGCCs presents cannot be accounted for by subtype isolation. Although a population of hotspots showed increased Ca^{2+} transients over the course of a train (Fig. 22), no individual VGCC subtype shows a strong preference for this activity. Indeed, all isolated VGCCs showed some level of inactivation over the course of the train.
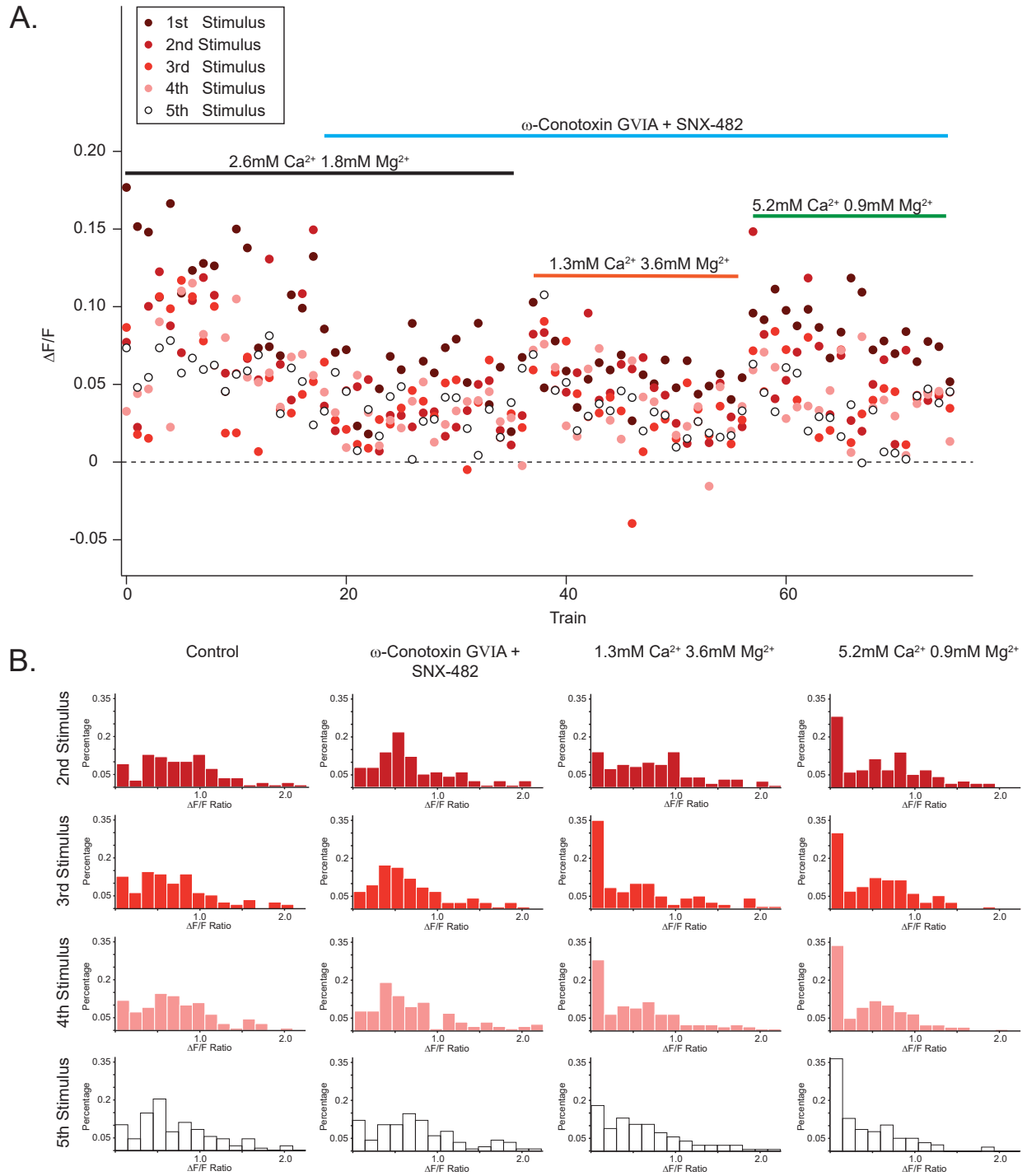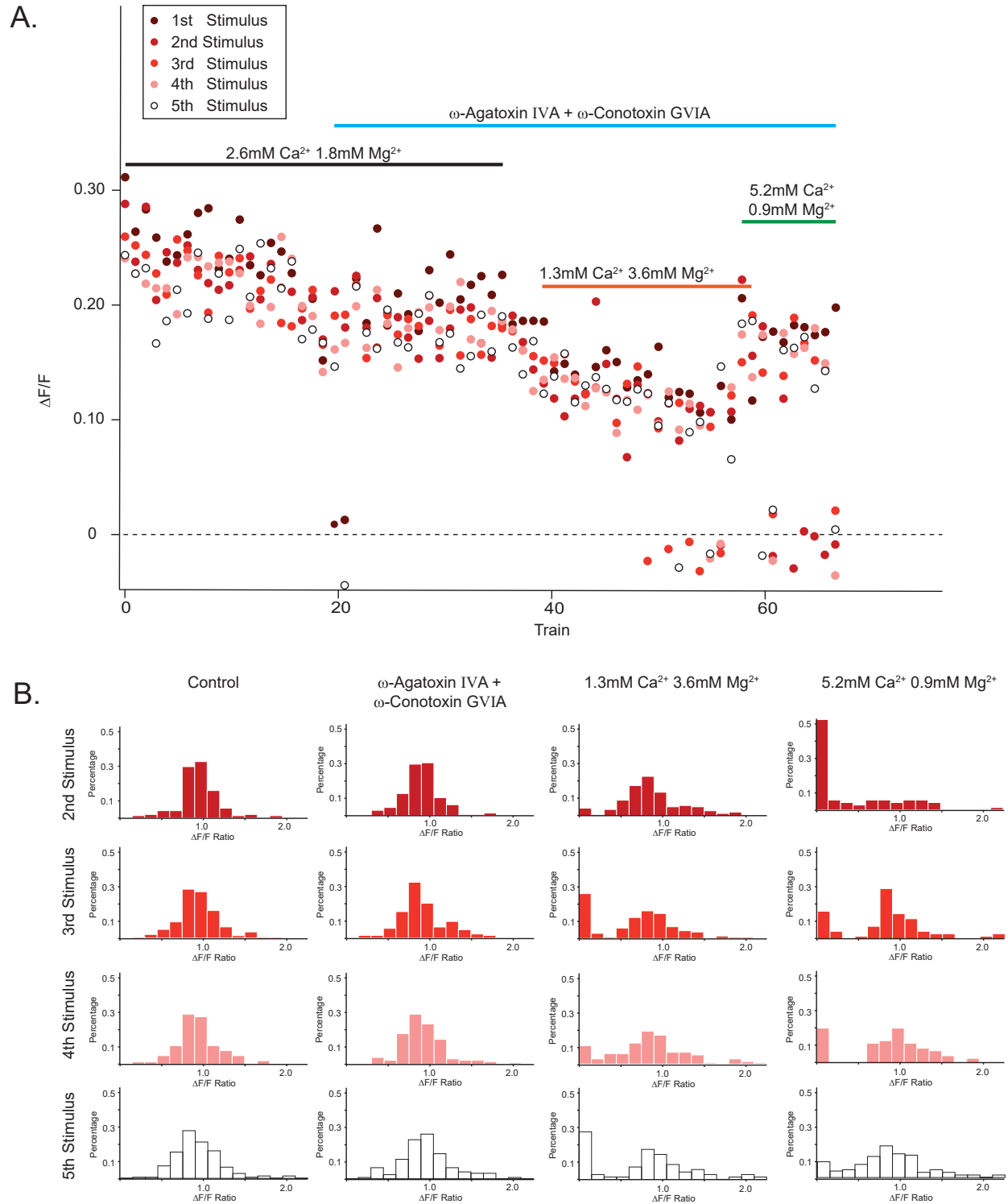
Figure 30. Example transients of calcium entry through isolated R-type VGCCs with 50hz stimulation and varying calcium and magnesium concentrations, in addition to histograms of all transients over all hotspots.

However, none of the individual VGCCs displayed [Ca^{2+}] dependent inactivation as strongly as when all VGCCs were present (Fig. 26). N-type channels resembled control hotspots the most, which is logical as N-type channels dominate in adult lamprey RS axons (Krieger et al., 1999; Photowala et al., 2005).
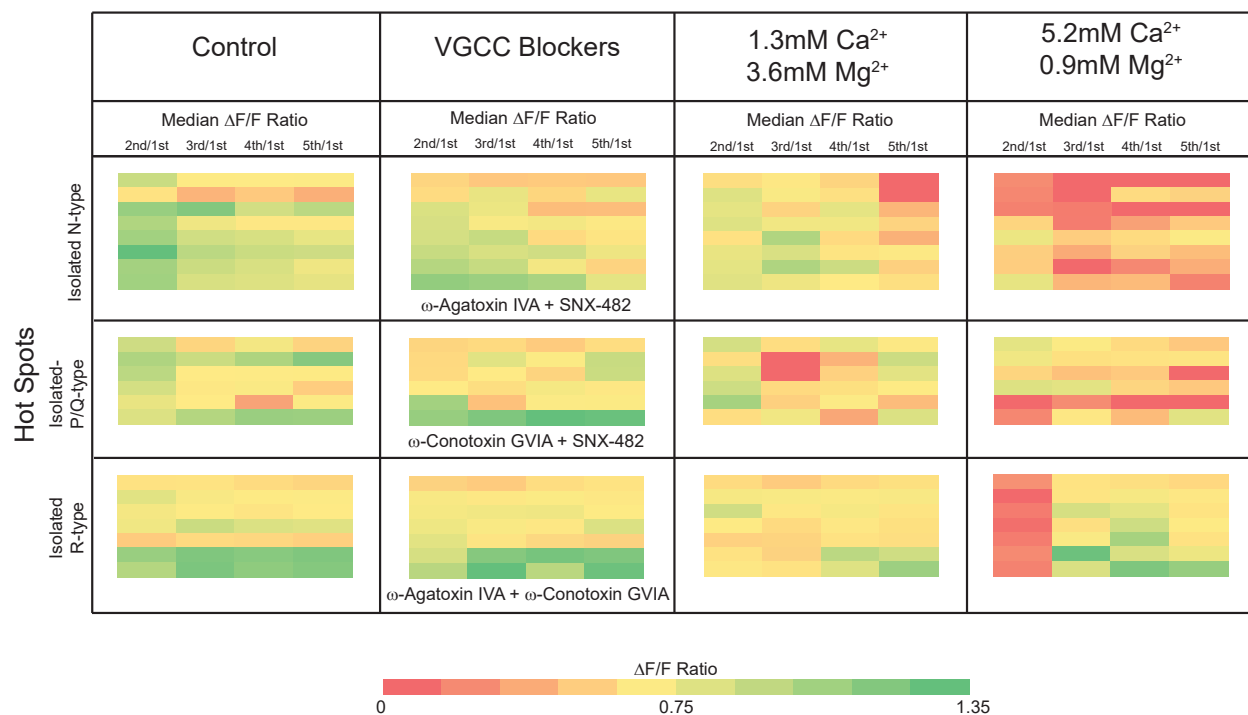
Figure 31. Heat Map of Calcium Transient Ratios through isolated VGCC subtypes over a 50Hz train of 5 stimuli across varying Calcium and Magnesium Concentrations. Each row represents the median ΔF/F Ratio to the 1st Ca^{2+} transient for a given hotspot over the course of the train.

This disparity between isolated VGCCs and the full complement of VGCCs suggests that the blockage of individual subtypes may have downstream effects, perhaps resulting in morphological changes in the active zone that alter Ca^{2+} transients. It is likely that active zone protein heterogeneity beyond VGCC subtype influences when a VGCC opens in response to an action potential and when it remains closed.

5.3 <u>**Discussion**</u>

Tight coupling of VGCCs to the fusion machinery at the active zone allows fast release of neurotransmitter in response to an action potential (Dodge and Rahamimoff, 1967; Heinemann et al., 1994; Schneggenburger and Neher, 2000). However, the likelihood of VGCC opening in response to each action potential has not been well studied. Utilizing a novel approach with the LLSM and taking advantage of a substantially improved signal to noise ratio, along with the use of lamprey giant reticulospinal axons that allow investigation of Ca^{2+} entry at individual active zones, I have shown that the probability of VGCC opening in response to a given action potential is stable at some active zones, and highly variable at others (Fig. 22). This is in stark contrast to older methods (either line-scanning confocal microscopy or wide field epifluorescence imaging) that did not allow us to observe this phenomenon and instead appeared to show that presynaptic Ca^{2+} transients were stable (Photowala et al., 2005). These previous results may have partially been due to the inability to resolve individual active zone transients over the diffuse background axonal signal. Observations made via the LLSM are more parsimonious with recordings of single Ca^{2+} channel conductance that showed individual VGCCs had low channel conductance, with only 1-4 channels opening at a time in a highly redundant population of VGCCs (Ramachandran, S., Thesis).

Ca^{2+} transients were stochastic in nature (Fig. 19), suggesting that populations of VGCCs were opening in response to a given stimulus. My methods are not able to determine the number of VGCCs in these cassettes. However, data from cell attached recordings and quantitative imaging indicate the number to be small perhaps even representing one VGCC, in line with previous studies showing only 1-4 channels open at once (Ramachandran dissertation). Over a train, VGCCs tend to drop out of participation, again in a stochastic nature (Fig. 21, 23), however some active zones instead show increased Ca^{2+} influx (Fig. 22). VGCCs are known to be modulated in a Ca^{2+}-dependent manner via CaM and downstream effects via CaMKII (Zamponi, 2003). The inactivation/facilitation of VGCC cassettes appears to follow this

Ca^{2+}-dependence for the majority of active zones, however, we did observe several hot spots that did not appear to have their probability of VGCC opening effected by $[Ca^{2+}]$ (Fig. 26).

Channel subtype partially explains this heterogeneity, with N-type channels showing the greatest degree of Ca^{2+} dependent inactivation, and R-type channels showing only transient inactivation (Fig. 31). However, no individual subtype could explain facilitation that was observed under control conditions (Fig. 22, 31). This leads us to believe that facilitation of Ca^{2+} influx over a train is not governed solely by VGCC subtype but rather by interactions that are disrupted when we apply channel blockers. For example, we know that all VGCC subtypes have some interaction with CaM, in addition to N and P/Q-type channels binding Syt-1 in low $[Ca^{2+}]$, as well as syntaxin-1A and SNAP-25 which lowers the inactivation voltage of VGCCs (Bezprozvanny et al., 1995; Wiser et al., 1996; Sheng et al., 1996; Zhong et al., 1999). By blocking VGCC subtypes we may be freeing up these proteins to find additional targets and modulating Ca^{2+} influx in unexpected ways.

By utilizing the LLSM I have been able to study Ca^{2+} transients at multiple active zones under physiologically relevant conditions in intact lamprey RS axons. This type of study has not been feasible before these advances in technology, as we have been limited in either field of view or speed of imaging. We have observed a large degree of variability in the behavior of VGCCs at individual active zones that appears to be stochastic in nature suggesting that open probability of VGCCs is relevant when studying P_r of a given synapse. This link will have to be more directly studied in future experiments.

6. DISCUSSION

Ca^{2+} plays a crucial role in the modulation of synaptic transmission. In this work I have studied this role from two angles: $G\beta\gamma$ inhibition which competes for Ca^{2+} binding, and variation of Ca^{2+} influx through VGCCs. The inhibition of synaptic transmission by the $G\beta\gamma$ subunit of the 5-HT-1B receptor is caused by competition between $G\beta\gamma$ and Syt-1 for binding of SNAP-25. When $G\beta\gamma$ binds SNAP-25 it modifies fusion to favor kiss-and-run (Photowala, 2006; Fang et al., 2008) . The resultant presynaptic inhibition is relieved in high $[Ca^{2+}]$ where Synaptotagmin outcompetes $G\beta\gamma$ for binding of SNAP-25. We studied the binding domains between $G\beta\gamma$ and SNAP-25 which led to the production of a mouse model that exhibits near normal synaptic transmission with reduced inhibition by 5-HT. Although the binding domains of $G\beta\gamma$ and Syt-1 were not found to be shared, and indeed the SNAP-25Δ3 did not mutate $G\beta\gamma$ binding domains directly, it is still likely that the binding of one protein occludes the other.

Relief of 5-HT inhibition occurs within 3 to 5 action potentials of a 50 Hz train (Gerachshenko et al., 2009). It is unclear whether the global $[Ca^{2+}]$ or the local $[Ca^{2+}]$ is more important for the relief of 5-HT mediated inhibition. The global rise in Ca^{2+} may reduce $G\beta\gamma$ binding sufficiently for subsequent transients to trigger release. In order for us to fully understand how Syt-1 outcompetes $G\beta\gamma$ during high frequency stimulation we must understand the dynamics of Ca^{2+} at active zones. Although we were not able to directly study $G\beta\gamma$ inhibition in tandem with our Ca^{2+} influx studies, we have begun to elucidate how VGGCs operate at individual synapses and have developed tools that will enable us to continue to study Ca^{2+} transients to further explore downstream effects of Ca^{2+} influx including the relief of $G\beta\gamma$ inhibition.

During high frequency stimulation, the global $[Ca^{2+}]$ rises steadily. This global rise in concentration is relatively small compared to the hyperlocal spikes produced in the nM region surrounding a VGCC during the brief window in which it is open. Global $[Ca^{2+}]$ may effect modulation of synaptic activity through Ca^{2+} targets such as Munc-13, RIM, Doc2, syt-7 and

complexin (Orita et al., 1997; Wang et al., 1997; Jackman et al., 2016; Walter et al., 2018). However, Syt-1 is highly sensitive to local $[Ca^{2+}]$ due to its relatively low affinity (Chapman et al., 2002). Since the local $[Ca^{2+}]$ is directly related to the probability of individual VGCC opening, understanding that probability is important for understanding the Ca^{2+}-synaptotagmin interaction as well as the ability for $G\beta\gamma$ to disrupt it.

Depending on the synapse, it has been estimated it only takes between one and five VGCCs opening to trigger release (Stanley, 1993; Shahrezaei et al., 2006; Bucurenciu et al., 2008) Our lab has previously shown that only 1-4 VGCCs open at a time amongst a larger population of VGCCs. I showed herein that Ca^{2+} transients were likewise variable and appeared to be stochastic in nature. Although our experiments did not directly study the relationship between Ca^{2+} influx at a single active zone and synaptic transmission, we did find active zones that did not reliably show opening of Ca^{2+} channels in response to an action potential. It is tempting to state that these active zones correspond to synapses that show a high number of synaptic transmission failures, however further studies must be done to prove this relationship.

Our data shows that local Ca^{2+} transients tend to be reduced under a paired pulse protocol as well as during high frequency stimulation, likely due to inactivation of VGCCs by Ca^{2+} dependent effectors. However, this is highly variable from active zone to active zone and from train to train. Some active zones display calcium dependent inhibition or facilitation of VGCCs, while others seem to be unaffected by $[Ca^{2+}]$. Although this may partially be due to VGCC subtype, in isolated studies, no individual subtype shared control condition characteristics. This suggests Ca^{2+} dependent effects on VGCCs are due to complex relationships between VGCC subtype and active zone microarchitecture which is disrupted when VGCC subtypes are blocked. Because Ca^{2+} transients are so brief, and synaptic transmission via Syt-1 requires large local $[Ca^{2+}]$ it is tempting to link the probability of VGCC opening to the probability of release. It would be interesting to see if the active zones we discovered that had PPRs <1 displayed STD and likewise if those synapses that had PPR >1

displayed STF. However, since global $[Ca^{2+}]$ rises even if an individual active zone fails to produce a Ca^{2+} transient, it is also possible that effects of global $[Ca^{2+}]$ from the summation of Ca^{2+} entry at all active zones lower the bar for release even when local VGCCs fail to open. Additionally, it is possible that the release of neurotransmitter throughout the train does not rely solely on Ca^{2+} binding to Syt-1 and instead employs additional Ca^{2+} sensors such as syt-7. Fully exploring these relationships in future studies will also aid in our understanding of how $G\beta\gamma$ inhibition is relieved under high frequency stimulation.

CITED LITERATURE

Abbott, L.F. and Regehr, W.G.: Synaptic computation. Nature 431:796-803, 2004

Acuna, C., Liu, X., Gonzalez, A., Südhof, T.C.: RIM-BPs mediate tight coupling of action potentials to Ca2+-triggered neurotransmitter release. Neuron 87:1234-1247, 2015

Ahmed, M. S., and Siegelbaum, S. A.: Recruitment of N-type Ca(21) channels during LTP enhances low release efficacy of hippocampal CA1 perforant path synapses. Neuron 63:372-385, 2009

Alabi A.A. and Tsien R.W.: Synaptic vesicle pools and dynamics. Cold Spring Harbor Perspectives in Biology 4:a013680, 2012

Arai, I. and Jonas, P.: Nanodomain coupling explains Ca(2)(+) independence of transmitter release time course at a fast central synapse. Elife 3:e04057, 2014

Aravamudan, B., Fergestad, T., Davis, W. S., Rodesch, C. K. and Broadie, K.: Drosophila UNC-13 is essential for synaptic transmission. Nature Neuroscience 2:965-971, 1999

Aravanis, A.M., Pyle, J.L., Harata, N.C., Tsien, R.W.: Imaging single synaptic vesicles undergoing repeated fusion events: kissing, running, and kissing again. Neuropharmacology 45:797-813, 2003

Armbruster, M., Messa, M., Ferguson, S.M., De Camilli, P. and Ryan, T.A.: Dynamin phosphorylation controls optimization of endocytosis for brief action potential bursts. eLife 2:e00845, 2013

Armstrong, C.M. and Matteson, D.R.: Two distinct populations of calcium channels in a clonal line of pituitary cells. Science 227:65-67, 1985

Atluri, P.P. and Regehr, W.G.: Determinants of the time course of facilitation at the granule cell to Purkinje cell synapse. Journal of Neuroscience 16:5661-5671.50, 1996

Augustin, I., Rosenmund, C., Südhof, T.C. and Brose, N.: Munc13-1 is essential for fusion competence of glutamatergic synaptic vesicles. Nature 400:45-461, 1999

Augustine, G.J., Adler, E.M., and Charlton, M.P.: (1991). The calcium signal for transmitter secretion from presynaptic nerve terminals. Annals of the New York Academy of Sciences 635:365-381, 1991

Bacaj, T., Wu, D., Yang, X.F., Morishita, W., Zhou, P., Xu, W., Malenka, R.C., Südhof, T.C.: Synaptotagmin-1 and synaptotagmin-7 trigger synchronous and asynchronous phases of neurotransmitter release. Neuron 80:947-959, 2013

Bai, J, Wang, C.T., Richards, D.A., Jackson, M.B. and Chapman, E.R.: Fusion pore dynamics are regulated by synaptotagmin t-SNARE interactions. Neuron 41:929-942, 2004

Bao, H., Goldschen-Ohm, M., Jeggle, P., Chanda, B., Edwardson, J.M. and Chapman, E.R.: Exocytotic fusion pores are composed of both lipids and proteins. Nature Structural Molecular Biology 23, 67-73, 2016

Bean, B.P.: Two kinds of calcium channels in canine atrial cells. Differences in kinetics, selectivity, and pharmacology. The Journal of General Physiology 86:1-30, 1985

Bennett, M.K., Calakos, N. and Scheller, R.H.: Syntaxin: a synaptic protein implicated in docking of synaptic vesicles at presynaptic active zones. Science 257:255-259, 1992

Bennett, M.K., and Scheller, R.H.: A molecular description of synaptic vesicle membrane trafficking. Annual Review of Biochemistry 63:63-100, 1994

Betke, K.M., Wells, C.A. and Hamm, H.E.: GPCR mediated regulation of synaptic transmission. Progress in Neurobiology 96:304-321, 2012

Betke, K.M., Rose, K.L., Friedman, D.B., Baucum, A.J., 2nd, Hyde, K., Schey, K.L. and Hamm, H.E.: Differential localization of G protein betagamma subunits. Biochemistry 53:2329-2343, 2014

Betz, A., Thakur, P., Junge, H. J., Ashery, U., Rhee, J. S., Scheuss, V., Rosenmund, C., Rettig, J. and Brose, N.: Functional interaction of the active zone proteins Munc13-1 and RIM1 in synaptic vesicle priming. Neuron 30:183-196, 2001

Bezprozvanny, I., Scheller, R.H., Tsien, R.W.: Functional impact of syntaxin on gating of N-type and Q-type calcium channels. Nature 378:623-626, 1995

Binz, T., Blasi, J., Yamasaki, S., Baumeister, A., Link, E., Südhof, T.C., Jahn, R. and Niemann, H.: Proteolysis of SNAP-25 by types E and A botulinal neurotoxins. Journal of Biological Chemistry 269:1617-1620, 1994

Blatow, M., Caputi, A., Burnashev, N., Monyer, H. and Rozov, A.:Ca2+ buffer saturation underlies paired pulse facilitation in calbindin-D28k-containing terminals. Neuron 38:79-88, 2003

Brown, D.A., Sihra, T.S.: Presynaptic signaling by heterotrimeric G-proteins. Handbook of Experimental Pharmacology 184:207-260, 2008

Blackmer, T., Larsen, E.C., Takahashi, M., Martin, T.F., Alford, S., and Hamm, H.E.: G protein betagamma subunit-mediated presynaptic inhibition: regulation of exocytotic fusion downstream of Ca2+ entry. Science 292:293-297, 2001

Blackmer, T., Larsen, E.C., Bartleson, C., Kowalchyk, J.A., Yoon, E.J., Preininger, A.M., Alford, S., Hamm, H.E., and Martin, T.F.: G protein betagamma directly regulates SNARE protein fusion machinery for secretory granule exocytosis. Nature Neuroscience 8:421-425, 2005

Blatow, M., Caputi, A., Burnashev, N., Monyer, H. and Rozov, A.: Ca2+ buffer saturation underlies paired pulse facilitation in calbindin-D28k-containing terminals. Neuron 38:79-88, 2003

Bleckert, A., Photowala, H., Alford, S.: Dual pools of actin at presynaptic terminals. Journal of Neurophysiology 107(12):3479-92, 2012

van den Bogaart, G., Holt, M.G., Bunt, G. Riedel, D., Wouters, F.S and Jahn, R.: One SNARE complex is sufficient for membrane fusion. Nature Structural and Molecular Biology 3:358-364, 2010

Böhme, M. A., Beis, C., Reddy-Alla, S., Reynolds, E., Mampell, M. M., Grasskamp, A. T., Lützkendorf, J. et al.: Active zone scaffolds differentially accumulate Unc13 isoforms to tune Ca 2C channel – vesicle coupling. Nature Neuroscience 19:1311-1320, 2016

Böhme, M. A., Grasskamp, A.T. and Walter, A.M.: Regulation of synaptic release-site Ca 2+ channel coupling as a mechanism to control release probability and short-term plasticity. FEBS Letters 592:3516-353, 2018

Bollmann, J.H., Sakmann, B. and Borst, J.G.: Calcium sensitivity of glutamate release in a calyx-type terminal. Science 289:953-957, 2000

Bornschein, G., and Schmidt, H.: Synaptotagmin Ca^{2+} sensors and their spatial coupling to presynaptic Ca_v channels in central cortical synapses. Frontiers in Molecular Neuroscience 11:494, 2019

Bourinet, E., Soong, T.W., Sutton, K., Slaymaker, S., Mathews, E., Monteil, A., Zamponi, G.W., Nargeot, J. and Snutch, T.P.: Splicing of alpha 1A subunit gene generates phenotypic variants of P- and Q-type calcium channels. Nature Neuroscience 2:407-415, 1999

Bourne, J., Morgan, J.R. and Pieribone, V.A.: Actin polymerization regulates clathrin coat maturation during early stages of synaptic vesicle recycling at lamprey synapses. Journal of Comparative Neurology 497:600-609, 2006

Breckenridge, L.J., Almers, W.: Currents through the fusion pore that forms during exocytosis of a secretory vesicle. Nature 328:814-817, 1987

Brodin, L., Grillner, S., Dubuc, R., Ohta, Y., Kasicki, S. and Hökfelt, T.: Reticulospinal neurons in lamprey: transmitters, synaptic interactions and their role during locomotion. Archives Italiennes de Biologie 126:317-345, 1998

Brodin, L. and Shupliakov, O.: Giant reticulospinal synapse in lamprey: molecular links between active and periactive zones. Cell and Tissue Research 326:301-310, 2006

Brose, N., Petrenko, A.G., Südhof, T.C., and Jahn, R.: Synaptotagmin: a calcium sensor on the synaptic vesicle surface. Science 256:1021-1025, 1992

Buchanan, J.T., Brodin, L., Dale, N. and Grillner, S.: Reticulospinal neurons activate excitatory amino acid receptors. Brain Research 408:321-325, 1987

Buchanan, J.T. and Grillner, S.: 5-Hydroxytryptamine depresses reticulospinal excitatory postsynaptic potentials in motoneurons of the lamprey. Neuroscience Letters 122:71-74, 1991

Buchanan, J.T.: Contributions of identifiable neurons and neuron classes to lamprey vertebrate neurobiology. Progress in Neurobiology 63(4):441-466, 2001

Bucurenciu, I., Kulik, A., Schwaller, B., Frotscher, M., and Jonas, P.: Nanodomain coupling between Ca21 channels and Ca21 sensors promotes fast and efficient transmitter release at a cortical GABAergic synapse. Neuron 57:536-545, 2008

Bucurenciu, I., Bischofberger, J., and Jonas, P.: A small number of open Ca2+ channels trigger transmitter release at a central GABAergic synapse.: Nature Neuroscience 13(1):19-21, 2010

Cabrera-Vera, T.M., Vanhauwe, J., Thomas, T.O., Medkova, M., Preininger, A., Mazzoni, M.R. and Hamm, H.E.: Insights into G protein structure, function, and regulation. Endocrine Reviews 24:765-781, 2003

Calloway, N., Gouzer, G., Xue, M. and Ryan, T. A. The active- zone protein Munc13 controls the use dependence of presynaptic voltage- gated calciumc hannels. eLife 4:e07728, 2015

Cao, Y.Q., Piedras-Rentería, E.S., Smith, G.B., Chen, G., Harata, N.C., and Tsien, R.W.: Presynaptic Ca2+ channels compete for channel type-preferring slots in altered neurotransmission arising from Ca2+ channelopathy. Neuron 43:387-400, 2004

Catterall, W.A.: Structure and regulation of voltage-gated Ca2+channels. Annual Review of Cell and Developmental Biology 16: 521-555, 2000

Catterall, W.A. and Few, A.P.: Calcium channel regulation and presynaptic plasticity. Neuron 59: 882-901, 2008

Catterall, W.A.: Ion channel voltage sensors: structure, function, and pathophysiology. Neuron 67:915-928, 2010

Ceccarelli, B., Hurlbut, W.P., Mauro, A.: Depletion of vesicles from frog neuromuscular junctions by prolonged tetanic stimulation. Journal of Cellular Biology 54:30-38, 1972

Chang, S., Trimbuch, T. and Rosenmund, C.: Synaptotagmin-1 drives synchronous Ca2+-triggered fusion by C2B-domain-mediated synaptic vesicle-membrane attachment. Nature Neuroscience 21:33-40, 2018

Chapman, E.R. and Jahn, R.: Calcium-dependent interaction of the cytoplasmic region of synaptotagmin with membranes-autonomous function of a single C2-homologous domain. Journal of Biological Chemistry 269:5735-5741, 1994

Chapman, E.R., Hanson, P.I., An, S. and Jahn, R.: Ca2+ regulates the interaction between synaptotagmin and syntaxin 1. Journal of Biological Chemistry 270:23667-23671, 1995

Chapman, E.R.: Synaptotagmin: a Ca2+ sensor that triggers exocytosis? Nature Reviews Molecular and Cellular Biology 3:498-508, 2002

Chaudhuri, D., Alseikhan, B.A., Chang, S.Y., Soong, T.W., Yue, D.T.: Developmental activation of calmodulin-dependent facilitation of cerebellar P-type Ca2+current. Journal of Neuroscience 25:8282-8294, 2005

Chaudhuri, D., Issa, J.B., and Yue, D.T.: Elementary mechanisms producing facilitation of Cav2.1 (P/Q-type) channels. The Journal of General Physiology 129:385-401, 2007

Chen, B-C., Legant, W.R., Wang, K., Shao, L., Milkie, D.E., Davidson, M.W., Janetopoulos, C., et al.: Lattice light-sheet microscopy: Imaging molecules to embryos at high spatiotemporal resolution. Science 346(6208):1257998, 2014

Chen, X., Tomchick, D.R., Kovrigin, E., Arac¸ D., Machius, M., Südhof, T.C. and Rizo, J.: Three-dimensional structure of the complexin/SNARE complex. Neuron 33:397-409, 2002

Chernomordik, L.V., Frolov, V.A., Leikina, E., Bronk, P. and Zimmerberg, J.: The pathway of membrane fusion catalyzed by influenza hemagglutinin: restriction of lipids, hemifusion, and lipidic fusion pore formation. Journal of Cell Biology 140:1369-1382, 1998

Chernomordik, L.V. and Kozlov, M.M.: Mechanics of membrane fusion. Nature Structural and Molecular Biology 15:675-683, 2008

Chiang, H.C., Shin, W., Zhao, W.D., Hamid, E., Sheng, J., Baydyuk, M., Wen, P.J., Jin, A., Momboisse, F. and Wu, L.G.: Post-fusion structural changes and their roles in exocytosis and endocytosis of dense-core vesicles. Nature Communications 5:3356, 2014

Chieregatti, E., Witkin, J.W. and Baldini, G.: SNAP-25 and synaptotagmin 1 function in Ca2+-dependent reversible docking of granules to the plasma membrane. Traffic 3:496-511, 2002

Christensen, S.M., Mortensen, M.W. and Stamou, D.G.: Single vesicle assaying of SNARE-synaptotagmin-driven fusion reveals fast and slow modes of both docking and fusion and intrasample heterogeneity. Biophysical Journal 100:957-967, 2011

Christie, J. M., Chiu, D. N. and Jahr, C. E.: Ca2-dependent enhancement of release by subthreshold somatic depolarization. Nature Neuroscience 14:62-68, 2010

Clapham, D.D. and Neer, E.J.: New roles for G-protein betagamma-dimers in transmembrane signalling. Nature 365:403-406, 1993

Clapham, D.E. and Neer, E.J.: G protein betagamma subunits. Annual Review of Pharmacology and Toxicology 37:167-203, 1997

Cochilla, A.J. and Alford, S.T.: Metabotropic glutamate receptor-mediated control of neurotransmitter release. Neuron 20(5):1007-1016, 1998

Cochilla, A.J. and Alford, S.T.: NMDA receptor-mediated control of presynaptic calcium and neurotransmitter release. The Journal of Neuroscience 19(1):193-205, 1999

Criado, M., Gil, A., Viniegra ,S., and Gutiérrez, L.M.: A single amino acid near the C terminus of the synaptosome associated protein of 25 kDa (SNAP-25) is essential for exocytosis in chromaffin cells. Proceedings of the National Academy of Science USA 96:7256-7261, 1999

Davies, J.N., Jarvis, S.E., and Zamponi,G.W.: Bipartite syntaxin 1A interactions mediate CaV2.2 calcium channel regulation. Biochemical and Biophysical Research Communications 411:562-568, 2011

Davletov, B.A., and Südhof, T.C.: A single C2 domain from synaptotagmin I is sufficient for high affinity Ca2+/phospholipid binding. J. Biological Chemistry 268:26386-26390, 1993

De Waard, M., Hering, J., Weiss, N., and Feltz, A.: How do G proteins directly control neuronal Ca2+ channel function? Trends in Pharmacological Sciences 26:427-436, 2005

Delaney, A.J., Crane, J.W., and Sah, P.: Noradrenaline modulates transmission at a central synapse by a presynaptic mechanism. Neuron 56:880-892, 2007

DeMaria, C.D., Soong, T.W., Alseikhan, B.A., Alvania, R.S. and Yue, D.T.: Calmodulin bifurcates the local Ca2+ signal that modulates P/Q-type Ca2+ channels. Nature 411:484-489, 2001

Dittman, J.S., Kreitzer, A.C. and Regehr, W.G.: Interplay between facilitation, depression, and residual calcium at three presynaptic terminals. Journal of Neuroscience 20:1374-1385, 2000

Dodge, Jr., F.A. and Rahamimoff,, R.: Co-operative action of calcium ions in transmitter release at the neuromuscular junction. Journal of Physiology 193:419-432, 1967

Dolphin, A.C.: G protein modulation of voltage-gated calcium channels. Pharmacological Reviews 55:607-627, 2003

Dubel, S.J., Starr, T.V., Hell, J., Ahlijanian, M.K., Enyeart, J.J., Catterall, W.A. and Snutch, T.P. Molecular cloning of the alpha-1 subunit of an omegaconotoxin-sensitive calcium channel. Proceedings of the National Academy of Science USA 89:5058-5062,1992

Dulubova, I., Sugita, S., Hill, S., Hosaka, M., Fernandez, I., Südhof, T.C. and Rizo, J.: A conformational switch in syntaxin during exocytosis: role of munc18. EMBO Journal 18:4372-4382, 1999

Dulubova, I., Khvotchev, M., Liu, S., Huryeva, I., Sudhof, T.C. and Rizo, J.: Munc-18 binds directly to the neuronal SNARE complex: Proceedings of the National Academy of Science 104:2697-2702, 2007

Edelstein, A., Amodaj, N., Hoover, K., Vale, R., Stuurman, N.: Computer control of microscopes using microManager. Current Protocols in Molecular Biology Chapter 14:Unit14 20, 2010

el Manira, A. and Bussières N.: Calcium channel subtypes in lamprey sensory and motor neurons. Journal of Neurophysiology 78:1334-1340, 1997

Erickson, M.G., Alseikhan, B.A., Peterson, B.Z. and Yue, D.T.: Preassociation of calmodulin with voltage-gated Ca(2+) channels revealed by FRET in single living cells. Neuron 31:973-985, 2001

Fang, Q., Berberian, K., Gong, L-W, Hafez, I., Sørensen, J.B., and Lindau, M.: The role of the C terminus of the SNARE protein SNAP-25 in fusion pore opening and a model for fusion pore mechanics. Proceedings of the National Academy of Science USA 105:15388-15392, 2008

Fang, Q., Zhao, Y., Herbst, A.D., Kim, B.N., and Lindau, M.: Positively charged amino acids at the SNAP-25 C terminus determine fusion rates, fusion pore properties, and energetics of tight SNARE complex zippering. Journal of Neuroscience 35:3230-3239, 2015

Fernandez, I., Ubach, J., Dulubova, I., Zhang, X., Südhof, T.C. and Rizo,J.: Three-dimensional structure of an evolutionarily conserved N-terminal domain of syntaxin 1A. Cell 94:841-849, 1998

Fernandez-Busnadiego, R., Zuber, B., Maurer, U.E., Cyrklaff, M., Baumeister, W., Lucic, V.: Quantitative analysis of the native presynaptic cytomatrix by cryoelectron tomography. Journal of Cellular Biology 188(1):145–156, 2010

Fernández-Chacón, R., Königstorfer, A., Gerber, S.H., Garcíía, J., Matos, M.F., Stevens, C.F., Brose, N., Rizo, J., Rosenmund, C., and Südhof, T.C.: Synaptotagmin I functions as a calcium regulator of release probability. Nature 410:41-49, 2001

Fernández-Chacón, R. and Alvarez de Toledo, G.: Cytosolic calcium facilitates release of secretory products after exocytotic vesicle fusion. FEBS Letters 363:221-225, 1995

Ferro-Novick, S., and Jahn, R.: Vesicle fusion from yeast to man Nature 370:191-193, 1994

Fesce, R., Grohovaz, F., Valtorta, F. and Meldolesi, J.: Neurotransmitter release: fusion or 'kiss-and-run'? Trends in Cell Biology 4:1-4, 1994

Fiebig, K.M., Rice, L.M., Pollock, E., and Brunger, A.T.: Folding by C2-domain peptides implicates synaptotagmin in exocytosis. intermediates of SNARE complex assembly. Nature Structural Biology 6:117-123, 1999

Forsythe, I.D., Tsujimoto, T., Barnes-Davies, M., Cuttle, M.F., Takahashi, T.: Inactivation of presynaptic calcium current contributes to synaptic depression at a fast central synapse. Neuron 20:797-807, 1998

Gandasi, N.R. and Barg, S.: Contact-induced clustering of syntaxin and munc18 docks secretory granules at the exocytosis site. Nature Communications 5:3914, 2014

Gandhi, S.P. and Stevens, C.F.: Three modes of synaptic vesicular recycling revealed by single-vesicle imaging. Nature 423:607-613, 2003

Gao, L., Shao, L., Chen, B.-C. and Betzig, E.: 3D live fluorescence imaging of cellular dynamics using Bessel beam plane illumination microscopy. Nature Protocols 9:1083-1101, 2014

Gao, Y., Zorman, S., Gundersen, G., Xi, Z., Ma, L., Sirinakis, G., Rothman, J.E. and Zhang, Y.: Single reconstituted neuronal SNARE complexes zipper in three distinct stages. Science 337:1340-1343, 2012

Gautam, N., Downes, G.B., Yan,K., Kisselev, O.: The G-protein betagmaa complex. Cell Signaling 10(7):447-455, 1998

Geppert, M., Goda, Y., Hammer, R.E., Li, C., Rosahl, T.W., Stevens, C.F., and Südhof, T.C.: Synaptotagmin I: a major Ca2+ sensor for transmitter release at a central synapse. Cell 79,717-727, 1994

Gerachshenko, T., Blackmer, T., Yoon, E.J., Bartleson, C., Hamm, H.E. and Alford, S.: G betagamma acts at the C terminus of SNAP-25 to mediate presynaptic inhibition. Nature Neuroscience 8:597-605, 2005

Gerachshenko, T., Schwartz, E., Bleckert, A. Photowala, H., Seymour, A., and Alford, S.: Presynaptic G-protein-coupled receptors dynamically modify vesicle fusion, synaptic cleft glutamate concentrations, and motor behavior. Journal of Neuroscience 29(33):10221-10233, 2009

Gerber, S.H., Rah, J.C., Min, S.W., Liu, X., de Wit, H., Dulubova, I., Meyer, A.C., Rizo, J. et al.: Conformational switch of syntaxin-1 controls synaptic vesicle fusion. Science 321:1507-1510, 2008

Gerona, R.R., Larsen, E.C., Kowalchyk, J.A. and Martin, T.F.: The C terminus of SNAP25 is essential for Ca2+-dependent binding of synaptotagmin to SNARE complexes. Journal of Biological Chemistry 275:6328-6336, 2000

Ghelani, T. and Sigrist, J.: Coupling the structural and functional assembly of synaptic release sites. Frontiers in Neuroanatomy 12:81, 2018

Gil, A., Gutiérrez, L.M., Carrasco-Serrano, C., Alonso, M.T., Viniegra, S., and Criado, M.: Modifications in the C terminus of the synaptosome-associated protein of 25 kDa (SNAP-25) and in the complementary region of synaptobrevin affect the final steps of exocytosis. Journal of Biological Chemistry 277:9904-9910, 2002

Goswami, S. P., Bucurenciu, I. and Jonas, P.: Miniature IPSCs in hippocampal granule cells are triggered by voltage-gated Ca2 channels via microdomain coupling. Journal of Neuroscience 32:14294-14304, 2012

Gracheva, E.O., Hadwiger, G., Nonet, M.L., and Richmond, J.E.: Direct interactions between C. elegans RAB-3 and Rim provide a mechanism to target vesicles to the presynaptic density. Neurosci Lett 444:137-142, 2008

Groffen, A.J., Martens, S., Arazola, R.D., Cornelisse, L.N., Lozovaya, N., de Jong, A.P.H.,Goriounova, N.A. et al.: Doc2b is a high-affinity Ca2+ sensor for spontaneous neurotransmitter release. Science 327(5973):1614-1618, 2010

Grote, E., Carr, C.M., and Novick, P.J.: Ordering the final events in yeast exocytosis. Journal of Cellular Biology 151:439-452, 2000

Gustafsson, J.S., Birinyi, A., Crum, J., Ellisman, M., Brodin, L. and Shupliakov, O.: Ultrastructural organization of lamprey reticulospinal synapses in three dimensions. Journal of Comparitive Neurology 450:167-182, 2002

Hallermann. S., Fejtova. A., Schmidt. H., Weyhersmuller, A., Silver, R.A., Gundelfinger, E.D. and Eilers, J.: Bassoon speeds vesicle reloading at a central excitatory synapse. Neuron 68: 710-723, 2010a

Hallermann, S., Heckmann, M. and Kittel, R.J.: Mechanisms of short-term plasticity at neuromuscular active zones of Drosophila. Human Frontier Science Program J4:72-84, 2010b

Hamid, E., Church, E., Wells, C.A., Zurawski, Z., Hamm, H.E. and Alford, S.: Modulation of neurotransmission by GPCRs is dependent upon the microarchitecture of the primed vesicle complex. Journal of Neuroscience 34:260-274, 2014

Hammarlund, M., Palfreyman, M.T., Watanabe, S., Olsen, S., and Jorgensen, E.M.: Open syntaxin docks synaptic vesicles. PLOS Biology 5:e198, 2007

Han, X., Wang, C. T., Bai, J., Chapman, E. R., and Jackson, M. B.: Transmembrane segments of syntaxin line the fusion pore of Ca2+-triggered exocytosis. Science 304,289-292, 2004

Han, Y., Kaeser, P.S., Südhof, T.C. and Schneggenburger, R.: RIM determines Ca2+ channel density and vesicle docking at the presynaptic active zone. Neuron 69:304-316, 2011

Hanson, P.I., Roth, R., Morisaki, H., Jahn, R., and Heuser, J.E.: Structure and conformational changes in NSF and its membrane receptor complexes visualized by quick-freeze/deep-etch electron microscopy. Cell 90:523-535, 1997

Harata, N.C., Pyle, J.L., Arvanis, A.M., Mozhayeva, M., Kavalali, E,T., and Tsien, R.W.: Limited numbers of recycling vesicles in small CNS nerve terminals: implications for neural signaling and vesicular cycling. TRENDS in Neurosciences 24:637-643, 2001

Harata, N.C., Choi, S., Pyle, J.L., Aravanis, A.M., Tsien, R.W.: Frequency dependent kinetics and prevalence of kiss-and-run and reuse at hippocampal synapses studied with novel quenching methods. Neuron 49:243-256, 2006

Harlow, M. L., Ress, D., Stoschek, A., Marshall, R. M. and McMahan U. J.: The architecture of active zone material at the frog's neuromuscular junction. Nature 409:479-484, 2001

Hata, Y., Slaughter, C.A. and Südhof, T.C.: Synaptic vesicle fusion complex contains unc-18 homologue bound to syntaxin. Nature 366:347-351, 1993

Hatsuzawa, K., Lang, T., Fasshauer, D., Bruns, D., and Jahn, R. The R-SNARE motif of tomosyn forms SNARE core complexes with syntaxin 1 and SNAP-25 and down-regulates exocytosis. Journal of Biological Chemistry 278:31159-31166, 2003

Heinemann, C., Chow, R.H., Neher, E. and Zucker, R.S.: Kinetics of the secretory response in bovine chromaffin cells following flash photolysis of caged Ca2+. Biophysical Journal 67:2546-2557, 1994

Hernandez, J.M., Stein, A., Behrmann, A., Riedel, D., Cypionka, A., Farsi, Z., Walla, P.J., Raunser, S. Jahn, R.: Membrane fusion intermediates via directional and full assembly of the SNARE complex. Science 336:1581-1584, 2012

Hess, D.T., Slater, T.M., Wilson, M.C., and Skene, J.H.P.: The 25 kDa Synaptosomal-associated Protein SNAP-25 Is the Major Methionine-Rich Polypeptide in Rapid Axonal Transport and a Major Substrate for Palmitoylation in Adult CNS. The Journal of Neuroscience 12:4634-4641, 1992

Heuser, J.E., Reese, T.S.: Evidence for recycling of synaptic vesicle membrane during transmitter release at the frog neuromuscular junction. Journal of Cellular Biology 1973(57):315-344, 1973

Heuser J.E., Reese, T.S., Dennis, M.J., Jan, Y., Jan, L., Evans, L.: Synaptic vesicle exocytosis captured by quick freezing and correlated with quantal transmitter release. Journal of Cell Biology 81(2): 275-300, 1979

Hibino, H., Pironkova, R., Onwumere, O., Vologodskaia, M., Hudspeth, A.J. and Lesage, F.: RIM binding proteins (RBPs) couple Rab3-interacting molecules (RIMs) to voltage-gated Ca(2+) channels. Neuron 34:411-423, 2002

Hille, B.: Modulation of ion-channel function by G-protein-coupled receptors. Trends in Neuroscience 17:531-536, 1994

Holroyd, P., Lang, T., Wenzel, D., De Camilli, P., and Jahn, R.: Imaging direct, dynamin-dependent recapture of fusing secretory granules on plasma membrane lawns from PC12 cells. Proceedings of the National Academy of Science USA 99:16806-16811, 2002

Hoppa, M. B., Lana, B., Margas, W., Dolphin, A. C. and Ryan, T. A.: alpha 2 delta expression sets presynaptic calcium channel abundance and release probability. Nature 486:122-125, 2012

Hoppa, M. B., Gouzer, G., Armbruster, M. and Ryan, T. A.: Control and plasticity of the presynaptic action potential waveform at small CNS nerve terminals. Neuron 84:778-789, 2014

Ikeda, S.R.: Voltage-dependent modulation of N-type calcium channels by G-protein betagamma subunits. Nature 380:255–-58, 1996

Ikeda, S.R. and Dunlap, K.: Voltage-dependent modulation of N-type calcium channels: role of G protein subunits. Advances in Second Messenger Phosphoprotein Research 33:131-151, 1999

Iremonger, K.J.and Bains, J.S.: Retrograde opioid signaling regulates glutamatergic transmission in the hypothalamus. Journal of Neuroscience 29:7349-7358, 2009

Ishizuka, T., Saisu, H., Odani, S. and Abe, T.: Synaphin: a protein associated with the docking/fusion complex in presynaptic terminals. Biochemical and Biophysical Research Communications 213:1107-1114, 1995

Jackman, S.L., Turecek, J., Belinsky, J.E. and Regehr, W.G.: The calcium sensor synaptotagmin 7 is required for synaptic facilitation. Nature 529:88-91, 2016

Jackman, S.L. and Regehr, W.G.: The mechanism and functions of synaptic facilitation. Neuron 94(3):447-464, 2017

Jarvis, S.E., Magga, J.M., Beedle, A.M., Braun, J.E., and Zamponi, G.W.: G protein modulation of N-type calcium channels is facilitated by physical interactions between syntaxin 1A and G betagamma. Journal of Biological Chemistry 275:6388-6394, 2000

Jarvis, S.E., Zamponi, G.W.: Distinct molecular determinants govern syntaxin1A-mediated inactivation and G-protein inhibition of N-type calcium channels. Journal Neuroscience 21:2939-2948, 2001

Jarvis, S.E., Barr, W., Feng, Z.P., Hamid, J. and Zamponi, G.W.: Molecular determinants of syntaxin 1 modulation of N-type calcium channels. Journal of Biological Chemistry 277:44399-44407, 2002

Jones, S.A., Shim, S.-H., He, J. and Zhuang, X. Fast, three-dimensional super-resolution imaging of live cells. Nature Methods 8:499–508,2011

Junge, H.J., Rhee, J.S., Jahn, O., Varoqueaux, F., Spiess, J., Waxham, M.N., Rosenmund, C. and Brose, N.: Calmodulin and Munc13 form a Ca2+ sensor/effector complex that controls short-term synaptic plasticity. Cell 118:389-401, 2004

Kaeser, P.S., Deng, L., Wang, Y., Dulubova, I., Liu, X., Rizo, J., and Südhof, T.C.: RIM proteins tether Ca2+ channels to presynaptic active zones via a direct PDZ-domain interaction. Cell 144:282–295, 2011

Kaneko, S., Cooper, C.B., Nishioka, N., Yamasaki, H., Suzuki, A., Jarvis, S.E., Akaike, A., Satoh, M. and Zamponi, G.W. Identification and characterization of novel human Ca(v)2.2 (alpha 1B) calcium channel variants lacking the synaptic protein interaction site. Journal of Neuroscience 22:82-92, 2002

Katz, B. and Miledi, R.: The role of calcium in neuromuscular facilitation. Journal of Physiology 195:481-492, 1968

Katz, B. and Miledi, R.: Further study of the role of calcium transmission. Journal of Physiology 207(3):789-801, 1970

Kavalali, E.T.: The mechanisms and functions of spontaneous neurotransmitter release. Nature Reviews Neurosceince 16:5-14, 2015

Kim, S.H., and Ryan, T.A.: Balance of calcineurin Aalpha and CDK5 activities sets release probability at nerve terminals. The Journal of Neuroscience 33(21):8937-8950, 2013

Kittel, R.J., Wichmann, C., Rasse, T.M., Fouquet, W., Schmidt, M., Schmid, A., Wagh, D.A., et al., Bruchpilot promotes active zone assembly, Ca2+ channel clustering, and vesicle release. Science 312:1051-1054, 2006

Klyachko, V.A. and Jackson, M.B.: Capacitance steps and fusion pores of small and large-dense-core vesicles in nerve terminals. Nature 418:89-92, 2002

Koch, W.J., Inglese, J., Stone, W.C., and Lefkowitz, R.J.: The binding site for the betagamma subunits of heterotrimeric G proteins on the beta-adrenergic receptor kinase. Journal of Biological Chemistry 268:8256-8260, 1993

Kochubey, O. and Schneggenburger, R.: Synaptotagmin increases the dynamic range of synapses by driving Ca2+-evoked release and by clamping a near-linear remaining Ca2+ sensor. Neuron 69(4): 736-748, 2011

Koushika, S. P., Richmond, J. E., Hadwiger, G., Weimer, R. M., Jorgensen, E. M., and Nonet, M. L.: A post-docking role for active zone protein Rim. Nature Neuroscience 4:997–1005, 2001

Komatsu, M., Schermerhorn, T., Aizawa, T., Sharp, G.W.: Glucose stimulation of insulin release in the absence of extracellular Ca2+ and in the absence of any increase in intracellular Ca2+ in rat pancreatic islets. Proceedings of the National Academy of Science USA 92(23): 10728-10732, 1995

Kononenko, N.L. and Haucke, V.: Molecular Mechaniss of Presynaptic Membrane Retrieval and Synaptic Vesivle formation: Neuron 85:484-496, 2015

Kozlov, M.M. and Chernomordik, L.V.: A mechanism of protein-mediated fusion: Coupling between refolding of the influenza hemagglutinin and lipid rearrangements. Biophysical Journal 75:1384-1396, 1998

Krieger, P., Büschges, A. and el Manira, A.: Calcium channels involved in synaptic transmission from reticulospinal axons in lamprey. Journal of Neurophysiology 81:1699-1705, 1999

Kümmel, D., Krishnakumar, S.S., Radoff, D.T., Li F., Giraudo, C.G., Pincet, F., Rothman, J.E. and Reinisch, K.M.: Complexin cross-links prefusion SNAREs into a zigzag array. Nature Structural Molecular Biology 18:927-933, 2011

Kyoung, M., Srivastava, A., Zhang, Y., Diao, J., Vrljic, M., Grob, P., Nogales, E., Chu, S., Brunger, A.T.: In vitro system capable of differentiating fast Ca2+-triggered content mixing from lipid exchange for mechanistic studies of neurotransmitter release. Proceedings of the National Academy of Science USA 108:E304-E313, 2011

Ladera C., del Carmen Godino, M., José Cabañero, M., Torres, M., Watanabe, M., Luján, R., Sánchez-Prieto, J.: Pre-synaptic GABA receptors inhibit glutamate release through GIRK channels in rat cerebral cortex. Journal of Neurochemistry 107:1506-1517, 2008

Lai, A.L., Tamm, L.K., Ellena, J.F. and Cafiso, D.S.: Synaptotagmin 1 modulates lipid acyl chain order in lipid bilayers by demixing phosphatidylserine. Journal of Biological Chemistry 286:25291-25300, 2011

Leal, K., Mochida, S., Scheuer, T., and Catterall, W. A., Fine-tuning synaptic plasticity by modulation of CaV2.1 channels with calcium sensor proteins. Proceedings of the National Academy of Science USA 109:17069-17074, 2012

Lee, A., Wong, S.T., Gallagher, D., Li, B., Storm, D.R., Scheuer, T., Catterall, W.A.: Ca2+/calmodulin binds to and modulates P/Q-type calcium channels. Nature 399:155-159, 1999

Lee, A., Zhou, H., Scheuer, T. and Catterall, W.A.: Molecular determinants of Ca(2+)/calmodulin-dependent regulation of Ca(v)2.1 channels. Proceedings of the National Academy of Science USA 100:16059-16064, 2003

Lindau, M., Hall, B.A., Chetwynd, A., Beckstein, O. and Sansom, M.S.P.: Coarse-grain simulations reveal movement of the synaptobrevin C-terminus inresponse to piconewton forces. Biophysical Journal 103:959-969, 2012

Littleton, J.T., Stern, M. Schulze, K., Perin, M., Bellen, H.J., Mutational analysis of drosophila synaptotagmin demonstrates its essential role in Ca(2+)-activated neurotransmitter release. Cell 74(6):1125-1134, 1993

Liu, H., Bai, H., Hui, E., Yang, L., Evans, C. S., Wang, Z., Kwon, S.E., Chapman, E.R.: Synaptotagmin 7 functions as a Ca(2+)-sensor for synaptic vesicle replenishment. eLife 3:e01524, 2014

Liu, C., Bickford, L.S., Held, R.G., Nyitrai, H., Südhof, T.C. and Kaeser, P.S.: The active zone protein family ELKS supports Ca2+ influx at nerve terminals of inhibitory hippocampal neurons. Journal of Neuroscience 34:12289-12303, 2014

Llinás, R. R.: Depolarization release coupling: an overview. Annals of the New York Academy of Sciences 635:3-17, 1991

Lodowski, D.T., Picher, j.A., Capel, W.D., Lefkowitz, R.J., Tesmer, J.J.G.: Keeping G proteins at bay: A complex between G protein-coupled recpetor kinase 2 and G betagamma. Science 300:1256-1262, 2003

Lübbert, M., Goral, R.O., Keine, C., Thomas, C., Guerrero-Given, D., Putzke, T., Satterfield, R., Kamasawa, N., and Young, Jr., S.M.: CaV2.1 alpha1 subunit expression regulates presynaptic CaV2.1 abundance and synaptic strength at a central synapse. Neuron 101:260-273, 2019

Luscher, C., Jan, L.Y., Stoffel, M., Malenka, R.C., Nicoll, R.A.: G protein-coupled inwardly rectifying K+ channels (GIRKs) mediate postsynaptic but not presynaptic transmitter actions in hippocampal neurons. Neuron 19(3):687-695, 1997

Mahal, L.K., Sequeira, S.M., Gureasko, J.M., and Söllner, T.H. Calcium-independent stimulation of membrane fusion and SNAREpin formation by synaptotagmin I. Journal of Cellular Biology 158:273-282, 2002

Martens, S., Kozlov, M.M. and McMahon, H.T. How synaptotagmin promotes membrane fusion. Science 316:1205–1208, 2007

Mazzoni ,M.R., Malinski ,J.A. and Hamm, H.E.: Structural analysis of rod GTP binding protein, Gt. Limited proteolytic digestion pattern of Gt with four proteases defines monoclonal antibody epitope. Journal of Biological Chemistry 266:14072-14081, 1991

McMahon, H.T., Missler, M., Li, C. and Südhof, T.C. Complexins: cytosolic proteins that regulate SNAP receptor function. Cell 83:111-119, 1995

Meer, D.P. and Buchanan, J.T.: Apamin reduces the late afterhyperpolarization of lamprey spinal neurons, with little effect on fictive swimming. Neuroscience Letters 143:1-4, 1992

Meinrenken, C. J., Borst, J. G. G. and Sakmann, B.: Calcium secretion coupling at calyx of Held governed by nonuniform channel vesicle topography. Journal of Neuroscience 22:1648-1667, 2002

Midorikawa, M. and Sakaba, T.: Kinetics of releasable synaptic vesicles and their plastic changes at hippocampal mossy fiber synapses. Neuron 96:1033-1040, 2017

Millar, A.G., Zucker, R.S., Ellis-Davies, G.C., Charlton, M.P. and Atwood, H.L.: Calcium sensitivity of neurotransmitter release differs at phasic and tonic synapses. Journal of Neuroscience 25:3113-3125, 2005

Minor, D.L., Jr. and Findeisen, F.: Progress in the structural understanding of voltage-gated calcium channel (CaV) function and modulation. Channels (Austin) 4:459-474, 2010

Misura ,K.M., Scheller, R.H., Weis W.I.: Three-dimensional structure of the neuronal-Sec1- syntaxin 1a complex. Nature 404:355-362, 2000

Miki, T., Kaufmann, W. A., Malagon, G., Gomez, L., Tabuchi, K., Watanabe, M., Shigemoto, R., Marty, A.: Numbers of presynaptic Ca2C channel clusters match those of functionally defined vesicular docking sites in single central synapses. Proceedings of the National Academy of Science USA 114:E5246-E5255, 2017

Mintz, I.M., Sabatini, B.L. and Regehr, W.G.: Calcium control of transmitter release at a cerebellar synapse. Neuron 15:675-688, 1995

Mochida, S., Few, A.P., Scheuer, T. and Catterall, W.A. Regulation of presynaptic Ca(V)2.1 channels by Ca2+ sensor proteins mediates short-term synaptic plasticity. Neuron 57:210-216, 2008

Mochida, S.: Presynaptic calcium channels. International Journal of Molecular Sciences 20(9):2217, 2019

Mohrmann, R., de Wit, H., Verhage, M., Neher, E., Sørensen, J.B.: Fast vesicle fusion in living cells requires at least three SNARE complexes. Science 330:502-505, 2010

Nakamura, Y., Harada, H., Kamasawa, N., Matsui, K., Rothman, J.S., Shigemoto, R., Silver, R.A., DiGregorio, D.A. and Takahashi, T.: Nanoscale distribution of presynaptic Ca(2+) channels and its impact on vesicular release during development. Neuron 85,145:158, 2015

Nanou, E., Sullivan, J.M., Scheuer, T. and Catterall, W.A.: Calcium sensor regulation of the CaV2.1 Ca2+ channel contributes to short-term synaptic plasticity in hippocampal neurons. Proceedings of the National Academy of Science USA 113:1062-1067, 2016

Naraghi, M., and Neher, E.: Linearized buffered Ca2+ diffusion in microdomains and its implications for calculation of [Ca2+] at the mouth of a calcium channel. Journal of Neuroscience 17,6961-6973, 1997

Neher, E.: Vesicle pools and Ca2+ microdomains: new tools for understanding their roles in neurotransmitter release. Neuron 20,389-399, 1998

Nishiki, T. and Augustine, G.J.: Dual roles of the C2B domain of synaptotagmin I in synchronizing Ca2+-dependent neurotransmitter release. Journal of Neuroscience 24:8542-8550, 2004a

Nishiki, T. and Augustine, G.J.: Synaptotagmin 1 synchronizes transmitter release in mouse hippocampal neurons. Journal of Neuroscience 24(27):6127-6312, 2004b

Oldham, W. M., and Hamm, H. E.: Heterotrimeric G protein activation by G protein-coupled receptors. Nature Reviews Molecular Cell Biology 9(1):60-71, 2008

Orita, S., Naito, A., Sakaguchi, G., Maeda, M., Igarashi, H., Sasaki, T., Takai, Y.: Physical and functional interaction of Doc2 and Munc13 in Ca2+-dependent exocytotic machinery. Journal of Biological Chemistry 272(26):16081-16084, 1997

Otto, H., Hanson, P.I. and Jahn, R.: Assembly and disassembly of a ternary complex of synaptobrevin, syntaxin, and SNAP-25 in the membrane of synaptic vesicles. Proceedings of the National Academy of Science USA 94:6197–6201, 1997

Oyler, G.A., Higgins, G.A., Hart, R.A., Battenberg, E., Billingsley, M., Bloom, F.E., and Wilson, M.C.:The identification of a novel synaptosomal-associated protein, SNAP-25, differentially expressed by neuronal subpopulations. Journal of Cellular Biology 109:3039-3052, 1989

Pangrsic, T., Gabrielaitis, M., Michanski, S., Schwaller, B., Wolf, F., Strenzke, N.and Moser, T.: EF-hand protein Ca2+ buffers regulate Ca2+ influx and exocytosis in sensory hair cells. Proceedings of the National Academy of Science USA 112:E1028-E1037, 2015

Patil, S.T., Zhang, L., Martenyi, F., Lowe, S.L., Jackson, K.A., Andreev, B.V., Avedisova, A.S. et al.: Activation of mGlu2/3 receptors as a new approach to treat schizophrenia: a randomized Phase 2 clinical trial. Nature Medicine 13:1102-1107, 2007

Perin, M.S., Fried, V.A., Mignery, G.A., Jahn, R., and Südhof ,T.C.: Phospholipid binding by a synaptic vesicle protein homologous to the regulatory region of protein kinase C. Nature 345:260–263, 1990

Perissinotti, P.P., Tropper, B.G. and Uchitel, O.D.: L-type calcium channels are involved in fast endocytosis at the mouse neuromuscular junction. European Journal of Neuroscience 27:1333-1344, 2008

Photowala, H., Freed, R. and Alford, S.: Location and function of vesicle clusters, active zones and Ca2+ channels in the lamprey presynaptic terminal. The Journal of Physiology (London) 569:119-135, 2005

Photowala, H., Blackmer, T., Schwartz, E., Hamm, H.E. and Alford, S.: G protein betagamma-subunits activated by serotonin mediate presynaptic inhibition by regulating vesicle fusion properties. Proceedings of the National Academy of Science USA 103:4281-4286, 2006

Planchon, T.A., Gao, L., Milkie, D.E., DAvidson, M.W, Galbraith, J.A., Galbraith and Betzig, E.: Rapid three-dimensional isotropic imaging of living cells using Bessel beam plane illumination. Nature Methods 8:417–423, 2011

Pobbati, A.V., Razeto, A., Böddener,M., Becke,r S., and Fasshauer, D.: Structural basis for the inhibitory role of tomosyn in exocytosis. Journal of Biological Chemistry 279:47192-47200, 2004

Rajapaksha, W.R., Wang, D., Davies, J.N., Chen, L., Zamponi, G.W. and Fisher, T.E.: Novel splice variants of rat CaV2.1 that lack much of the synaptic protein interaction site are expressed in neuroendocrine cells. The Journal of Biological Chemistry 283:15997-16003, 2008

Reddy-Alla, S., Böhme, M. A., Reynolds, E., Beis, C., Grasskamp, A. T., Mampell, M. M., Maglione, M. et al.: Stable positioning of Unc13 restricts synaptic vesicle fusion to defined release sites to promote synchronous neurotransmission. Neuron 95:1350.e12-1364.e12, 2017

Rettig, J., Sheng, Z.H., Kim, D.K., Hodson, C.D., Snutch, T.P., Catterall, W.A.: Isoform-specific interaction of the 1A subunits of brain Ca2+channels with the presynaptic proteins syntaxin and SNAP-25. Proceedings of the National Academy of Science USA 93:7363-7368, 1996

Rhee, J.S., Betz, A., Pyott, S., Reim, K., Varoqueaux, F., Augustin, I., Hesse, D., et al.: Beta phorbol ester- and diacylglycerol-induced augmentation of transmitter release is mediated by Munc13s and not by PKCs. Cell 108:121-133, 2002

Richmond, J. E., Davis, W. S. and Jorgensen, E. M.: UNC-13 is required for synaptic vesicle fusion in C. elegans. Nature Neuroscience 2:959-964, 1999

Richmond, J.E., Weimer, R.M., and Jorgensen, E.M.: An open form of syntaxin bypasses the requirement for UNC-13 in vesicle priming. Nature 412(6844):338-41, 2001

Rickman, C. and Davletov, B.: Mechanism of calcium-independent synaptotagmin binding to target SNAREs. Journal of Biological Chemistry 278:5501-5504, 2003

Risselada, H.J., Kutzner, C. and Grubmuller, H.: Caught in the act: visualization of SNARE-mediated fusion events in molecular detail. ChemBioChem 12:1049-1055, 2011

Rosa, J.M., Nanclares, C., Orozco, A., Colmena, I., de Pascual, R., García, A.G. and Gandía, L.: Regulation by L-type calcium channels of endocytosis: an overview. Journal of Molecular Neuroscience 48:360-367, 2012

Rose, G.J., and Fortune, E.S.: Frequency-dependent PSP depression contributes to low-pass temporal filtering in Eigenmannia. The Journal of Neuroscience 19:7629-7639, 1999

Rovainen, C.M.: Synaptic interactions of reticulospinal neurons and nerve cells in the spinal cord of the sea lamprey. Journal of Comparitive Neurology 154:207-223, 1974

Rowan, M. J., Tranquil, E. and Christie, J. M.: Distinct Kv channel subtypes contribute to differences in spike signaling properties in the axon initial segment and presynaptic boutons of cerebellar interneurons. Journal of Neuroscience 34:6611-6623, 2014

Rowan, M. J., DelCanto, G., Yu, J. J., Kamasawa, N. and Christie, J. M.: Synapse- level determination of action potential duration by K(+) channel clustering in axons. Neuron 91:370-383, 2016

Ryan, T.A.: Kiss-and-run, fuse-pinch-and-linger, fuse-and collapse: the life and times of a neurosecretory granule. Proceedings of the National Academy of Science USA 100:2171-2173, 2003

Sabatini, B.L., and Regehr, W.G.: Timing of neurotransmission at fast synapses in the mammalian brain. Nature 384:170-172, 1996

Sakamoto, H., Ariyoshi, T., Kimpara, N., Sugao, K., Taiko, I., Takikawa, K., Asanuma, D. et al.: Synaptic weight set by Munc13-1 supramolecular assemblies. Nature Neuroscience 21:41-49, 2018

Saviane, C. and Silver, R.A.: Fast vesicle reloading and a large pool sustain high bandwidth transmission at a central synapse. Nature 439:983-987, 2006

Schaub, J.R., Lu, X., Doneske, B., Shin, Y and McNew J.A.: Hemifusion arrest by complexin is relieved by Ca2+-synaptotagmin I. Nature Structural and Molecular Biology 13:748-750, 2006

Schiavo, G., Santucci, A., Dasgupta, B.R., Mehta, P.P., Jontes, J., Benfenati, F., Wilson, M.C., and Montecucco, C.: Botulinum neurotoxins serotypes A and E cleave SNAP-25 at distinct COOH-terminal peptide bonds. FEBS Letters 335:99-103, 1993

Schiavo, G., Osborne, S.L., Sgouros, J.G.: Synaptotagmins: more isoforms than functions? Biochemical and Biophysical Research Communications 248(1): 1-8, 1998

Schmidt, H., Brachtendorf, S., Arendt, O., Hallermann, S., Ishiyama, S., Bornschein, G., Gall, D., Schiffmann, S.N., Heckmann, M., Eilers, J.: Nanodomain coupling at an excitatory cortical synapse. Current Biology 23:244–249, 2013

Schneggenburger, R. and Neher, E. Intracellular calcium dependence of transmitter release rates at a fast central synapse. Nature 406:889-893, 2000

Schneider, C.A., Rasband, W.S., Eliceiri, K.W.: NIH Image to ImageJ: 25 years of image analysis. Nature Methods 9:671-675, 2012

Schoch, S., Castillo, P.E., Jo, T. Mukherjee, K. Geppert, M., Wang, Y., Schmitz, F., Malenka, R.C., Südhof, T.C.: RM1-alpha forms a protein scaffold for regulating neurotransmitter release at the active zone. Nature 415:321-326, 2002

Schwaller, B.: Cytosolic Ca2+ buffers. Cold Spring Harbor Perspectives in Biology 2:a004051, 2010

Schwartz, E.J., Gerachshenko, T., Alford, S.: 5-HT prolongs ventral root bursting via presynaptic inhibition of synaptic activity during fictive locomotion in lamprey. Journal Neurophsiology 93:980-988, 2005

Schwartz, E.J., Blackmer, T. Gerachshenko, T. and Alford, S.: Presynaptic G-protein-coupled receptors regulate synaptic cleft glutamate via transient vesicle fusion. Journal of Neuroscience 27:5857-5868, 2007

Schuette, C.G., Hatsuzawa, K., Margittai, M., Stein, A., Riedel, D., Küster, P., König, M., Seidel, C. and Jahn, R.: Determinants of liposome fusion mediated by synaptic SNARE proteins. Proceedings of the National Academy of Science 101(9):2858-2863, 2004

Scott, J.K., Huang, S.F., Gangadhar, B.P., Samoriski, G.M., Clapp, P., Gross, R.A., Taussig, R. and Smrcka, A.V.: Evidence that a protein-protein interaction 'hot spot' on heterotrimeric G protein betagamma subunits is used for recognition of a subclass of effectors. EMBO Journal 20:767-776, 2001

Shahrezaei, V., Cao, A. and Delaney, K. R.: Ca21 from one or two channels controls fusion of a single vesicle at the frog neuromuscular junction. Journal of Neuroscience 26:13240-13249, 2006

Sharma, S. and Lindau, M.: The fusion pore, 60 years after the first cartoon. FEBS Letters 592:3542-3562, 2018

Sheng, J., He, L., Zheng, H., Xue, L., Luo, F., Shin, W., Sun, T., Kuner, T., Yue, D. T., and Wu, L. G.: Calcium-channel number critically influences synaptic strength and plasticity at the active zone. Nature Neuroscience 15:998-1006, 2012

Sheng, Z.H., Rettig, J., Takahashi, M. and Catterall, W.A.: Identification of a syntaxin-binding site on N-type calcium channels. Neuron 13:1303-1313, 1994

Sheng, Z.H., Rettig, J., Cook, T. and Catterall, W.A.: Calcium-dependent interaction of N-type calcium channels with the synaptic core complex. Nature 379:451-454, 1996

Sheng, Z.H., Yokoyama, C.T., Catterall, W.A., Interaction of the synprint site of N-type Ca2+channels with the C2 B domain of synaptotagmin I. Proceedings of the National Academy of Science USA 94:5405-5410, 1997

Shimazaki, Y., Nishiki, T., Omori ,A., Sekiguchi, M., Kamata, Y., Kozaki ,S., and Takahashi, M.: Phosphorylation of 25-kDa synaptosome-associated protein. Possible involvement in protein kinase C-mediated regulation of neurotransmitter release. Journal of Biological Chemistry 271:14548-14553, 1996

Shin, O.H., Lu, J., Rhee, J.S., Tomchick, D.R., Pang, Z.P.P., Wojcik, S.M., Camacho-Perez, M., et al.: Munc13 C2B domain is an activity-dependent Ca2+ regulator of synaptic exocytosis. Nat. Struct. Mol. Biol. 17, 280–288, 2010

Sieber, J.J., Willig, K.I., Kutzner, C., Class, G., Harke, B. Donnert, G., Rammner, B., et al.: Anatomy and dynamics of a supramolecular membrane protein cluster. Science 317:1072-1076, 2007

Simms, B.A. and Zamponi, G.W.: Neuronal voltage-gated calcium channels: structure, function, and dysfunction. Neuron 82(1):24-45, 2014

Simon, M.I., Strathmann, M.P., Gautam, N.: Diversity of G proteins in signal transduction. Science 252(5007):802-808, 1991

Sirota, M.G., Di Prisco, G.V., Dubuc, R.: Stimulation of the mesenphalic locomotor region elicits controlled swimming in semi-intact lampreys. European Journal of Neuroscience 12(11):4081-4092, 2000

Smrcka, A.V.: G protein betagamma subunits: central mediators of G protein-coupled receptor signaling. Cellular and Molecular Life Sciences 65:2191-2214, 2008

Smyth, A.M., Duncan, R.R., and Rickman, C.: Munc18-1 and Syntaxin1: unraveling the interactions between the dynamic duo. Cellular and Molecular Neurobiology 30:1309-1313, 2010

Söllner, T., Whiteheart, S.W., Brunner, M., Erdjument-Bromage, H., Geromanos, S., Tempst, P. and Rothman, J.E.: SNAP receptors implicated in vesicle targeting and fusion. Nature 362:318-324, 1993

Soong, T.W., Stea, A., Hodson, C.D., Dubel, S.J., Vincent, S.R. and Snutch, T.P.: Structure and functional expression of a member of the low voltage-activated calcium channel family. Science 260:1133-1136, 1993

Sørensen, J.B., Wiederhold, K., Müller, E.M., Milosevic, I., Nagy, G., de Groot, B.L., Grubmüller, H. and Fasshauer, D.: Sequential N- to C-terminal SNARE complex assembly drives priming and fusion of secretory vesicles. EMBO Journal 25:955-966, 2006

Sondek, J., Bohm, A., Lambright, D.G., Hamm, H.E. and Sigler, P.B.: Crystal structure of a G-protein betagamma dimer at 2.1Å resolution. Nature 379:369-374, 1996

Spafford, J.D., Munno, D.W., Van Nierop, P., Feng, Z.P., Jarvis, S.E., Gallin, W.J., Smit, A.B., Zamponi, G.W. and Syed, N.I.: Calcium channel structural determinants of synaptic transmission between identified invertebrate neurons. The Journal of Biological Chemistry 278:4258-4267, 2003

Stanika, R.I., Villanueva, I., Kazanina, G., Andrews, S.B. and Pivovarova, N.B.: Comparative impact of voltage-gated calcium channels and NMDA receptors on mitochondria-mediated neuronal injury. The Journal of Neuroscience 32:6642-6650, 2012

Stanley, E.F.: Single calcium channels and acetylcholine release at a presynaptic nerve terminal. Neuron 11:1007–1011, 1993

Su, S.C., Seo, J., Pan, J.Q., Samuels, B.A., Rudenko, A., Ericsson, M., Neve, R.L., Yue, D.T., Tsai, L.H.: Regulation of N-type voltage-gated calcium channels and presynaptic function by cyclin-dependent kinase 5. Neuron 75(4):675-687, 2012

Südhof, T.C.: The synaptic vesicle cycle. Annual Review Neuroscience 27:509-547, 2004

Südhof, T.C., Rothman, J.E.: Membrane fusion: grappling with SNARE and SM proteins. Science 323(5913):474-477, 2009

Südhof, T.C.: Neurotransmitter Release: The Last Millisecond in the Life of a Synaptic Vesicle Neuron 80:675-690, 2013

Sutton, R.B., Fasshauer, D., Jahn, R. and Brunger A.T.: Crystal structure of a SNARE complex involved in synaptic exocytosis at 2.4Å resolution. Nature 395:347-353, 1998

Sutton, R.B., Ernst, J.A., Brunger, A.T.: Crystal structure of the cytosolic C2A-C2B domains of synaptotagmin III. Implications for Ca(+2)-independent snare complex interaction. Journal of Cell Biology 147(3):589-98, 1999

Swanson, C.J., Bures, M., Johnson, M.P., Linden, A.M., Monn, J.A., and Schoepp, D.D.: Metabotropic glutamate receptors as novel targets for anxiety and stress disorders. Nature Reviews Drug Discovery 4:131-144, 2005

Tadross, M.R., Dick, I.E. and Yue, D.T.: Mechanism of local and global Ca2+ sensing by calmodulin in complex with a Ca2+ channel. Cell 133:1228-1240, 2008

Takahashi, M., Freed, R., Blackmer, T and Alford, S.: Calcium influx-independent depression of transmitter release by 5-HT at lamprey spinal cord syanpses. Journal of Physiology 532.3:323-336, 2001

Takamori, S., Holt, M., Stenius, K., Lemke, E.A., Gronborg, M., Riedel, D., Urlaub, H., et al.: Molecular anatomy of a trafficking organelle. Cell 127:831–846, 2006

Tang, J., Maximov, A., Shin, O-H., Dai, H., Rizo, J and Südhof, T.C.: A Complexin/Synaptotagmin 1 switch controls fast synaptic vesicle exocytosis. Cell 126:1175-1187, 2006

Tang, J.: Complexins. Encyclopedia of Neuroscience (Larry RS ed) 1–7, Academic Press, Oxford, 2009

Taschenberger, H., Woehler, A., and Neher, E.: Superpriming of synaptic vesicles as a common basis for intersynapse variability and modulation of synaptic strength. Proceedings of the National Academy of Science USA 113:e4548-e4557, 2016

Tedford, H.W., Zamponi, G.W.: Direct G protein modulation of Cav2 calcium channels. Pharmacological Reviews 58:837-862, 2006

Teng, F.Y., Wang, Y., Tang, B.L., 2001. The syntaxins. Genome Biology Reviews 2(11):3012.1-3012.7, 2001

Tippens, A.L., Pare, J.F., Langwieser, N., Moosmang, S., Milner, T.A., Smith, Y., Lee, A.: Ultrastructural evidence for pre- and postsynaptic localization of Cav1.2 L-type Ca2+ channels in the rat hippocampus. Journal of Comparative Neurology 506(4):569-583, 2008

Tong, X. J., López-Soto E.J., Li, L. Liu, H., Nedelcu, D., Lipscombe, D., Hu, Z., Kaplan, J.M.: Retrograde synaptic inhibition is mediated by alpha- neurexin binding to the alpha2delta subunits of N- type calcium channels. Neuron 95:326-340, 2017

Tsien, R.W., Ellinor, P.T., Horne, W.A.: Molecular diversity of voltage-dependent Ca2+ channels. Trends in Pharmacological Sciences 12:349-354, 1991

Tucker, W.C., Weber, T. and Chapman, E.R.: Reconstitution of Ca2+-regulated membrane fusion by synaptotagmin and SNAREs. Science 304:435-438, 2004

Van Hook, M.J., and Thoreson, W.B.: Rapid synaptic vesicle endocytosis in cone photoreceptors of salamander retina. Journal of Neuroscience 32:18112-18123, 2012

Van Hook, W.J., Babai, N. Zurawski, Z., Yim, Y.Y., Hamm, H.E. and Thoreson, W.B.: A presynaptic group III mGluR recruits g betagamma/SNARE interactions to inhibit synaptic transmission by cone photoreceptors in the vertebrate retina. The Journal of Neuroscience 37(17):4618-4634, 2017

Vanderbeld, B. and Kelly, G.M.: New thoughts on the role of the beta-gamma subunit in G-protein signal transduction. Biochemistry and Cell Biology 78:537-550, 2000

Voets, T., Moser, T., Lund, P., Chow, R.H., Geppert, M., Südhof, T.C. and Neher, E.: Intracellular calcium dependence of large dense-core vesicle exocytosis in the absence of synaptotagmin I. Proceedings of the National Academy of Science 98:11680-11685, 2001

Vyleta, N.P. and Jonas, P.: Loose coupling between Ca2+ channels and release sensors at a plastic hippocampal synapse. Science 343:665-670, 2014

Wadel, K., Neher, E. and Sakaba, T.: The coupling between synaptic vesicles and Ca2+ channels determines fast neurotransmitter release. Neuron 53:563-575, 2007

Wallen, P., Buchanan, J.T., Grillner, S., Hill, R.H., Christenson, J. and Hokfelt, T.: Effects of 5 hydroxytryptamine on the afterhyperpolarization, spike frequency regulation, and oscillatory membrane properties in lamprey spinal cord neurons. Journal of Neurophysiology 61:759-768, 1989

Walter, A.M., Bohme, M.A. and Sigrist, S.J.: Vesicle release site organization at synaptic active zones. Neuroscience Research 127:3-13, 2018

Wang, L. Y., Fedchyshyn, M. J. and Yang, Y. M.: Action potential evoked transmitter release in central synapses: insights from the developing calyx of held. Molecular Brain 2:36, 2009

Wang, Y., Okamoto, M., Schmitz, F., Hofman, K. and Südhof, T. C.: RIM is a putative Rab3A-effector in regulating synaptic vesicle fusion. Nature 388:593-598, 1997

Washbourne, P., Thompson, P.M., Carta, M., Costa, E.T., Mathews, J.R., Lopez-Benditó, G., Molnár, Z. et al.: Genetic ablation of the t-SNARE SNAP-25 distinguishes mechanisms of neuroexocytosis. Nature Neuroscience 5:19-26, 2002

Watanabe, S., Rost, B.R., Camacho-Perez, M., Davis, M.W., Sohl-Kielczynski, B., Rosenmund, C., Jorgensen, E.M.: Ultrafast endocytosis at mouse hippocampal synapses. <u>Nature</u> 504:242-247, 2013

Weber, A.M., Wong, F.K., Tufford, A.R., Schlichter, L.C., Matveev, V. and Stanley, E.F.: N-type Ca2+ channels carry the largest current: implications for nanodomains and transmitter release. <u>Nature Neuroscience</u> 13:1348-1350, 2010

Weber, T., Zemelman, B.V., McNew, J.A., Westermann, B., Gmachi, M., Parlati, F., Söllner, T.H., Rothman, J.E.: SNAREpins: Minimal Machinery for membrane fusion. <u>Cell</u> 92:759-772, 1998

Weimbs, T., Low, S.H., Chapin, S.J., Mostov, K.E., Bucher, P. and Hofmann, K.: A conserved domain is present in different families of vesicular fusion proteins: A new superfamily. <u>Proceedings of the National Academy of Science USA</u> 94:3046-3051, 1997

Weimer, R.M., Richmond, J.E.: Synaptic vesicle docking: a putative role for the Munc18/Sec1 protein family. <u>Current Topics in Developmental Biology</u>. 65, 83-113, 2005

Wells, C.A., Zurawski, Z., Betke, K.M., Yim, Y.Y., Hyde, K., Rodriguez, S., Alford, S. and Hamm, H.E.: Gbetagamma inhibits exocytosis via interaction with critical residues on soluble N ethylmaleimide-sensitive factor attachment protein-25. <u>Molecular Pharmacology</u> 82:1136-1149, 2012

Wen, H., Linhoff, M.W., McGinley, M.J., Li, G-L., Corson, G.M., Mandel, G. and Brehm, P.: Distinct roles for two synaptotagmin isoforms in synchronous and asynchronous transmitter release at zebrafish neuromuscular junction. <u>Proceedings of the National Academy of Science USA</u> 107:13906-1391, 2010

Weng, G., Li, J., Dingus, J., Hildebrandt, J.D., Weinstein, H., and Iyengar, R.: G betagamma subunit interacts with a peptide encoding region 956–982 of adenylyl cyclase 2. Cross-linking of the peptide to free G betagamma but not the heterotrimer. <u>Journal of Biological Chemistry</u> 271:26445-26448, 1996

Wheeler, D.B., Randall, A. and Tsien, R.W.: Roles of N-type and Q-type Ca2+ channels in supporting hippocampal synaptic transmission. <u>Science</u> 264:107-111, 1994

Williams, C., Chen, W., Lee, C.-H., Yaeger, D., Vyleta, N. P. and Smith, S. M.: Coactivation of multiple tightly coupled calcium channels triggers spontaneous release of GABA. <u>Nature Neuroscience</u> 15:1195-1197, 2012

Wikstrom, M., Hill, R., Hellgren, J. and Grillner, S.: The action of 5-HT on calcium-dependent potassium channels and on the spinal locomotor network in lamprey is mediated by 5-HT1A-like receptors. <u>Brain Research</u> 678:191-199, 1995.

Wiser, O., Bennett, M.K., Atlas, D.: Functional interaction of syntaxin and SNAP-25 with voltage-sensitive L- and N-type Ca2+ channels. <u>EMBO Journal</u> 15:4100-4110, 1996

Wu, D., Hu, Q., Yan, Z., Chen, W., Yan, C., Huang, X., Zhang, J. et al.: Structural basis of ultraviolet-B perception by UVR8. <u>Nature</u> 484:214-219, 2012

Wu, J., Yan, Z., Li, Z., Qian, X., Lu, S., Dong, M., Zhou, Q., Yan, N.: Structure of the voltage- gated calcium channel Ca(v)1.1 at 3.6Å resolution. Nature 537:191-196, 2016

Wu, L.G., Westenbroek, R.E., Borst, J.G., Catterall, W.A. and Sakmann, B. Calcium channel types with distinct presynaptic localization couple differentially to transmitter release in single calyx-type synapses. Journal of Neuroscience 19:726-736, 1999

Wu, X.S., Zhang, Z., Zhao, W.D., Wang, D., Luo, F., and Wu, L.G.: Calcineurin is universally involved in vesicle endocytosis at neuronal and nonneuronal secretory cells. Cell Reports 7:982-988, 2014

Xu, J., Mashimo, T. and Südhof, T. C.: Synaptotagmin-1, -2, and -9: Ca21 sensors for fast release that specify distinct presynaptic properties in subsets of neurons. Neuron 54:567-581, 2007

Xu, J., McNeil, B., Wu, W., Nees, D., Bai, L., and Wu, L.-G.: GTP-independent rapid and slow endocytosis at a central synapse. Nature Neuroscience 11:45–53, 2008

Xu, T., Binz, T., Niemann, H. and Neher, E.: Multiple Kinetic components of exocytosis distinguished by neurotoxin sensitivity. Nature Neuroscience 1:192-100, 1998

Xu, Y., Zhu, S-W. and Li, Q-W.: Lamprey: a model for vertebrate evolutionary research. Zoological Research 37:263-269, 2016

Yokoyama, C.T., Sheng, Z.H., Catterall, W.A.: Phosphorylation of the synaptic protein interaction site on N-type calcium channels inhibits interactions with SNARE proteins. Journal of Neuroscience 17:6929-6938, 1997

Yokoyama, C.T., Myers, S.J., Fu, J., Mockus, S.M., Scheuer, T., Catterall, W.A.: Mechanism of SNARE protein binding and regulation of CaV2 channels by phosphorylation of the synaptic protein interaction site. Molecular and Cellular Neuroscience 28:1-17, 2005

Yoon, E.J., Gerachshenko, T., Spiegelberg, B.D., Alford, S., Hamm, H.E.: G betagamma interferes with Ca2+-dependent binding of synaptotagmin to the soluble Nethylmaleimide-sensitive factor attachment protein receptor (SNARE) complex. Molecular Pharmacology 72:1210-1219, 2007

Yoon, E.J., Hamm, H.E. and Currie, K.P.: G protein betagamma subunits modulate the number and nature of exocytotic fusion events in adrenal chromaffin cells independent of calcium entry. Journal of Neurophsyiology 100:2929-2939, 2008

Yu, F.H., Yarov-Yarovoy, V., Gutman, G.A., Catterall, W.A.: Overview of molecular relationships in the voltage-gated ion channel superfamily. Pharmacological Reviews 57:387-395, 2005

Zampighi, G.A., Zampighi, L.M., Fain, N., Lanzavecchia, S., Simon, S.A., Wright, E.M.: Conical electron tomography of a chemical synapse: Vesicles docked to the active zone are hemi-fused. Biophysical Journal 91:2910-2918, 2006

Zamponi, G.W.: Regulation of presynaptic calcium channels by synaptic proteins. Journal of Pharmacological Sciences 92:79-83, 2003

Zakharenko, S.S., Zablow, L., Siegelbaum, S.A.: Altered presynaptic vesicle release and cycling during mGluR-dependent LTD. Neuron 35:1099-1110, 2002

Zelenin, P. V: Reticulospinal neurons controlling forward and backward swimming in the lamprey. The Journal of Neurophysiology 105:1361-1371, 2011

Zhang, Q., Li, Y., Tsien, R.W.: The dynamic control of kiss-and-run and vesicular reuse probed with single nanoparticles. Science 323:1448-1453, 2009

Zhang, X.L., Upreti, C. and Stanton, P.K.: G betagamma and the C terminus of SNAP-25 are necessary for long-term depression of transmitter release. PLOS One 6:e20500, 2011

Zhang, X., Rizo, J. and Südhof, T.C Mechanism of phospholipid binding by the C2A domain of synaptotagmin I. Biochemistry 37:12395–12403, 1998

Zhang, X., Kim-Miller, M.J., Fukuda, M., Kowalchyk, J.A. and Martin, T.F.: Ca2+-dependent synaptotagmin binding to SNAP-25 is essential for Ca2+-triggered exocytosis. Neuron 34:599-611, 2002

Zhao, W.D., Hamid, E., Shin, W., Wen, P.J., Krystofiak, E.S., Villarreal, S.A., Chiang, H.C., Kachar, B. and Wu, L.G.: Hemi-fused structure mediates and controls fusion and fission in live cells. Nature 534:548-552, 2016

Zhao, Y., Fang, Q., Straub, S.G., Lindau, M., and Sharp, G.W.: Noradrenaline inhibits exocytosis via the G protein betagamma subunit and refilling of the readily releasable granule pool via the alphai1/2 subunit. Journal of Physiology 588:3485–3498, 2010

Zhao Y, Fang Q, Herbst AD, Berberian KN, Almers W and Lindau M.: Rapid structural change in synaptosomal-associated protein 25 (SNAP25) precedes the fusion of single vesicles with the plasma membrane in live chromaffin cells. Proceedings of the National Academy of Science USA 110:14249-14254, 2013

Zhen, M. and Jin, Y.: The liprin protein SYD-2 regulates the differentiation of presynaptic termini in C. elegans. Nature 401:371-375, 1999

Zhong, H., Yokoyama, C.T., Scheuer, T., Catterall, W.A.: Reciprocal regulation of P/Q-type Ca2+ channels by SNAP-25, syntaxin and synaptotagmin. Nature Neuroscience 2:939-941, 1999

Zhou, Q., Lai, Y. Bacaj, T., Zhao, M., Lyubimov, A.Y., Uervirojnangkoorn, M., Zeldin, O.B., Brewster, A.S., Sauter, N.K., et al.,: Architecture of the synaptotagmin-SNARE machinery for neuronal exocytosis. Nature 525:62-67, 2015

Zurawski, Z., Rodriguez, S., Hyde, K., Alford, S.T., Hamm, H.E.: G beta gamma Binds to the Extreme C Terminus of SNAP25 to Mediate the Action of G(i/o)-Coupled G Protein-Coupled Receptors Molecular Pharmacology 89(1),75-83, 2016

Zurawski, Z. Thompson Gray, A.D., Brady, L.J., Page, B., Church, E.C. Harris, N.A., Dohn, M.R., et al.: Disabling the Gbetagamma-SNARE interaction disrupts GPCR-mediated presynaptic inhibition, leading to physiological and behavioral phenotypes. Science Signaling 12:eaat8595, 2019a

Zurawski, Z., Yim, Y.Y., Alford, S.T. and Hamm, H.E.: The expanding roles and mechanisms of G protein-mediated presynaptic inhibition. Journal of Biological Chemistry Reviews 294(5):1661-1670, 2019b

APPENDIX A

UIC UNIVERSITY OF ILLINOIS
AT CHICAGO

Office of Animal Care and Institutional
Biosafety Committee (OACIB) (M/C 672)
Office of the Vice Chancellor for Research
206 Administrative Office Building
1737 West Polk Street
Chicago, Illinois 60612

8/15/2019

Simon Alford
Biological Sciences
M/C 067

Dear Dr. Alford:

The protocol indicated below was reviewed in accordance with the Animal Care Policies and Procedures of the University of Illinois at Chicago and **renewed on 8/15/2019.**

Title of Application: Dynamic Interactions Between G Proteins and Calcium at SNARE Complexes
ACC NO: 17-139
Original Protocol Approval: 8/15/2017 **(3 year approval with annual continuation required).**
Current Approval Period: 8/15/2019 **to** 8/15/2020

Funding: *Portions of this protocol are supported by the funding sources indicated in the table below.*
Number of funding sources: 2

Funding Agency	Funding Title			Portion of Funding Matched
NIH via subcontract from	Mechanisms of synaptic dysfunction in Parkinson's and other synuclein-linked diseases (Institutional # 00322318)			Other: Matched to SOW in subcontract from MBL
Funding Number	**Current Status**	**UIC PAF NO.**	**Performance Site**	**Funding PI**
R01 NS 078165 (original v., yrs 7-11)	Funded		UIC for subconstract	Simon Alford (for subcontract at UIC)
Funding Agency	**Funding Title**			**Portion of Funding Matched**
NIH via subcontract from	Optimization of Modulators of Gbg-SNARE Interaction (Institutional # 00005925)			Other: linked to 16-199 Form G
Funding Number	**Current Status**	**UIC PAF NO.**	**Performance Site**	**Funding PI**
R01MH101679- (A1 version)	Funded	2013-07033	UIC For Subcontract from Venderbilt Univ.	Simon Alford (PI for subcontract at UIC)

This institution has Animal Welfare Assurance Number A3460.01 on file with the Office of Laboratory Animal Welfare, NIH. **This letter may only be provided as proof of IACUC approval for those specific funding sources listed above in which all portions of the grant are matched to this ACC protocol.**

Thank you for complying with the Animal Care Policies and Procedures of the UIC.

Sincerely,

Amy Lasek

Amy Lasek, PhD
Chair, Animal Care Committee
AL/*kg*
cc: BRL, ACC File, Lisa Hoffman

APPENDIX B

March 11, 2019

Shelagh Rodriguez
Biological Sciences
University of Illinois at Chicago
932 N. Oakley Blvd.
Chicago, IL 60622

Email: shelagh.rodriguez@gmail.com

Dear Shelagh Rodriguez:

This is to grant you permission to reproduce the following figures in your dissertation titled "5-HT Modulates the Mode of Fusion Events Through the Interaction of Gbetagamma, Calcium-synaptotagmin and SNARE proteins" for the University of Illinois at Chicago:

Figures 1-8 and Tables 1-2 from CA Wells, Z Zurawski, KM Betke, YY Yim, K Hyde, S Rodriguez, S Alford, and HE Hamm (2012) Gβγ Inhibits Exocytosis via Interaction with Critical Residues on Soluble N-Ethylmaleimide-Sensitive Factor Attachment Protein-25, *Mol Pharmacol*, 82(6): 1136-1149; DOI: https://doi.org/10.1124/mol.112.080507

Permission to reproduce the figures is granted for any format or medium including print and electronic. The authors and the source of the materials must be cited in full, including the article title, journal title, volume, year, and page numbers.

Sincerely yours,

Richard Dodenhoff
Journals Director

February 28, 2019

Shelagh Rodriguez
Biological Sciences
University of Illinois at Chicago
932 N. Oakley Blvd.
Chicago, IL 60622

Email: shelagh.rodriguez@gmail.com

Dear Shelagh Rodriguez:

This is to grant you permission to reproduce the following figures in your dissertation titled "5-HT Modulates the Mode of Fusion Events Through the Interaction of Gbetagamma, Calcium-synaptotagmin and SNARE proteins" for the University of Illinois at Chicago:

Figures 1-7 from Z Zurawski, S Rodriguez, K Hyde, S Alford, and HE Hamm (2016) Gβγ Binds to the Extreme C Terminus of SNAP25 to Mediate the Action of Gi/o-Coupled G Protein–Coupled Receptors, *Mol Pharmacol*, 89(1):75-83; DOI: https://doi.org/10.1124/mol.115.101600

Permission to reproduce the figures is granted for any format or medium including print and electronic. The authors and the source of the materials must be cited in full, including the article title, journal title, volume, year, and page numbers.

Sincerely yours,

Richard Dodenhoff
Journals Director

VITA

Shelagh Rodriguez
932 N. Oakley Blvd, Chicago IL, 60622
Phone: 312-543-6345
shelagh.rodriguez@gmail.com

Education:

Ph. D Candidate, University of Illinois at Chicago, 2010 - Present
Concentration: Neurobiology, Synaptic Transmission
Research: 5-HT Modulates the Mode of Fusion Events Through the Interaction of Gβ, Ca^{2+}-Synaptotagmin and SNARE proteins
Primary Investigator: Simon Alford

B.S, Biology, University of Illinois at Chicago, 2010
Minor: Mathematics

Publications:

G beta gamma SNARE Interactions and Their Behavioral Effects
Alford, S; Hamm, H; Rodriguez, S; Zurawski, Z
NEUROCHEMICAL RESEARCH Volume: 44 Issue: 3 Pages: 636-649 Published MAR 2019

G beta gamma Binds to the Extreme C Terminus of SNAP25 to Mediate the Action of G(i/o)-Coupled G Protein-Coupled Receptors
Zurawski, Z; Rodriguez, S; Hyde, K; Alford, S; Hamm, HE
MOLECULAR PHARMACOLOGY Volume: 89 Issue: 1 Pages: 75-83 Published: JAN 2016

G beta gamma Inhibits Exocytosis via Interaction with Critical Residues on Soluble N-Ethylmaleimide-Sensitive Factor Attachment Protein-25
Wells, CA; Zurawski, Zack; Betke, KM; Yim, YY; Hyde, K; Rodriguez, S; Alford, S; Hamm, HE
MOLECULAR PHARMACOLOGY Volume: 82 Issue: 6 Pages: 1136-1149 Published: DEC 2012

Conference Posters:

Rodriguez, S; Ramachandran, S; Church, EC; Potcoava, M; Alford, S.T. Quantal fluctuation in transmitter release can be accounted for by fluctuations in presynaptic Ca2+ entry. Poster Presented by Simon Alford at: Society for Neuroscience Annual Meeting; 2018 November 3-7; San Diego, CA

Rodriguez, S; Ramachandran, S; Church, E.C; Aldord, S.T. Stimulus-evoked Ca2+ influx at a single active zone varies through a variable and small population of voltage-gated Ca2+ channels. Poster Presented by Shelagh Rodriguez at: Society for Neuroscience Annual Meeting; 2017 November 11-15; Washington, DC

Conference Papers:

Potcoava, MC; Rodriguez, S; Zurawski, Z; Alford, S. Lattice Light-Sheet and Self-Interference Incoherent Digital Holography. Paper presented by Mariana Potcoava at: Digital Holography and Three-Dimensional Imaging; 2019 May 19-23; Bordeaux France

Potcoava, MC; Rodriguez, S; Alford, S. Ca2+ Decomposition into Signal and Noise Components for Multisite Ca2+ Imaging. Paper presented by Mariana Potcoava at: Clinical and Translational Biophotonics; 2018 April 3-6; Hollywood, FL

Research Skills and Experience:

Research Assistant: 2017 - Present
University of Illinois at Chicago

Extensive experience with the lamprey as a model organism, including;
 Electrophysiology: sharp-electrode recording, voltage-clamp recording, paired cell
   recording, patch-clamp recording,
 Fluorescence imaging: wide-field microscopy, confocal microscopy, lattice light sheet
   microscopy
 Dissection: isolated axon preparation, slice preparation with a Vibratome
 Developed techniques for introduction of Calcium dyes to multiple axons simultaneously

Experience with additional model systems:
 Electrophysiology using chromaffin cells and mouse hippocampal cultures
 Mouse behavioral assays such as spontaneous alternation and Rota-rod.
 Aseptic technique and preparing mouse hippocampal cultures.

Laboratory Management:
 Acted as Laboratory Safety Manager: ensuring compliance with university safety
 protocols, organized and secured hazardous materials
 Maintained stock of chemicals and equipment
 Performed required upkeep of electrophysiological rigs and cooling systems
 Assisted in design of cooling chambers for electrophysiological recordings

Proficient with:
 IgorPro
 ImageJ
 AxoGraph
 Adobe Illustrator
 Microsoft Excel

Teaching Experience:

Teaching Assistant 2010 - 2017
University of Illinois at Chicago
Courses: Cells and Organisms, Homeostasis, Genetics, Microbiology

> Cells and Organisms, Genetics, Microbiology: Instructed students in lab experiments and discussion sessions, as well as assisting with preparation work for the labs. Prepared lectures for small sections of students based on course material.

> Homeostasis: Held review sessions for students twice a week to explain difficult material. Lectured the full complement of 300 students when the professor was absent.

Community Involvement:

Presented Anatomy and Botany demonstrations at Andrew Jackson Language Academy's annual Science Night: 2015 - 2016

Volunteered as an Elementary School Science Fair Judge at Andrew Jackson Language Academy and Mark T. Skinner West Elementary School: 2013 - 2016

Volunteered at Expanding Your Horizons Annual Seminar: 2016

Volunteered as a High School Science Fair Judge at Lincoln Park High School: 2015